

57

**Exact Conservation of Quantum Numbers
B, S and Q in the Statistical Description
of High Energy Collisions**

by

Mark Marais

A thesis submitted in fulfilment of the
requirements for the M.Sc. degree
in the Department of Physics
University of Cape Town
South Africa

March 1997

The University of Cape Town has been given
the right to reproduce this thesis in whole
or in part. Copyright is held by the author.

The copyright of this thesis vests in the author. No quotation from it or information derived from it is to be published without full acknowledgement of the source. The thesis is to be used for private study or non-commercial research purposes only.

Published by the University of Cape Town (UCT) in terms of the non-exclusive license granted to UCT by the author.

**Exact Conservation of Quantum Numbers
B, S and Q in the Statistical Description
of High Energy Collisions**

Mark Marais

*Department of Physics, University of Cape Town
Rondebosch 7700, South Africa*

Abstract

High energy collisions are studied assuming that particles can be described by a hadron gas in thermal and chemical equilibrium.

The exact conservation of baryon number, strangeness and charge are explicitly taken into account. For heavy ions the effect arising from the neutron surplus becomes important and leads to a substantial increase in e.g. the π^-/π^+ ratio. Special emphasis is therefore put on the exact conservation of charge. Comparison with experimental results from the E866 collaboration at BNL is made.

*It is sufficiently clear that all things are changed, and
nothing really perishes, and that the sum of matter
remains absolutely the same.*

Francis Bacon
De Natura Rerum

Preface

The material presented divides naturally into two components. In the first part, Chapters 1 to 3, the basic ideas of a hadron gas model assuming thermal and chemical equilibrium are reviewed. Formulations of the partition function are developed in Chapter 4 to include exact conservation of baryon number, strangeness and charge. Particle number calculations are performed for all particles in the hadronic spectrum. In Chapter 5 results from the model are discussed and compared to results from the E866 collaboration at BNL.

Chapter 1 begins with a review and historical perspective of the development of a thermodynamical picture of high energy collisions. The basic assumptions of a thermal model are presented and the different formalisms which are available for describing such a model are discussed. The chapter closes with a brief look at various experimental observables.

Chapter 2 is an overview of results obtained from a dynamical hadron gas model containing longitudinal and transverse flow. This is compared to the case of a stationary fireball and with data from NA35 at CERN.

The third chapter reviews techniques for determining the total partition function of hadronic gases and looks at what effect the exact conservation of quantum numbers has on it. The general formalism for a restricted partition function is also presented.

The partition functions for the full hadronic spectrum including exact charge conservation emerge in Chapter 4. Expressions for particle number production, $\langle N \rangle$, for the full range of particles are derived from the partition functions using well established techniques. The viability of a transformation in the equations from charge, Q , to the z-component of isospin, I_3 , is also discussed in detail.

In Chapter 5 results using the model are presented and, comparisons made with recent experimental data for $Au - Au$ collisions at BNL. Deviations of particle ratios from the isospin symmetric cases can clearly be seen for the cases where isospin symmetry is broken.

Appendix A deals with π^+ , π^- production in a π , p , n isospin symmetric gas.

Appendix B presents the mathematical analysis for the viability of transforming from Q to I_3 in the equations.

And finally, Appendix C contains expressions for $\langle N \rangle$ of all particles in the hadronic spectrum.

Contents

1	A New Form of Matter ?	2
1.1	Introduction	2
1.2	Existence of Fireballs	3
1.3	Thermodynamical Approach	5
1.4	Experimental Observables	8
1.5	Signatures of the QGP	8
1.6	The Future	9
2	Dynamic Fireball Model	10
2.1	Longitudinal Flow	10
2.2	Transverse Flow and m_T Scaling	12
2.3	Conclusion	15
3	The Hadron Gas Partition Function	16
3.1	For a Hadronic Gas with total Baryon number B	17
3.1.1	In the Canonical Ensemble	17
3.2	Including Baryons and Mesons	19
3.2.1	Adding Deltas	19
3.2.2	Adding Mesons	20
3.3	General Formalism for a “Restricted Partition Function”	20
3.4	Bessel Function Representation of Z	21
4	Exact Baryon, Strangeness, Charge Conservation	23
4.1	Simpler Cases of the Hadron Gas	24

4.1.1	A π^+ , π^- Gas	24
4.1.2	A Proton-Antiproton Gas	25
4.2	The Complete Hadronic Partition Function	26
4.2.1	Case 1: Baryon number = $0, \pm 1$, Strangeness = $0, \pm 1$, Charge = $0, \pm 1$. .	26
4.2.2	Transforming from B, S, Q , to B, S, I_3	30
4.2.3	Case 2: Baryon number = $0, \pm 1$, Strangeness = $0, \pm 1, \pm 2$, Charge = $0, \pm 1$	31
4.2.4	Case 3: Baryon number = $0, \pm 1$, Strangeness = $0, \pm 1, \pm 2, \pm 3$, Charge = $0, \pm 1$	33
4.2.5	Case 4: Baryon number = $0, \pm 1$, Strangeness = $0, \pm 1, \pm 2, \pm 3$, Charge = $0, \pm 1, \pm 2$	34
4.3	Particle Numbers for a Gas with B, S, Q Conservation	35
4.3.1	Case 1: Baryon number = $0, \pm 1$, Strangeness = $0, \pm 1$, Charge = $0, \pm 1$. .	36
5	Results obtained using the B, S, Q Calculations	38
5.1	Seeing beyond B, S Conservation with B, S, Q	38
5.2	Comparisons with the BNL E866 data	40
5.3	Summary and Conclusions	45
A	π^+, π^- Production in a π, p, n Gas	47
B	Analysis of a Q to I_3 Transformation	49
C	Particle Number Expressions	51
C.0.1	Case 2: Baryon number = $0, \pm 1$, Strangeness = $0, \pm 1, \pm 2$, Charge = $0, \pm 1$	51
C.0.2	Case 3: Baryon number = $0, \pm 1$, Strangeness = $0, \pm 1, \pm 2, \pm 3$, Charge = $0, \pm 1$	54
C.0.3	Case 4: Baryon number = $0, \pm 1$, Strangeness = $0, \pm 1, \pm 2, \pm 3$, Charge = $0, \pm 1, \pm 2$	57

List of Figures

1.1	<i>Phase diagram of hadronic matter depicting the transition from hadrons to quarks.</i>	3
1.2	<i>a) The central region opening up after the collision between target and projectile nucleus. b) Central plateau region corresponding to the central region where the average multiplicity of particles per interval of rapidity is approximately constant.</i>	4
1.3	<i>a) N_p^{Exact} / N_p^{GC} ratio and, b) $N_{\bar{p}}^{Exact} / N_{\bar{p}}^{GC}$ ratio as a function of interaction volume radius for a proton-antiproton gas with exact baryon number conservation for different cases of B.</i>	7
2.1	<i>π^- y spectrum comparing fit from model containing longitudinal flow (solid line) with experimental data from NA35 (cross-hairs) and a purely thermal model (dotted line). The dashed line shows resonance decay contributions to the longitudinal flow model [32].</i>	11
2.2	<i>Extraction of η_{\max} from the rapidity distribution of hadrons [32].</i>	12
2.3	<i>y spectrum of p, K^0, Λ, and $\bar{\Lambda}$ with longitudinal flow in comparison with $S + S$ data from NA35 [32].</i>	13
2.4	<i>Comparison of the theoretical spectra with the E802 Si + Au data [32].</i>	14
2.5	<i>a) purely thermal π^- m_T- spectrum including resonance decays from a stationary fireball model and, b) the same spectrum generated using a transverse flow model. Both a) and b) are compared to the NA35 data [32].</i>	14
5.1	<i>A plot of the known (stable) nuclides to show the deviation of neutron number, N, from Z as N increases [47].</i>	39
5.2	<i>Plot showing the deviation from one for the π^-/π^+ ratio as the neutron surplus increases. The n/p ratio is also shown as a dotted line.</i>	39

LIST OF FIGURES

5.3	<i>Experimental particle ratios at mid-rapidity as a function of centrality [48]. . . .</i>	41
5.4	<i>The π^-/π^+ ratio plotted as a function of B for different values of the temperature with $B/2Q$ remaining fixed at 1 and 1.5.</i>	42
5.5	<i>The K^+/π^+ ratio plotted as a function of B.</i>	42
5.6	<i>The K^-/π^+ ratio plotted as a function of B.</i>	43
5.7	<i>The K^+/K^- ratio plotted as a function of B.</i>	43
5.8	<i>The \bar{p}/π ratio plotted as a function of B.</i>	44
5.9	<i>The p/π^+ ratio plotted as a function of B.</i>	45

List of Tables

4.1	Table showing z-component of isospin assignments for particles decaying by the weak or electromagnetic interactions	31
-----	---	----

Chapter 1

A New Form of Matter ?

“The study of the N-N interaction gives insight into the change in the structure of the quark wave functions during the collision process. An alternative, albeit simplistic approach, is to consider nuclear matter as a collection of bags like the holes in Swiss cheese, and to study the structure of the system as it is compressed.” [1]

1.1 Introduction

Of great interest and excitement in studying relativistic heavy ion collisions is the possibility of producing a completely new phase of matter, namely, a quark-gluon plasma (QGP), if the energy density produced in the collisions is sufficiently high.

A beam of projectile particles is collided with a target and under extreme high conditions of energy density and/or temperature, the hadronic matter in the ensuing fireball could undergo a phase transition by the individual hadrons dissolving or, fusing together, freeing their quark-gluon constituents to form the conjectured plasma (a weakly interacting Fermi and Bose gas[2]). This new state of matter is an almost inevitable consequence of QCD (quantum chromodynamics) which predicts that strongly interacting matter will form a hadron gas at low temperatures and a plasma of quarks and gluons at high temperatures [3]-[6]. Between these two phases is a transition or intermediate phase where colour becomes deconfined and chiral symmetry is restored. The quarks become massless in the final plasma phase.

Experiments performed at accelerators, such as at Brookhaven and CERN, yield information about particle numbers produced at certain projectile energies and targets.

The conditions necessary for the existence of the plasma phase are possibly also satisfied in the cores of neutron stars where the density may be as high as 10-20 times that of ordinary nuclear matter [7]. A diagrammatic representation depicting the different phases of hadronic matter is shown in Figure 1.1.

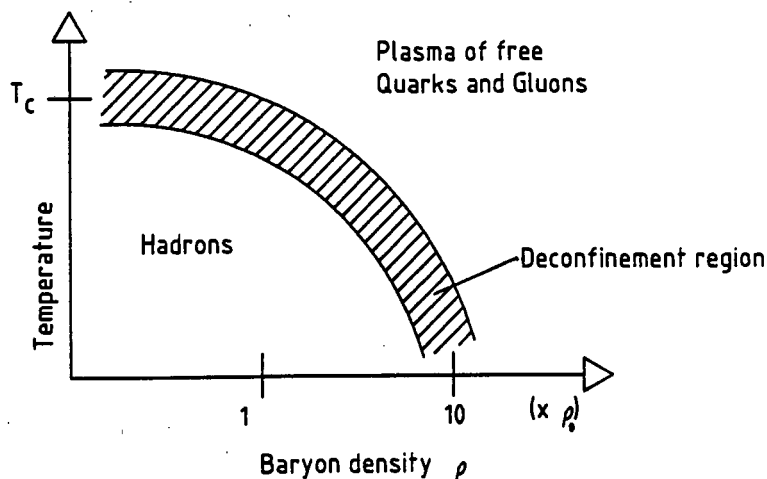


Figure 1.1: Phase diagram of hadronic matter depicting the transition from hadrons to quarks.

1.2 Existence of Fireballs

The idea of a “fireball” - a region in space where, after a collision, the energy of the longitudinal motion is largely transferred to transverse degrees of freedom [2] or, a cluster of highly excited hadronic matter sticking together for a very short period of time and where the hadron gas phases move with collective motion [8, 9], had begun with Heisenberg’s claim in 1936 [10] that a single elementary hadron-hadron collision can give rise to multiple secondary particle production (eleven years before the discovery of the pion!). The first Hydrogen bubble chamber pictures proved Heisenberg correct. Thus, in a single nucleus-nucleus collision a domain in space will arise from which many secondary particles will emanate. This region of production can be thought of as the “fireball”.

In a nucleus-nucleus collision the two nuclei overlap either partially as in a peripheral collision

or, totally, as in a central collision. A volume of hot hadronic matter is created consisting of a central region containing few baryons and, two highly excited baryon-rich fragmentation regions. The central region consists mainly of mesons with an equal amount of quarks and antiquarks. This scenario is illustrated in Figure 1.2.

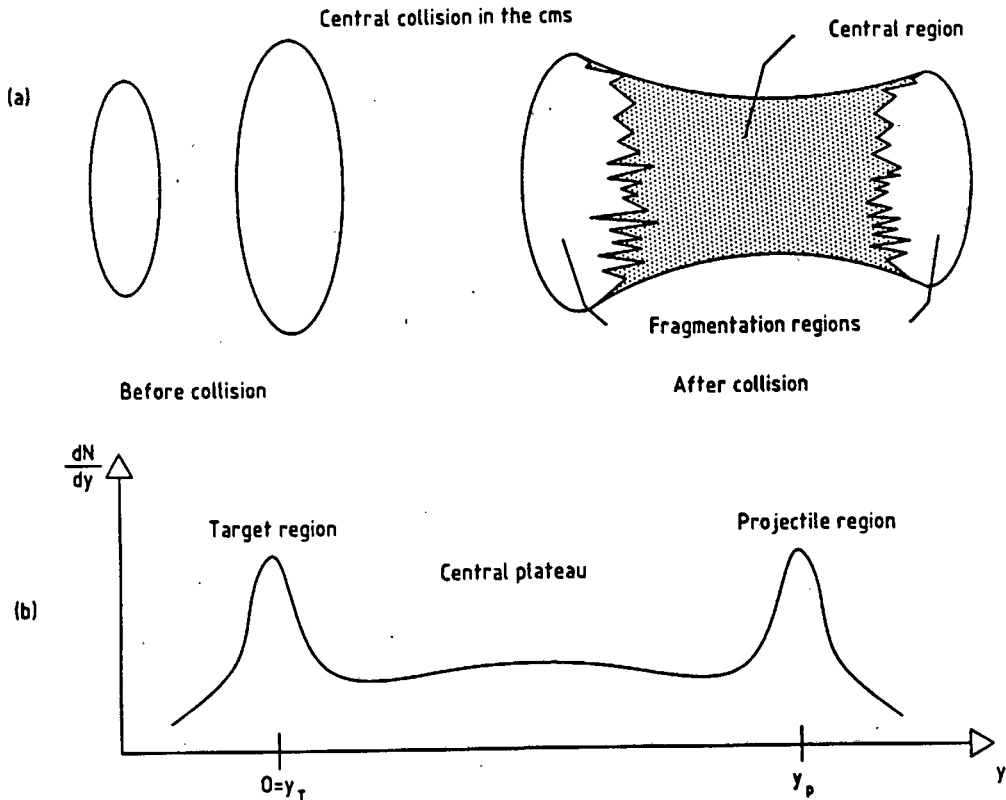


Figure 1.2: a) The central region opening up after the collision between target and projectile nucleus. b) Central plateau region corresponding to the central region where the average multiplicity of particles per interval of rapidity is approximately constant.

The fireball is characterized by the following physical variables:

- energy density,
- baryon number density and
- total volume.

The energy density in the central and fragmentation regions have been found to be of comparable magnitude according to modern estimates which put it in the range of $0.3 - 1.5 \text{ GeV}/\text{fm}^3$ for compressional energy and, a few GeV/fm^3 for heat energy [7].

1.3 Thermodynamical Approach

In 1937 Weisskopf was the first to show quantitatively that thermodynamics and/or statistics might be applied to such a small system as a nucleus [12] because of the large level density of heavy nuclei at high excitation energy. The ideas of Koppe [13, 14] and Fermi [15] (1948/1950) of a statistical model for particle production were first applied in the late forties to pion-nucleon and nucleon-nucleon collisions and were simply taken over to the case of $N\bar{N}$ annihilation [16]. These early models worked surprisingly well in describing pion multiplicities, momentum spectra and branching ratios [17]-[21].

The birth of the *Statistical Bootstrap Model* (SBM) in 1964 by Hagedorn followed on the developments preceding it and, one of the most important phenomenological indications of the ‘thermal behaviour’ of strong interactions and the thermal-like multihadron production in hadron-hadron collisions, is the ‘universal’ soft- p_T distribution plotted against $\sqrt{p_T^2 + m^2}$ i.e. the universal slope of transverse mass. With the momentum distribution thus plotted, all particles from a thermalized emitter should show the same universal exponential behaviour (“ m_T scaling”). Although the systematic deviation from a purely exponential m_T at low values of p_T (“low p_T anomaly”) can be quantitatively explained by the steeper m_T spectra of resonance decays, hard scattering phenomena characterized by a power-like tail in the transverse momenta at higher energies and, by an increase in $\langle p_T \rangle$ for higher multiplicity events, cannot however be explained within the SBM phenomenological framework.

Statistical modelling of particle production assumes that the particles produced in the fireball have interacted sufficiently so that a common temperature may be used to describe all species in the gas. Production rates of the different hadronic species in the fireball provide a good probe of locally thermalized sources in hadronic collisions since, being a Lorentz invariant quantity, it is not affected by collective motions of the gas [11]. All the thermal manifestations in nuclei-nuclei collisions can be thought of as the outcome of a single fundamental property of strong interactions, namely, that they have an exponential mass spectrum $\rho(m) \sim \exp(m/T_0)$ where T_0 is the singular phase transition temperature [9]. It is now understood that this is a consequence of quark confinement and that T_0 is related to QCD string tension. However, it is not clear what the physical mechanisms are that underlie the assumption of local thermodynamical

equilibrium.

A statistical description of particle production provides us with several formalisms which can be used to describe events following a collision. The most often used ones are the:-

- Canonical
- Grand Canonical and,
- Mixed Canonical

descriptions. At relativistic energies particles can be created from kinetic energy therefore, the canonical description for fixed particle number N , cannot be used. Thus with respect to particle number, we are forced in the relativistic scenario to use the grand canonical description. However, with respect to conservation laws which *do* impose constraints on particle number production, a choice between the different formalisms above becomes evident. Hagedorn pointed out in 1968 that the canonical formalism would be more appropriate to use in high energy proton-proton collisions because of small particle numbers and small interaction volumes and, showed that the production of anti- He^3 is wrong by seven orders of magnitude when the grand canonical formalism is applied in its standard form [8]. This theme has since been considerably developed and expanded in the literature [22]-[27]. It is also found (ref. [44]) that for large interaction volumes a description using the grand canonical ensemble can be justified but, for smaller systems such as in a $p - p$ collision, corrections arising solely from exact strangeness and baryon number conservation cannot be neglected.

The effect of imposing exact baryon number conservation on the statistical description of hadronic gas models has been investigated for a free pointlike proton-antiproton gas and the results compared to the grand canonical ensemble where baryon number holds only as an average over many ensembles [28]. It is found that in the large volume limit both descriptions are identical and a detailed investigation of small volumes shows that if the volume radius is larger than 5 fm and/or the baryon number is larger than 50, finite volume corrections are negligible and it is justified to use the grand canonical ensemble (see Fig. 1.3).

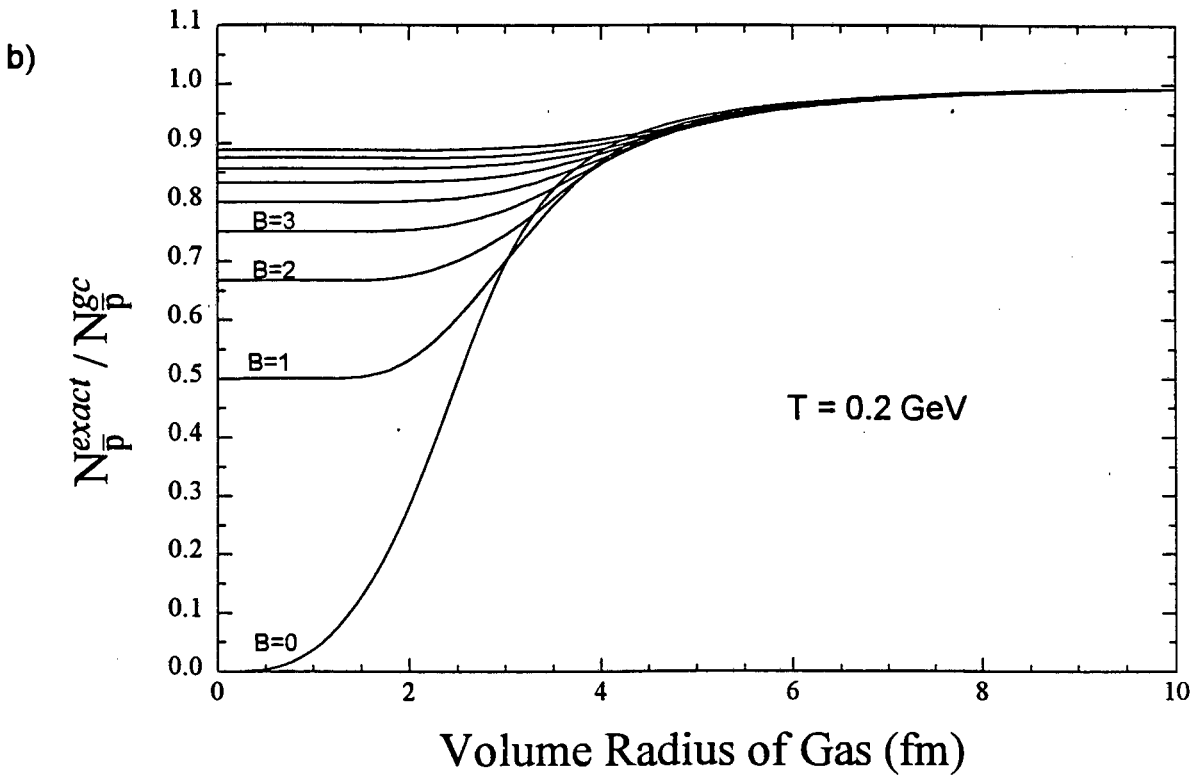
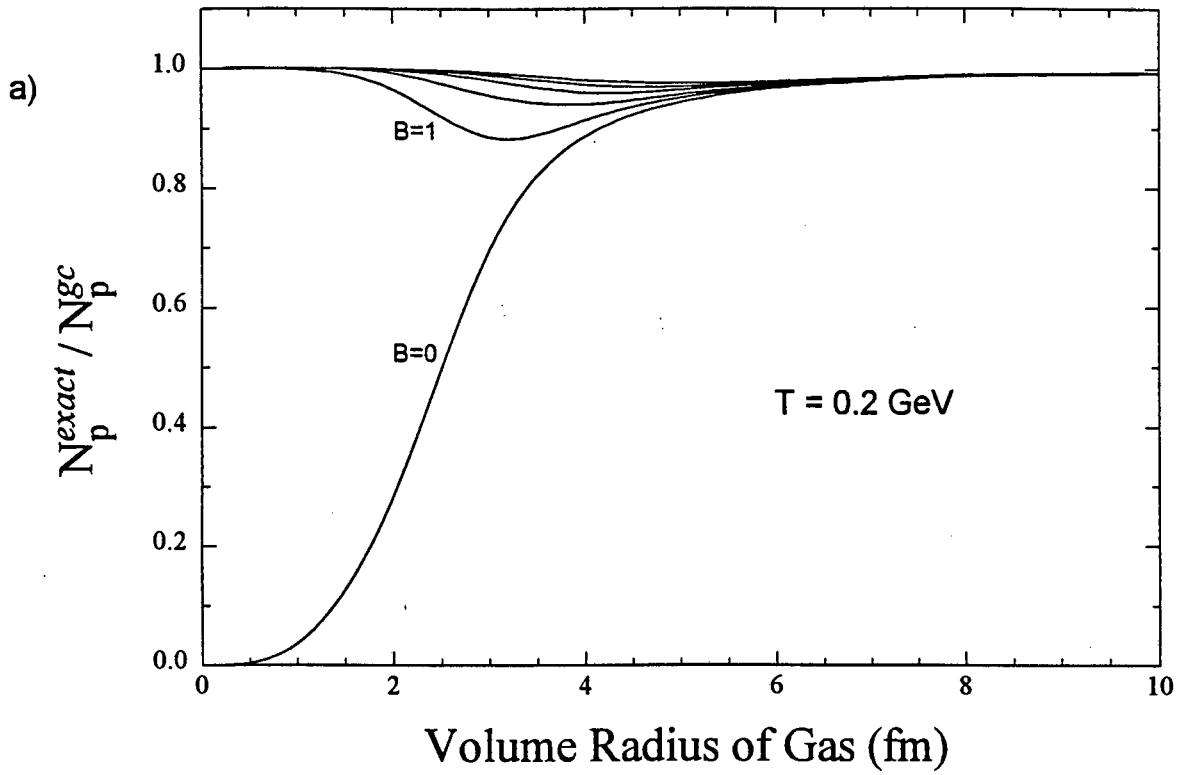


Figure 1.3: a) N_p^{Exact} / N_p^{GC} ratio and, b) $N_{\bar{p}}^{Exact} / N_{\bar{p}}^{GC}$ ratio as a function of interaction volume radius for a proton-antiproton gas with exact baryon number conservation for different cases of B .

1.4 Experimental Observables

Experimental observables from collisions can be divided into two categories. These are:

- global hadronic observables (e.g. transverse energy E_T , charged particle distributions, p_T distributions, particle production cross-sections and two-particle correlations).

They provide information about the system at freeze-out such as energy density and size.

- signature observables i.e. observables which could serve as possible signatures for the phase transition to a QGP (e.g. dileptons, direct photons, J/ψ suppression, strangeness enhancement).

A brief synopsis of a few proposed signatures for the QGP follows.

1.5 Signatures of the QGP

Direct Photons

A photon produced in the QGP will leave the plasma with a probability much smaller than that of hadrons to interact and, would retain the memory of the plasma temperature. This makes it a good signature of the QGP provided it can be distinguished from photons produced by hadronic decays e.g. $\pi^0 \rightarrow 2\gamma$ and $\eta \rightarrow 3\pi^0 \rightarrow 6\gamma$. Since the pions are mainly radiated off the surface and photons are produced throughout the fireball, very heavy ion collisions may result in a fairly large n_γ/n_π ratio ($\simeq 0.2$ for e.g. uranium).

J/ψ Suppression

J/ψ consists of the bound pair $c\bar{c}$ and its production in the plasma can be detected via the decay into muon pairs i.e. $J/\psi \rightarrow \mu^+ + \mu^-$. Muons, like photons, have no strong interactions and thus, if they are produced in the QGP, will leave without interacting. The muons will also carry with them the memory of conditions in the plasma such as temperature. The suppression of J/ψ production had been predicted by Matsui and Satz [29] prior to any experimental data. They attributed this to the formation of a QGP which would have a strong colour field thereby inhibiting the attractive potential necessary for c and \bar{c} quarks to bind. Experimental results

from the NA38 experiment at CERN confirmed this prediction but alternative interpretations have been forwarded. These broadly fall into two categories namely, those which assume a QGP has been formed and, those which attribute the suppression to inelastic collisions of the J/ψ with extremely dense hadronic matter created in the collision.

Strangeness Enhancement

The enhancement of strange particles particularly strange antibaryon production in a QGP phase as opposed to the hadron gas phase hinges on the fact that the rate of strange pair production in the QGP via gluon fusion is faster than by hadronic processes in the hadron gas (a few fm/c as opposed to a few 10 to 100 fm/c). Strange phase space saturation thus proceeds much faster in the QGP.

Another distinguishing feature between a QGP and a hadron gas as far as strangeness neutrality goes is that strangeness conservation in a QGP requires a vanishing strange quark chemical potential i.e. $\mu_S = 0$ independent of temperature or baryon chemical potential, μ_B , while in a hadron gas strangeness neutrality depends on a variety of strange mesons and baryons all of whose abundances depend on μ_B [30].

In all experimental results both enhancement and $\mu_S = 0$ is obtained. It is found that an analysis using the QGP equations of state [31] describe the data better than a hadron gas description. However, the possibility of some other as yet unknown mechanism which would describe these features cannot be excluded.

1.6 The Future

Is a QGP formed? Today there is debate about the possible formation of this conjectured new phase of matter. The quest for the QGP is reaching a decisive phase with experimental evidence seemingly mounting in favour of its production. It is hoped that a new round of experiments at the CERN Large Hadron Collider (LHC) and at the Brookhaven Relativistic Heavy Ion Collider (RHIC) will provide the answers to many questions surrounding the search.

Chapter 2

Dynamic Fireball Model

The hadron gas model imbued with collective transverse and longitudinal flow provides the static Hagedorn model with additional features of internal consistency. It is compared with a stationary fireball model in terms of transverse mass and rapidity spectra.

Hadron gas models assume the production of a thermal system which expands until it reaches freeze-out at which point all the hadronic resonances decay into the lightest stable particles. It has been shown by Heinz *et al* [32] that a thermal picture which incorporates collective longitudinal and transverse flow gives excellent fits to the observed hadron spectra from $S + S$ collisions at CERN. An overview of these results are presented.

2.1 Longitudinal Flow

Evidence for longitudinal flow can be extracted from experimental data.

We begin with rapidity distributions. Experimentally, much broader than expected thermal rapidity distributions are obtained. This had prompted Hagedorn [33] to postulate a longitudinal flow velocity field (or a superposition of several thermal emitters moving with different velocities relative to the observer). The rapidity distribution of π^- as measured by NA35 is much wider than a stationary fireball picture, even with resonance decays, could predict. It thus appears from the data that the momentum distribution of the pions is influenced by the direction of the colliding nuclei. Thus an anisotropic momentum distribution results. This is explained very well by Bjorken's boost-invariant model [34] which is based on the inside-

outside cascade picture of secondary particle production. Although this has been formulated for asymptotically high energies it can be modified to beam energy by restricting η , the flow or boost angle, to the interval $(\eta_{\min}, \eta_{\max})$ [35]. This is done for the rapidity distribution which is then the integral over uniformly distributed thermal sources i.e.

$$\frac{dn}{dy}(y) = \int_{\eta_{\min}}^{\eta_{\max}} d\eta \frac{dn_{th}}{dy}(y - \eta) \quad (2.1)$$

Comparisons of: theoretical fits incorporating longitudinal flow, purely thermal fits and, data from NA35, are shown in Figure 2.1.

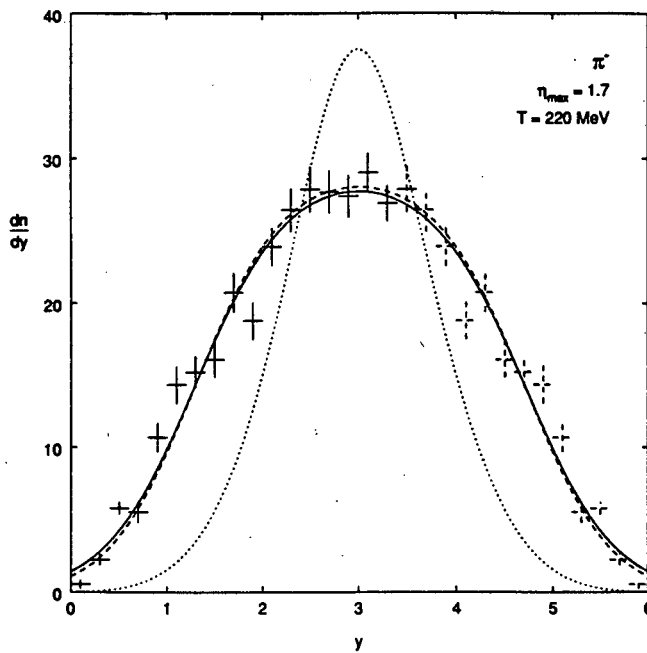


Figure 2.1: π^- y spectrum comparing fit from model containing longitudinal flow (solid line) with experimental data from NA35 (cross-hairs) and a purely thermal model (dotted line). The dashed line shows resonance decay contributions to the longitudinal flow model [32].

The value of $\eta_{\max} = 1.7$ for pions can be extracted from the rapidity distribution independent of the temperature. The same value for η_{\max} can also be obtained in this way for all produced particles (see Fig. 2.2). The protons are exceptional in that they still carry with them a large fraction of their initial beam energy.

Strange particles should also be a good indicator of collective flow since they are not present in the original nuclei but only produced later. This means that, unlike protons, they are

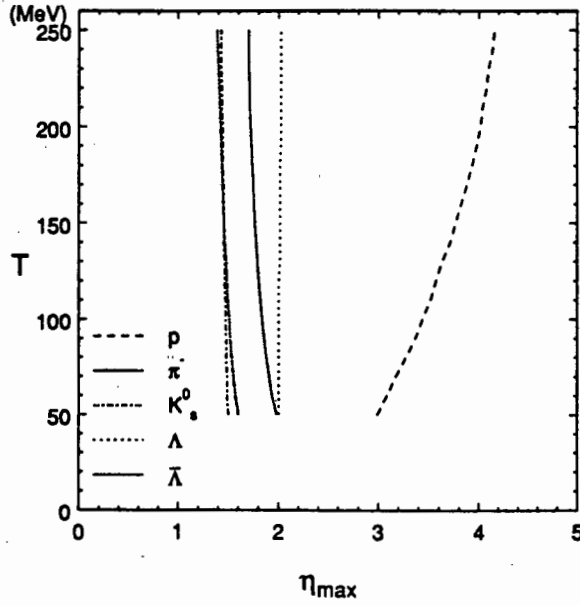


Figure 2.2: Extraction of η_{\max} from the rapidity distribution of hadrons [32].

uncontaminated by a cold spectator component. The exception could be the $\bar{\Lambda}$'s which may or may not retain some memory of the initial production process. This question has not been completely resolved. Because of their bigger mass, strange particles should also show a more accentuated flow component against random thermal motion as in the case of pions. This can be seen in the y spectrum of strange particles (Fig. 2.3).

2.2 Transverse Flow and m_T Scaling

As we have seen, longitudinal flow velocity influences the rapidity spectrum and shows very little sensitivity to the temperature (seen when determining $\eta_{\max} = 1.7$). The main effect of transverse flow on the other hand would be a flattening of the transverse mass spectrum and it is this we focus on.

The slope at large m_T for the transverse mass spectrum can be calculated analytically from expressions for the invariant momentum spectrum. The following expression for the slope is obtained:

$$\lim_{m_T \rightarrow 0} \frac{d}{dm_T} \ln \frac{dN}{dm_T^2} \approx \frac{1}{T} \sqrt{\frac{1 - v_T/c}{1 + v_T/c}} \equiv \frac{1}{T_{app}} \quad (2.2)$$

This can be interpreted in terms of an “apparent” or blueshifted temperature (T_{app}) in which thermal and flow effects are mixed. The total spectra can be seen as a superposition of spectra with different blueshift factors. With this in mind we can proceed to look at the effect of

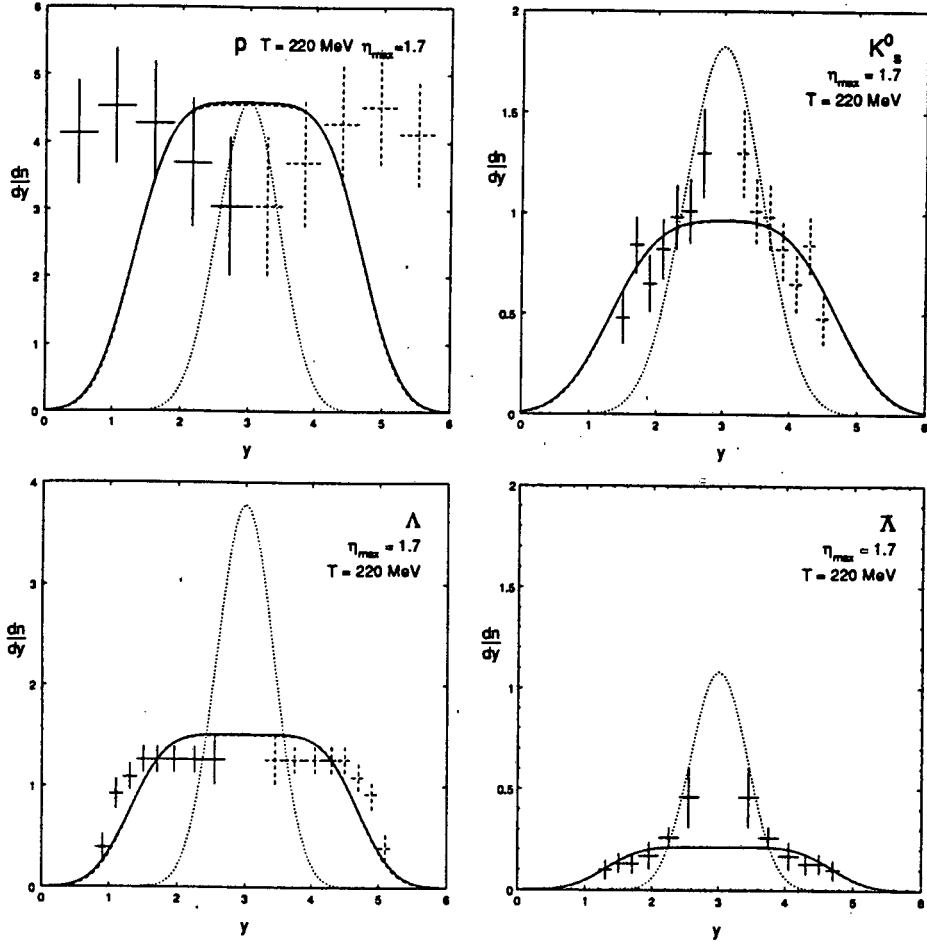


Figure 2.3: y spectrum of p , K^0 , Λ , and $\bar{\Lambda}$ with longitudinal flow in comparison with $S + S$ data from NA35 [32].

transverse flow on m_T scaling and, in particular, the flattening of the curve at low p_T .

At low p_T ($p_T < m$) visible distortions are seen in the momentum spectra from $Si + Au$ collisions at the Brookhaven AGS E802 collaboration (Fig. 2.4). This can also be seen in results from the E814 collaboration at the AGS. Assuming transverse flow, the flattening effect can be explained by a boost in the transverse momentum of emitted particles according to $p_T = p_T + mv_T$ as a result of collective flow. The peak of the Maxwell distribution shifts towards finite values of p_T leading to the flattening at low p_T . The effect becomes more pronounced with increasing mass. At high p_T ($p_T \gg m$) m_T scaling is recovered.

For the π^- m_T -spectrum (including resonance decays) a good fit at lower fireball temperatures is obtained with the data by using the theoretical model containing transverse flow.

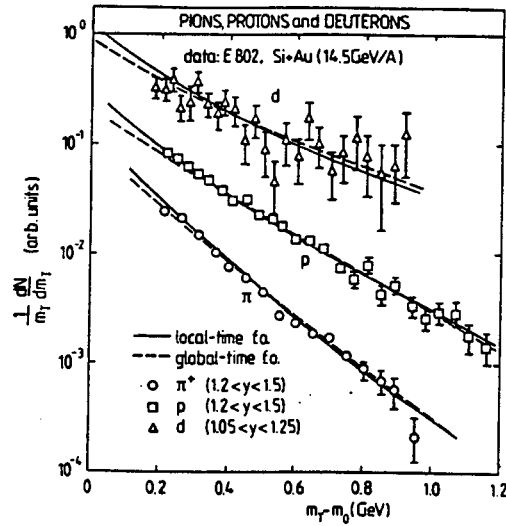
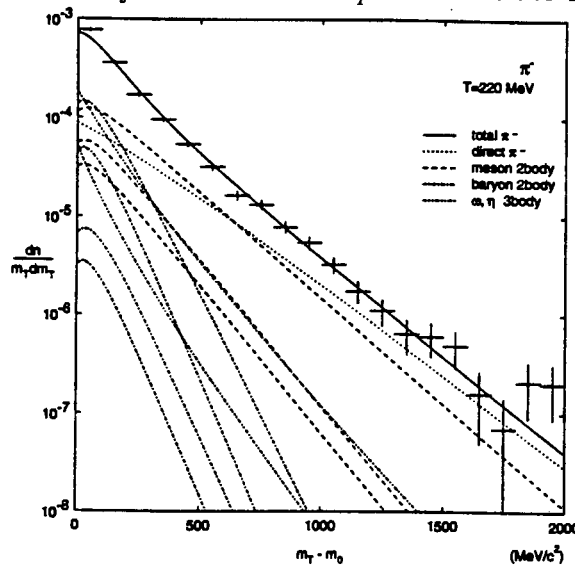


Figure 2.4: Comparison of the theoretical spectra with the E802 Si + Au data [32].

a)



b)

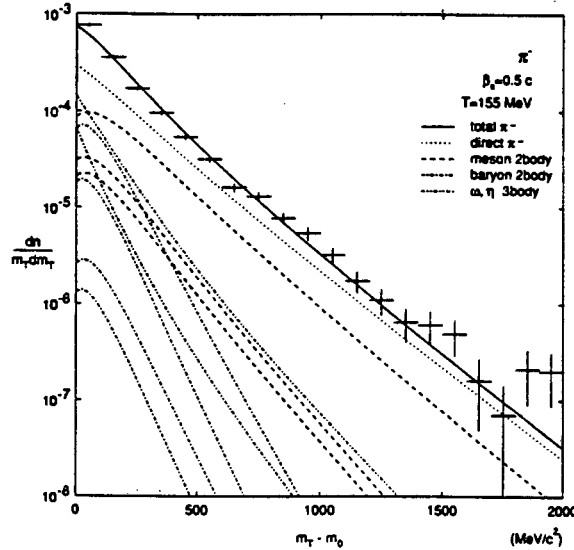


Figure 2.5: a) purely thermal π^- m_T -spectrum including resonance decays from a stationary fireball model and, b) the same spectrum generated using a transverse flow model. Both a) and b) are compared to the NA35 data [32].

2.3 Conclusion

A hadron gas model with collective flow provides good parametrization of observed $S+S$ hadron spectra at CERN. Evidence for transverse flow, however, remains largely circumstantial and a stronger confirmation of the tendencies attributed to flow phenomena needs to be established in the new round of really heavy ion collisions ($Au + Au$ or $Pb + Pb$) for collective flow to be placed on a firmer footing.

Chapter 3

The Hadron Gas Partition Function

The rapid development of hadronic gas models used in the description of relativistic heavy ion collisions is largely based on the hypothesis that the energy available in the collision of two such heavy nuclei is equipartitioned among the accessible degrees of freedom. It must be noted however that this does not necessarily imply the whole system participates in this thermalization [2].

In this chapter the methods of determining the total partition function for a hadronic gas, which tells us how the particles in the gas are partitioned or split between the different energy levels, are reviewed. Starting with the simple case of a gas consisting of fermions of a single species (particles and antiparticles e.g. protons and antiprotons) which possesses a conserved, additive quantum number (e.g. baryon number), other particles from the hadronic spectrum, such as pions, are gradually incorporated in the build up to a general formalism for the partition function. The methods presented here will be used in later chapters to obtain expressions for partition functions which contain up to three conserved quantum numbers and from which the expressions for particle number production in a thermalized hadronic gas will be derived. In this section we use baryon number as our conserved quantity to illustrate how the exact conservation of an additive quantum number influences the partition function.

3.1 For a Hadronic Gas with total Baryon number B

3.1.1 In the Canonical Ensemble

The partition function for the assemblies in a canonical ensemble is defined as

$$Z_C = \sum_i e^{-\epsilon_i/T} \quad (3.1)$$

where ϵ_i is the energy of the state denoted by i .

The above equation can be written in the following way to denote a gas with total baryon number, B , and, consisting only of protons and antiprotons:

$$\begin{aligned} Z_B &= \sum_i \langle i | e^{-\epsilon_i/T} | i \rangle \\ &= \text{Tr} \left[e^{-\frac{\hat{H}}{T}} \right] \\ &= \sum_{\text{all states}} e^{-\frac{1}{T} \{ \epsilon^0 n_p^0 + \epsilon^1 n_p^1 \dots + \epsilon^0 n_{\bar{p}}^0 + \epsilon^1 n_{\bar{p}}^1 + \dots \}} \end{aligned} \quad (3.2)$$

where the trace sums diagonal elements only.

We note that n_p and $n_{\bar{p}}$ equals the number of protons and antiprotons respectively and, $n_p^0 + n_p^1 + n_p^2 + \dots + n_p^\infty - n_{\bar{p}}^0 - n_{\bar{p}}^1 - n_{\bar{p}}^2 - \dots - n_{\bar{p}}^\infty = \text{Baryon number, } B$.

The partition function in equation 3.2 may be split into component parts and, may also be extended to include a gas containing pions as well. After doing this one obtains

$$\begin{aligned} Z_B &= \sum_{n_p^1=0}^{\infty} \frac{e^{-\epsilon_p^0 n_p^0/T}}{n_p^0!} \sum_{n_p^1=0}^{\infty} \frac{e^{-\epsilon_p^1 n_p^1/T}}{n_p^1!} \dots \sum_{n_p^\infty=0}^{\infty} \frac{e^{-\epsilon_p^\infty n_p^\infty/T}}{n_p^\infty!} \\ &\quad \sum_{n_{\bar{p}}^0=0}^{\infty} \frac{e^{-\epsilon_{\bar{p}}^0 n_{\bar{p}}^0/T}}{n_{\bar{p}}^0!} \dots \sum_{n_{\bar{p}}^1=0}^{\infty} \frac{e^{-\epsilon_{\bar{p}}^1 n_{\bar{p}}^1/T}}{n_{\bar{p}}^1!} \\ &\quad \sum_{n_\pi^0=0}^{\infty} \frac{e^{-\epsilon_\pi^0 n_\pi^0/T}}{n_\pi^0!} \dots \sum_{n_\pi^\infty=0}^{\infty} \frac{e^{-\epsilon_\pi^\infty n_\pi^\infty/T}}{n_\pi^\infty!} \end{aligned} \quad (3.3)$$

The division by $n!$ is necessary because in the product of summations, each term will occur $n!$ times. The product of sums in equation 3.3 may be evaluated by noting that $e^x = \sum_{n=0}^{\infty} \frac{x^n}{n!}$.

Therefore

$$\begin{aligned} Z_B &= \exp \left\{ e^{-\frac{\epsilon_p^0}{T}} \right\} \exp \left\{ e^{-\frac{\epsilon_p^1}{T}} \right\} \dots \exp \left\{ e^{-\frac{\epsilon_p^\infty}{T}} \right\} \\ &\quad \cdot \exp \left\{ e^{-\frac{\epsilon_{\bar{p}}^0}{T}} \right\} \exp \left\{ e^{-\frac{\epsilon_{\bar{p}}^1}{T}} \right\} \dots \exp \left\{ e^{-\frac{\epsilon_{\bar{p}}^\infty}{T}} \right\} \end{aligned}$$

$$\begin{aligned}
& \cdot \exp \left\{ e^{-\frac{\epsilon_0}{T}} \right\} \exp \left\{ e^{-\frac{\epsilon_1}{T}} \right\} \dots \exp \left\{ e^{-\frac{\epsilon_\infty}{T}} \right\} \\
= & \exp \left\{ \sum_{i=0}^{\infty} e^{-\frac{\epsilon_i}{T}} \right\} \exp \left\{ \sum_{i=0}^{\infty} e^{-\frac{\epsilon_i}{T}} \right\} \exp \left\{ \sum_{i=0}^{\infty} e^{-\frac{\epsilon_i}{T}} \right\} \\
& \text{sums over energy states}
\end{aligned} \tag{3.4}$$

The wave-function of a quantum mechanical system such as that described by equation 3.4 moving in free space is $\Psi = \Psi_o \exp i(k_x x + k_y y + k_z z)$ where the propagation constants are given by $k_x = \frac{2\pi}{\lambda_x} = \frac{2n\pi}{L_x}$, $k_y = \frac{2\pi}{\lambda_y} = \frac{2n\pi}{L_y}$ and $k_z = \frac{2\pi}{\lambda_z} = \frac{2n\pi}{L_z}$ [36]. In order to describe the partition function in the continuum limit we consider the system contained in a box with sides of length L_x , L_y and L_z , orientated along x, y and z coordinate axes respectively. In the thermodynamic limit we consider the limit as $V \rightarrow \infty$ therefore $L \rightarrow \infty$ so that, after applying boundary conditions, sums over single particle levels can be replaced by an integral over wavenumbers [36, 37, 38], i.e.

$$\sum \rightarrow g \int d^3 n = gV (2\pi)^{-3} \int d^3 k = gV \int \frac{d^3 p}{(2\pi)^3} \tag{3.5}$$

where g is the degeneracy of each single particle momentum state (g counts the respective independent degrees of freedom of particles) e.g. g is equal to 1 for spinless particles. Also note that in the continuum limit $\epsilon \rightarrow \sqrt{p^2 + m^2}$.

Therefore, for $V \rightarrow \infty$, equation 3.4 becomes

$$\begin{aligned}
Z_B &= \exp \left\{ V \int \frac{d^3 p}{(2\pi)^3} e^{-\frac{E_p}{T}} \right\} \\
&\cdot \exp \left\{ V \int \frac{d^3 p}{(2\pi)^3} e^{-\frac{E_{\bar{p}}}{T}} \right\} \\
&\cdot \exp \left\{ V \int \frac{d^3 p}{(2\pi)^3} e^{-\frac{E_{\pi}}{T}} \right\}
\end{aligned} \tag{3.6}$$

This equation corresponds to the case $B = 0$. In general however, we have $n_p = n_{\bar{p}} + B$.

Equation 3.5 holds well if the volume of a system is sufficiently large and the density of energy states is sufficiently high. For small volumes this integral approximation can be modified to take into account finite size correction effects via geometrical considerations and von Neumann(+) or Dirichlet(-) boundary conditions where + and - refers to the \pm in equation 3.7 respectively [39]. The resulting improvement is given below:

$$\sum \rightarrow g \int = \int \frac{V}{2\pi^2} k^2 dk \pm \frac{S}{8\pi} k dk + \frac{L}{8\pi} dk \tag{3.7}$$

V , S and L are the volume, surface and circumference of a sphere since spherical symmetry for the system is assumed. Thus, for a spherical volume, only one parameter for the system emerges namely, the radius.

The partition function may be further evaluated by including the following delta function i.e.

$$\delta_{n_p, n_{\bar{p}}+B} = \frac{1}{2\pi} \int_0^{2\pi} e^{i(n_p - n_{\bar{p}} - B)\psi} d\psi \quad (3.8)$$

Making use of the delta function, the partition function in equation 3.4 can thus be written as

$$Z_B = \int_0^{2\pi} d\psi e^{-iB\psi} \exp \left\{ \sum_{i=0}^{\infty} e^{i\psi - \frac{\epsilon_i}{T}} \right\} \exp \left\{ \sum_{i=0}^{\infty} e^{-i\psi - \frac{\epsilon_i}{T}} \right\} \exp \left\{ \sum_{i=0}^{\infty} e^{-\frac{\epsilon_i}{T}} \right\} \quad (3.9)$$

therefore

$$\begin{aligned} Z_B &= \frac{1}{2\pi} \int_0^{2\pi} d\psi e^{-iB\psi} \exp \left\{ V \int \frac{d^3p}{(2\pi)^3} e^{i\psi - \frac{E_p}{T}} \right\} \\ &\quad \cdot \exp \left\{ V \int \frac{d^3p}{(2\pi)^3} e^{-i\psi - \frac{E_{\bar{p}}}{T}} \right\} \\ &\quad \cdot \exp \left\{ V \int \frac{d^3p}{(2\pi)^3} e^{-\frac{E_{\pi}}{T}} \right\} \end{aligned} \quad (3.10)$$

Defining $V \int \frac{d^3p}{(2\pi)^3} e^{-\frac{E}{T}} = Z_1(T, V)$ (the single particle partition function), we obtain the following from equation 3.10

$$Z_B = \frac{1}{2\pi} \int_0^{2\pi} d\psi e^{-iB\psi} \exp \left\{ Z_1^p e^{i\psi} + Z_1^{\bar{p}} e^{-i\psi} + Z_1^{\pi} \right\} \quad (3.11)$$

For $B = 0$, equation 3.11 becomes

$$Z_{B=0} = \frac{1}{2\pi} \int_0^{2\pi} d\psi \exp \left\{ Z_1^p e^{i\psi} + Z_1^{\bar{p}} e^{-i\psi} + Z_1^{\pi} \right\} \quad (3.12)$$

Since $Z_1^p = Z_1^{\bar{p}}$, we can write $Z_1^p e^{i\psi} + Z_1^{\bar{p}} e^{-i\psi} = Z_1^p 2 \cos \psi$.

3.2 Including Baryons and Mesons

3.2.1 Adding Deltas

In general, for a gas containing nucleons and deltas in the canonical ensemble, we have

$$Z_B = \frac{1}{2\pi} \int_0^{2\pi} d\psi e^{-iB\psi} \exp \left\{ Z_1^N e^{i\psi} + Z_1^{\Delta} e^{i\psi} + Z_1^{\bar{N}} e^{-i\psi} + Z_1^{\bar{\Delta}} e^{i\psi} \right\}$$

$$\begin{aligned}
&= \frac{1}{2\pi} \int_0^{2\pi} d\psi e^{-iB\psi} \exp \left\{ \left(Z_1^N + Z_1^\Delta \right) e^{i\psi} + \left(Z_1^{\bar{N}} + Z_1^{\bar{\Delta}} \right) e^{-i\psi} \right\} \\
&= \frac{1}{2\pi} \int_0^{2\pi} d\psi e^{-iB\psi} \exp \left\{ \left(Z_1^{N,\Delta} \right) e^{i\psi} + \left(Z_1^{\bar{N},\bar{\Delta}} \right) e^{-i\psi} \right\}
\end{aligned} \tag{3.13}$$

where

$$\begin{aligned}
Z_1^{N,\Delta} &= Z_1^N + Z_1^\Delta \\
Z_1^{\bar{N},\bar{\Delta}} &= Z_1^{\bar{N}} + Z_1^{\bar{\Delta}} \\
Z_1^N &= Z_1^p + Z_1^n
\end{aligned}$$

and

$$Z_1^N = \underbrace{(2 \times 2)}_{\text{p,n spins}} \cdot V \int \frac{d^3 p}{(2\pi)^3} e^{-\frac{E}{T}}$$

3.2.2 Adding Mesons

Following from equation 3.13, we find that mesons may be included in a similar way i.e.

$$Z_{B+M} = \frac{1}{2\pi} \int_0^{2\pi} d\psi e^{-iB\psi} \exp \left\{ \left(Z_1^{N,\Delta} \right) e^{i\psi} + \left(Z_1^{\bar{N},\bar{\Delta}} \right) e^{-i\psi} + Z_1^M \right\} \tag{3.14}$$

with

$$Z_1^M = Z_1^\pi + Z_1^\varpi + Z_1^\rho + Z_1^\psi + \dots$$

3.3 General Formalism for a “Restricted Partition Function”

When imposing exact baryon number conservation what we are really interested in is a restricted partition function which satisfies the requirements of conserving only baryon number. This is obtained by restricting the statistical trace and hence the sum in equation 3.1 only to states which have the appropriate quantum numbers. One thus limits the amount of accessible states available to the system. This “restricting” process is essentially obtained by “slicing” in the correct factors using delta function representations. The delta functions thus exclude all unwanted states by forcing the sum to be performed only over states fulfilling a required quantum number configuration. An analysis [40] reveals that in the factor defined as the fugacity

namely; $\lambda = e^{\beta\mu}$ where $\beta = \frac{1}{T}$, $\beta\mu$ is replaced by the parametrization $i\psi$ ($0 < \psi < 2\pi$) from which follows a generating function for all restricted partition functions i.e.

$$Z_n = \frac{1}{2\pi} \int_0^{2\pi} d\psi e^{-in\psi} Z(\psi) \quad (3.15)$$

where

$$Z(\psi) = Z(\lambda = e^{i\psi}) = \text{Tr} \left[e^{-\beta\hat{H} + i\psi\hat{N}} \right] \quad (3.16)$$

Detailed derivations may also be found in [22, 41].

The symmetry group for additive quantum numbers, such as baryon number used in the previous examples and charge, which we encounter in the next chapter, is the abelian Lie group $U(1)$. The generalization of the partition function to include non-abelian symmetries has however been done, see [22, 23, 24].

The construction of a canonical partition function to include exact baryon number and strangeness conservation has been done by Hagedorn and Redlich [26] using group theoretical projection techniques based on the use of group characters. The form of this partition function is given below as:

$$Z_{B,S} = \frac{1}{2\pi} \int_0^{2\pi} d\phi e^{-iS\phi} \cdot \frac{1}{2\pi} \int_0^{2\pi} d\psi e^{-iB\psi} Z(T, V, \phi, \psi) \quad (3.17)$$

where ϕ represents the projection angle for strangeness. It can be seen that the above equation may be extended to include more conserved quantum numbers such as electric charge, charm and beauty.

3.4 Bessel Function Representation of Z

In the next chapter extensive use will be made of Bessel functions to rewrite the partition functions in “closed” form i.e. in terms of infinite sums over Bessel functions (the infinite sums arising from delta function representations which will be introduced). This form proves convenient for computer calculation of numerical results.

Use will be made of the following integral representation of the Bessel function of order B i.e.:

$$I_B(x) = \frac{1}{2\pi} \int_0^{2\pi} d\theta \exp(x \cos \theta) \exp(-iB\theta) \quad (3.18)$$

As a simple illustration we apply this to equation 3.12 for a proton-antiproton-pion gas. The partition function for this gas can thus be written as

$$Z_B = I_B (2Z^p) \exp Z^\pi \quad (3.19)$$

This section thus concludes our review of the hadron gas partition function the application of which will be extended in the next chapter.

Chapter 4

Exact Baryon, Strangeness, Charge Conservation

Up till now a maximum of two conserved quantities have been considered when formulating partition functions in studies of hadron gases. These have been baryon number and strangeness.

A third conserved quantity is now added.

In this chapter the work done by Cleymans, Redlich, Suhonen and others such as [42, 43, 44] describing particle production in hadronic gas systems obeying Maxwell-Boltzmann statistics for which strangeness and baryon number are exactly conserved, and, which contain particles with strangeness up to and including three, is extended to include exact charge conservation. Our restricted partition function thus has to be extended to incorporate an additional quantum number which, being additive, allows us to remain within the abelian Lie group $U(1)$.

In the first section we start by considering a gas consisting of particles having only charge as a quantum number (particles without baryon number or strangeness in this case) i.e. we consider a gas consisting of pions only. A proton-antiproton gas, which has baryon number and charge, is also discussed. In addition, a gas consisting of pions, neutrons and protons, is discussed in Appendix A.

In the second section the full hadronic spectrum is taken into account and the partition functions for the four cases examined, namely; a gas containing particles of $|strangeness| \leq 1$, $|strangeness| \leq 2$, $|strangeness| \leq 3$ and, $|strangeness| \leq 3, |charge| \leq 2$, are derived. The partition functions will then be used in the third section to obtain expressions for particle

number production in each of the four cases discussed.

A transformation from B, S, Q to B, S, I_3 where I_3 is the conserved quantum number of the z-component for isospin, will be discussed immediately after case one.

4.1 Simpler Cases of the Hadron Gas

4.1.1 A π^+ , π^- Gas

We start with the partition function restricted to charged pions i.e.

$$Z = \frac{1}{2\pi} \int_0^{2\pi} d\alpha. e^{-iQ\alpha} \exp \left\{ \frac{Z^\pi e^{i\alpha} + Z^\pi e^{-i\alpha}}{2Z^\pi \cos \alpha} \right\} \quad (4.1)$$

The angle α is used to label charge and Z^π is the single particle partition for pions. This equation may also be written in terms of a bessel function representation to yield the following equation in closed form

$$Z = I_Q (2Z^\pi) \quad (4.2)$$

The number of π^+ s and π^- s produced may be calculated by introducing a chemical potential μ for each charged state of pions, as one would in the grand canonical case, differentiating with respect to μ and, setting the chemical potential to zero according to the following:

$$\langle N \rangle = \left. \frac{T}{Z} \frac{\partial Z}{\partial \mu} \right|_{\mu=0}$$

After doing this, the following is obtained:

$$\begin{aligned} \langle N_{\pi^+} \rangle &= I_{Q-1} (2Z^\pi) / I_Q (2Z^\pi) \\ \langle N_{\pi^-} \rangle &= I_{Q+1} (2Z^\pi) / I_Q (2Z^\pi) \end{aligned} \quad (4.3)$$

If I_3 , the z-component of isospin, for the gas is zero overall (note: $Q = I_3 + \frac{B}{2}$, a point which will be discussed in detail later in the chapter), then $Q = 0$ (since $B = 0$). The expressions for the pion numbers thus become:

$$\begin{aligned} \langle N_{\pi^+} \rangle &= I_{-1} (2Z^\pi) / I_0 \\ \langle N_{\pi^-} \rangle &= I_{+1} (2Z^\pi) / I_0 \end{aligned} \quad (4.4)$$

We note that, since $I_{+1} = I_{-1}$ in general, the following is true: $\langle N_{\pi^+} \rangle = \langle N_{\pi^-} \rangle$ as one would expect in the special case of $I_3 = 0$ above.

4.1.2 A Proton-Antiproton Gas

The partition function for a proton-antiproton gas is given by

$$Z = \frac{1}{(2\pi)^2} \int_0^{2\pi} d\psi \exp(-iB\psi) \int_0^{2\pi} d\alpha \exp(-iQ\alpha) \cdot \exp \left(Z^p \left(\underbrace{\exp(i(\psi + \alpha))}_{\text{proton}} + \underbrace{\exp(-i(\psi + \alpha))}_{\text{antiproton}} \right) \right) \quad (4.5)$$

The angles ψ and α are used to label baryon number and charge respectively. The angles may also be “decoupled” so that equation 4.5 can be written as

$$Z = \underbrace{\frac{1}{2\pi} \int_0^{2\pi} d\psi \exp(-i(B + n_{\text{proton}})\psi)}_{\delta_{-B-n_{\text{proton}}}} \cdot \underbrace{\frac{1}{2\pi} \int_0^{2\pi} d\alpha \exp(-i(Q + n_{\text{proton}})\alpha)}_{\delta_{-Q-n_{\text{proton}}}} \cdot \frac{1}{2\pi} \int_0^{2\pi} d\gamma \exp \left(2Z^p \cos \underbrace{(\psi + \alpha)}_{=\gamma} \right) \exp(-i(-n_{\text{proton}})\gamma) \quad (4.6)$$

Therefore

$$\begin{aligned} Z &= \sum_{n_{\text{proton}}=-\infty}^{\infty} I_{-n} (2Z^p) \delta_{-B-n_{\text{proton}}} \delta_{-Q-n_{\text{proton}}} \\ &= \sum_{n_{\text{proton}}=-\infty}^{\infty} I_{B+Q+n} (2Z^p) \end{aligned} \quad (4.7)$$

Finding proton and antiproton numbers using the same method as we did for the pions, the following expressions are obtained:

$$\begin{aligned} \langle N_p \rangle &= \frac{1}{Z} \sum_{n_p=-\infty}^{\infty} I_{B+Q+n_{\text{proton}}-2} (2Z^p) \\ \langle N_{\bar{p}} \rangle &= \frac{1}{Z} \sum_{n_p=-\infty}^{\infty} I_{B+Q+n_{\text{proton}}+2} (2Z^p) \end{aligned} \quad (4.8)$$

4.2 The Complete Hadronic Partition Function

4.2.1 Case 1: Baryon number = 0,±1, Strangeness = 0,±1, Charge = 0,±1

Starting with the basic integral as presented by Hagedorn and Redlich [26] with the angle ψ labelling the baryons, ϕ labelling the strange particles and, introducing the angle α to label charge, one has for the canonical partition function assuming Boltzmann statistics:

$$\begin{aligned}
Z_{B,S,Q}^1(T,V) = & \frac{1}{(2\pi)^3} \int_0^{2\pi} d\phi \exp(-iS\phi) \int_0^{2\pi} d\psi \exp(-iB\psi) \int_0^{2\pi} d\alpha \exp(-iQ\alpha) \\
& \cdot \exp(Z^{\pi^0}) \\
& \cdot \exp(Z^{K^0} (\exp(i\phi) + \exp(-i\phi))) \\
& \cdot \exp(Z^n (\exp(i\psi) + \exp(-i\psi))) \\
& \cdot \exp(Z^{\pi^\pm} (\exp(i\alpha) + \exp(-i\alpha))) \\
& \cdot \exp(Z^{\Lambda^0} (\exp i(\psi - \phi) + \exp(-i(\psi - \phi)))) \\
(*) & \cdot \exp(Z (\exp(i(\psi + \phi)) + \exp(-i(\psi + \phi)))) \\
& \cdot \exp(Z^{K^\pm} (\exp(i(\phi + \alpha)) + \exp(-i(\phi + \alpha)))) \\
(*) & \cdot \exp(Z (\exp(i(\phi - \alpha)) + \exp(-i(\phi - \alpha)))) \\
& \cdot \exp(Z^p (\exp(i(\psi + \alpha)) + \exp(-i(\psi + \alpha)))) \\
& \cdot \exp(Z^{\Delta^-} (\exp(i(\psi - \alpha)) + \exp(-i(\psi - \alpha)))) \\
(*) & \cdot \exp(Z (\exp(i(\phi + \psi + \alpha)) + \exp(-i(\phi + \psi + \alpha)))) \\
& \cdot \exp(Z^{\Sigma^+} (\exp(i(-\phi + \psi + \alpha)) + \exp(-i(-\phi + \psi + \alpha)))) \\
& \cdot \exp(Z^{\Sigma^-} (\exp(i(-\phi + \psi - \alpha)) + \exp(-i(-\phi + \psi - \alpha)))) \\
(*) & \cdot \exp(Z (\exp(i(\phi + \psi - \alpha)) + \exp(-i(\phi + \psi - \alpha)))) \tag{4.9}
\end{aligned}$$

In the notation for the partition function viz., $Z_{B,S,Q}^1$, the superscript 1 refers to a gas in which the strangeness of the constituent particles do not exceed $|strangeness| = 1$ and, the subscripts B , S and Q imply that net baryon number(B), strangeness(S) and charge are conserved(Q). Single particle partition functions for various particles are given by $Z^{particle}$.

The various combinations in which baryon number, strangeness and charge can occur for case 1, together with the corresponding particles for each combination, are shown in table 4.1. The combinations labelled by (*) in equation 4.9 do not occur in nature and will therefore be omitted from subsequent calculations. The pairwise contributions of particles and antiparticles will give rise to the cosine of the angles.

The partition function can thus be written as

$$\begin{aligned}
Z_{B,S,Q}^1(T,V) = & \frac{1}{(2\pi)^3} \int_0^{2\pi} d\phi \exp(-iS\phi) \int_0^{2\pi} d\psi \exp(-iB\psi) \int_0^{2\pi} d\alpha \exp(-iQ\alpha) \\
& \cdot \exp[2Z^{K^0} \cos \phi + 2Z^n \cos \psi + 2Z^{\pi^\pm} \cos \alpha + 2Z^{\Lambda^0} \cos(\psi - \phi) \\
& + 2Z^{K^\pm} \cos(\phi + \alpha) + 2Z^p \cos(\psi + \alpha) + 2Z^{\Delta^-} \cos(\psi - \alpha) \\
& + 2Z^{\Sigma^+} \cos(-\phi + \psi + \alpha) + 2Z^{\Sigma^-} \cos(-\phi + \psi - \alpha)] \cdot \exp(Z^{\pi^0}) \quad (4.10)
\end{aligned}$$

Introducing ones in the form of delta functions allow the decoupling of the angles ϕ , ψ , and α which would otherwise prevent the integral from being solved analytically for the case where strangeness is plus/minus two, three or four.

Using the following (Fourier) representation of the delta function:

$$\delta(x) = \frac{1}{2\pi} \sum_{n=-\infty}^{\infty} \exp(inx)$$

and, introducing

$$\int \delta(x) dx = 1$$

allows one to write

$$\int \delta(x) dx = \frac{1}{2\pi} \sum_{n=-\infty}^{\infty} \int_0^{2\pi} \exp(inx) dx = 1$$

Choosing the variable x to be λ , κ , γ , δ^- , σ^+ , and σ^- respectively, where

$$\lambda = \psi - \phi$$

$$\kappa = \phi + \alpha$$

$$\gamma = \psi + \alpha$$

$$\delta^- = \psi - \alpha$$

$$\sigma^+ = -\phi + \psi + \alpha$$

$$\sigma^- = -\phi + \psi - \alpha$$

we obtain the following

$$\begin{aligned}
\int \delta(\lambda - \psi + \phi) d\lambda &= \frac{1}{2\pi} \sum_{n_\lambda=-\infty}^{\infty} \int_0^{2\pi} \exp(in_\lambda(\lambda - \psi + \phi)) d\lambda \\
\int \delta(\kappa - \phi - \alpha) d\kappa &= \frac{1}{2\pi} \sum_{n_\kappa=-\infty}^{\infty} \int_0^{2\pi} \exp(in_\kappa(\kappa - \phi - \alpha)) d\kappa \\
\int \delta(\gamma - \psi - \alpha) d\gamma &= \frac{1}{2\pi} \sum_{n_\gamma=-\infty}^{\infty} \int_0^{2\pi} \exp(in_\gamma(\gamma - \psi - \alpha)) d\gamma \\
\int \delta(\delta^- - \psi + \alpha) d\delta^- &= \frac{1}{2\pi} \sum_{n_{\delta^-}=-\infty}^{\infty} \int_0^{2\pi} \exp(in_{\delta^-}(\delta^- - \psi + \alpha)) d\delta^- \\
\int \delta(\sigma^+ + \phi - \psi - \alpha) d\sigma^+ &= \frac{1}{2\pi} \sum_{n_{\sigma^+}=-\infty}^{\infty} \int_0^{2\pi} \exp(in_{\sigma^+}(\sigma^+ + \phi - \psi - \alpha)) d\sigma^+ \\
\int \delta(\sigma^- + \phi - \psi + \alpha) d\sigma^- &= \frac{1}{2\pi} \sum_{n_{\sigma^-}=-\infty}^{\infty} \int_0^{2\pi} \exp(in_{\sigma^-}(\sigma^- + \phi - \psi + \alpha)) d\sigma^-
\end{aligned}$$

therefore

$$\begin{aligned}
Z_{B,S,Q}^1(T, V) &= \frac{1}{(2\pi)^3} \int_0^{2\pi} d\phi \exp(-iS\phi) \int_0^{2\pi} d\psi \exp(-iB\psi) \int_0^{2\pi} d\alpha \exp(-iQ\alpha) \\
&\cdot \exp[2Z^{K^0} \cos \phi + 2Z^n \cos \psi + 2Z^{\pi^\pm} \cos \alpha + 2Z^{\Lambda^0} \cos(\psi - \phi) \\
&+ 2Z^{K^\pm} \cos(\phi + \alpha) + 2Z^p \cos(\psi + \alpha) + 2Z^{\Delta^-} \cos(\psi - \alpha) \\
&+ 2Z^{\Sigma^+} \cos(-\phi + \psi + \alpha) + 2Z^{\Sigma^-} \cos(-\phi + \psi - \alpha)] \exp(Z^{\pi^0}) \\
&\cdot \frac{1}{2\pi} \sum_{n_\lambda=-\infty}^{\infty} \int_0^{2\pi} \exp(in_\lambda(\lambda - \psi + \phi)) d\lambda \\
&\cdot \frac{1}{2\pi} \sum_{n_\kappa=-\infty}^{\infty} \int_0^{2\pi} \exp(in_\kappa(\kappa - \phi - \alpha)) d\kappa \\
&\cdot \frac{1}{2\pi} \sum_{n_\gamma=-\infty}^{\infty} \int_0^{2\pi} \exp(in_\gamma(\gamma - \psi - \alpha)) d\gamma \\
&\cdot \frac{1}{2\pi} \sum_{n_{\delta^-}=-\infty}^{\infty} \int_0^{2\pi} \exp(in_{\delta^-}(\delta^- - \psi + \alpha)) d\delta^- \\
&\cdot \frac{1}{2\pi} \sum_{n_{\sigma^+}=-\infty}^{\infty} \int_0^{2\pi} \exp(in_{\sigma^+}(\sigma^+ + \phi - \psi - \alpha)) d\sigma^+ \\
&\cdot \frac{1}{2\pi} \sum_{n_{\sigma^-}=-\infty}^{\infty} \int_0^{2\pi} \exp(in_{\sigma^-}(\sigma^- + \phi - \psi + \alpha)) d\sigma^- \tag{4.11}
\end{aligned}$$

Making use of the delta functions to decouple the angles for each combination of quantum numbers i.e. for each set of particles subscribing to a particular set of quantum numbers, one

has for the partition function

$$\begin{aligned}
Z_{B,S,Q}^1(T,V) = & \sum_{n_\lambda=-\infty}^{\infty} \sum_{n_\kappa=-\infty}^{\infty} \sum_{n_\gamma=-\infty}^{\infty} \sum_{n_{\delta^-}=-\infty}^{\infty} \sum_{n_{\sigma^+}=-\infty}^{\infty} \sum_{n_{\sigma^-}=-\infty}^{\infty} \\
& \left\{ \frac{1}{2\pi} \int_0^{2\pi} \exp(2Z^{K^0} \cos \phi) \exp(-i(S - n_\lambda + n_\kappa - n_{\sigma^+} - n_{\sigma^-}) \phi) d\phi \right. \\
& \cdot \frac{1}{2\pi} \int_0^{2\pi} \exp(2Z^n \cos \psi) \exp(-i(B + n_\lambda + n_\gamma + n_{\delta^-} + n_{\sigma^+} + n_{\sigma^-}) \psi) d\psi \\
& \cdot \frac{1}{2\pi} \int_0^{2\pi} \exp(2Z^{\pi^\pm} \cos \alpha) \exp(-i(Q + n_\kappa + n_\gamma - n_{\delta^-} + n_{\sigma^+} - n_{\sigma^-}) \alpha) d\alpha \\
& \cdot \frac{1}{2\pi} \int_0^{2\pi} \exp(2Z^{\Lambda^0} \cos \lambda) \exp(-i(-n_\lambda) \lambda) d\lambda \\
& \cdot \frac{1}{2\pi} \int_0^{2\pi} \exp(2Z^{K^\pm} \cos \kappa) \exp(-i(-n_\kappa) \kappa) d\kappa \\
& \cdot \frac{1}{2\pi} \int_0^{2\pi} \exp(2Z^p \cos \gamma) \exp(-i(-n_\gamma) \gamma) d\gamma \\
& \cdot \frac{1}{2\pi} \int_0^{2\pi} \exp(2Z^{\Delta^-} \cos \delta^-) \exp(-i(-n_{\delta^-}) \delta^-) d\delta^- \\
& \cdot \frac{1}{2\pi} \int_0^{2\pi} \exp(2Z^{\Sigma^+} \cos \delta^-) \exp(-i(-n_{\sigma^+}) \sigma^+) d\sigma^+ \\
& \cdot \frac{1}{2\pi} \int_0^{2\pi} \exp(2Z^{\Sigma^-} \cos \sigma^-) \exp(-i(-n_{\sigma^-}) \sigma^-) d\sigma^- \\
& \cdot \exp(Z^{\pi^0}) \left. \right\} \tag{4.12}
\end{aligned}$$

The deltas will be taken out at this stage to maintain isospin symmetry and re-included in case 4 with their isospin symmetric partner in the baryon decuplet, the Δ^{++} .

Using the following integral representation of the Bessel function of order B :

$$I_B(x) = \frac{1}{2\pi} \int_0^{2\pi} d\theta \exp(x \cos \theta) \exp(-iB\theta)$$

allows one to write the partition function in terms of bessel functions in the following closed form

$$\begin{aligned}
Z_{B,S,Q}^1(T,V) = & \left\{ \sum_{n_\lambda=-\infty}^{\infty} \sum_{n_\kappa=-\infty}^{\infty} \sum_{n_\gamma=-\infty}^{\infty} \sum_{n_{\sigma^+}=-\infty}^{\infty} \sum_{n_{\sigma^-}=-\infty}^{\infty} I_{S-n_\lambda+n_\kappa-n_{\sigma^+}-n_{\sigma^-}}(2Z^{K^0}) \right. \\
& \cdot I_{B+n_\lambda+n_\gamma+n_{\sigma^+}+n_{\sigma^-}}(2Z^n) I_{Q+n_\kappa+n_\gamma+n_{\sigma^+}-n_{\sigma^-}}(2Z^{\pi^\pm}) I_{-n_\lambda}(2Z^{\Lambda^0}) \\
& \cdot I_{-n_\kappa}(2Z^{K^\pm}) I_{-n_\gamma}(2Z^p) I_{-n_{\sigma^+}}(2Z^{\Sigma^+}) I_{-n_{\sigma^-}}(2Z^{\Sigma^-}) \left. \right\} \\
& \cdot \exp(Z^{\pi^0}) \tag{4.13}
\end{aligned}$$

where the net baryon number, strangeness and charge are given by B , S , and Q respectively.

4.2.2 Transforming from B, S, Q , to B, S, I_3

In nuclei-nuclei collisions of high baryon number content and high charge content (e.g. Sulphur on Sulphur where $B(\text{sulphur}) = 32$ and $Q(\text{sulphur}) = 16$), we consider whether it becomes useful for computational purposes to change from B, S, Q to B, S, I_3 where I_3 is the conserved quantum number for the z-component of isospin. This involves a transformation from Q to I_3 according to the following prescription

$$\frac{Q}{e} = \frac{B}{2} + \frac{S}{2} + I_3$$

(Gell-Mann 1953, Nishijima 1955) [45, 46]

i.e.

$$I_3 = Q - \frac{B + S}{2}$$

For Sulphur on Sulphur for instance, this means a change from $B = 32, S = 0$ and $Q = 16$ to $B = 32, S = 0$ and $I_3 = 0$. We thus investigate whether in the closed form of the expressions for the partition functions and the ensuing expressions for the particle numbers, a lower order of bessel functions will result which, in computational terms, could mean less strain in the calculation of those bessel functions containing Q as an index.

The conversions from Q to I_3 for the different physically possible combinations in all four cases, are summarized in table 4.1.

The angle α will now be used to label I_3 and ϕ and ψ are changed to ϕ' and ψ' respectively to accommodate the inclusion of isospin since there will be no particles of “pure” strangeness or “pure” baryon number without possessing isospin as well. The question remains whether this transformation will make it numerically easier to calculate the bessel functions. It is shown in Appendix B that the procedure does not in fact help since Q will be replaced by $I_3 + B + S$ in the integral representations which will have limits of integration going from 0 to π . Thus, computationally, nothing would be gained in the transformation.

Table 4.1: Table showing z-component of isospin assignments for particles decaying by the weak or electromagnetic interactions

B	S	Q	I_3						
			$-\frac{3}{2}$	-1	$-\frac{1}{2}$	0	$+\frac{1}{2}$	+1	$+\frac{3}{2}$
0	0	0				π^0, η			
0	0	∓ 1		π^-				π^+	
1	0	0			n, Δ^0				
1	0	1					p, Δ^+		
1	0	-1	Δ^-						
1	0	2							Δ^{++}
1	-1	0				Λ^0, Σ^0			
1	-1	-1		Σ^-					
1	-1	1						Σ^+	
0	∓ 1	∓ 1			K^-		K^+		
0	1	0			K^0				
1	-2	0					Ξ^0		
1	-2	-1			Ξ^-				
1	-3	-1				Ω^-			

4.2.3 Case 2: Baryon number = 0, ± 1 , Strangeness = 0, $\pm 1, \pm 2$, Charge = 0, ± 1

In this case one includes the Ξ and $\bar{\Xi}$ particles which have strangeness ∓ 2 respectively. The Z^Ξ terms in the partition function contain the 2ϕ angle for $|\text{strangeness}| = 2$ and the angle α for charge.

Making the above inclusions, the partition function in its integral form may thus be written as

$$\begin{aligned}
Z_{B,S,Q}^2(T,V) = & \frac{1}{(2\pi)^3} \int_0^{2\pi} d\phi \exp(-iS\phi) \int_0^{2\pi} d\psi \exp(-iB\psi) \int_0^{2\pi} d\alpha \exp(-iQ\alpha) \\
& \cdot \exp[2Z^{K^0} \cos \phi + 2Z^n \cos \psi + 2Z^{\pi^\pm} \cos \alpha + 2Z^{\Lambda^0} \cos \lambda \\
& + 2Z^{K^\pm} \cos \kappa + 2Z^p \cos \gamma + 2Z^{\Sigma^+} \cos \sigma^+ \\
& + 2Z^{\Sigma^-} \cos \sigma^- + 2Z^{\Xi^0} \cos(\psi - 2\phi) \\
& + 2Z^{\Xi^-} \cos(\psi - 2\phi - \alpha)] \exp(Z^{\pi^0})
\end{aligned} \tag{4.14}$$

Introducing the variables ξ for Ξ^0 and ξ^- for Ξ^- , we obtain

$$\begin{aligned}\xi &= \psi - 2\phi \\ \xi^- &= \psi - 2\phi - \alpha\end{aligned}$$

Two additional delta functions may thus be introduced namely;

$$\begin{aligned}\int \delta(\xi - \psi + 2\phi) d\xi &= \frac{1}{2\pi} \sum_{n_\xi=-\infty}^{\infty} \int_0^{2\pi} \exp(in_\xi(\xi - \psi + 2\phi)) d\xi \\ \int \delta(\xi^- - \psi + 2\phi + \alpha) d\xi^- &= \frac{1}{2\pi} \sum_{n_{\xi^-}=-\infty}^{\infty} \int_0^{2\pi} \exp(in_{\xi^-}(\xi^- - \psi + 2\phi + \alpha)) d\xi^-\end{aligned}$$

Using the delta functions with variables ranging from λ to ξ^- in the usual way to decouple the angles, one obtains

$$\begin{aligned}Z_{B,S,Q}^2(T,V) &= \sum_{n_\lambda=-\infty}^{\infty} \sum_{n_\kappa=-\infty}^{\infty} \sum_{n_\gamma=-\infty}^{\infty} \sum_{n_{\sigma^+}=-\infty}^{\infty} \sum_{n_{\sigma^-}=-\infty}^{\infty} \sum_{n_\xi=-\infty}^{\infty} \sum_{n_{\xi^-}=-\infty}^{\infty} \\ &\cdot \left\{ \frac{1}{2\pi} \int_0^{2\pi} \exp(2Z^{K^0} \cos \phi) \right. \\ &\cdot \exp(-i(S - n_\lambda + n_\kappa - n_{\sigma^+} - n_{\sigma^-} - 2n_\xi - 2n_{\xi^-})\phi) d\phi \\ &\frac{1}{2\pi} \int_0^{2\pi} \exp(2Z^n \cos \psi) \\ &\cdot \exp(-i(B + n_\lambda + n_\gamma + n_{\sigma^+} + n_{\sigma^-} + n_\xi + n_{\xi^-})\psi) d\psi \\ &\frac{1}{2\pi} \int_0^{2\pi} \exp(2Z^{\pi^\pm} \cos \alpha) \\ &\cdot \exp(-i(Q + n_\kappa + n_\gamma + n_{\sigma^+} - n_{\sigma^-} - n_{\xi^-})\alpha) d\alpha \\ &\frac{1}{2\pi} \int_0^{2\pi} \exp(2Z^{\Lambda^0} \cos \lambda) \exp(-i(-n_\lambda)\lambda) d\lambda \\ &\frac{1}{2\pi} \int_0^{2\pi} \exp(2Z^{K^\pm} \cos \kappa) \exp(-i(-n_\kappa)\kappa) d\kappa \\ &\frac{1}{2\pi} \int_0^{2\pi} \exp(2Z^P \cos \gamma) \exp(-i(-n_\gamma)\gamma) d\gamma \\ &\frac{1}{2\pi} \int_0^{2\pi} \exp(2Z^{\Sigma^+} \cos \sigma^+) \exp(-i(-n_{\sigma^+})\sigma^+) d\sigma^+ \\ &\frac{1}{2\pi} \int_0^{2\pi} \exp(2Z^{\Sigma^-} \cos \sigma^-) \exp(-i(-n_{\sigma^-})\sigma^-) d\sigma^- \\ &\frac{1}{2\pi} \int_0^{2\pi} \exp(2Z^{\Xi^0} \cos \xi) \exp(-i(-n_\xi)\xi) d\xi \\ &\left. \frac{1}{2\pi} \int_0^{2\pi} \exp(2Z^{\Xi^-} \cos \xi^-) \exp(-i(-n_{\xi^-})\xi^-) d\xi^- \right\} \cdot \exp(Z^{\pi^0}) \quad (4.15)\end{aligned}$$

which, in closed form reads

$$\begin{aligned}
Z_{B,S,Q}^2(T,V) = & \left\{ \sum_{n_\lambda=-\infty}^{\infty} \sum_{n_\kappa=-\infty}^{\infty} \sum_{n_\gamma=-\infty}^{\infty} \sum_{n_{\sigma^+}=-\infty}^{\infty} \sum_{n_{\sigma^-}=-\infty}^{\infty} \sum_{n_\xi=-\infty}^{\infty} \sum_{n_{\xi^-}=-\infty}^{\infty} \right. \\
& I_{S-n_\lambda+n_\kappa-n_{\sigma^+}-n_{\sigma^-}-2n_\xi-2n_{\xi^-}} (2Z^{K^0}) I_{B+n_\lambda+n_\gamma+n_{\sigma^+}+n_{\sigma^-}+n_\xi+n_{\xi^-}} (2Z^n) \\
& I_{Q+n_\kappa+n_\gamma+n_{\sigma^+}-n_{\sigma^-}-n_{\xi^-}} (2Z^{\pi^\pm}) I_{-n_\lambda} (2Z^{\Lambda^0}) I_{-n_\kappa} (2Z^{K^\pm}) \\
& I_{-n_\gamma} (2Z^p) I_{-n_{\sigma^+}} (2Z^{\Sigma^+}) I_{-n_{\sigma^-}} (2Z^{\Sigma^-}) I_\xi (2Z^{\Xi^0}) \\
& \left. I_{-n_{\xi^-}} (2Z^{\Xi^-}) \right\} \cdot \exp(Z^{\pi^0}) \tag{4.16}
\end{aligned}$$

4.2.4 Case 3: Baryon number = 0, ±1, Strangeness = 0, ±1, ±2, ±3, Charge = 0, ±1

In case 3 we include the Ω and $\bar{\Omega}$ particles which have strangeness ± 3 respectively. The Z^{Ω^-} term in the partition function contains the 3ϕ angle for $|\text{strangeness}| = 3$.

From first principles one has

$$\begin{aligned}
Z_{B,S,Q}^3(T,V) = & \frac{1}{(2\pi)^3} \int_0^{2\pi} d\phi \exp(-iS\phi) \int_0^{2\pi} d\psi \exp(-iB\psi) \int_0^{2\pi} d\alpha \exp(-iQ\alpha) \\
& \cdot \exp[2Z^{K^0} \cos \phi + 2Z^n \cos \psi + 2Z^{\pi^\pm} \cos \alpha + 2Z^{\Lambda^0} \cos \lambda \\
& + 2Z^{K^\pm} \cos \kappa + 2Z^p \cos \gamma + 2Z^{\Sigma^+} \cos \sigma^+ \\
& + 2Z^{\Sigma^-} \cos \sigma^- + 2Z^{\Xi^0} \cos \xi + 2Z^{\Xi^-} \cos \xi^- \\
& + 2Z^{\Omega^-} \cos(-3\phi + \psi - \alpha)] \exp(Z^{\pi^0}) \tag{4.17}
\end{aligned}$$

A delta function with the variable ω may be written as

$$\int \delta(\omega + 3\phi - \psi + \alpha) d\omega = \frac{1}{2\pi} \sum_{n_\omega=-\infty}^{\infty} \int_0^{2\pi} \exp(in_\omega(\omega + 3\phi - \psi + \alpha)) d\omega$$

Using the all the delta functions derived thusfar, one obtains in closed form

$$\begin{aligned}
Z_{B,S,Q}^3(T,V) = & \left\{ \sum_{n_\lambda=-\infty}^{\infty} \sum_{n_\kappa=-\infty}^{\infty} \sum_{n_\gamma=-\infty}^{\infty} \sum_{n_{\sigma^+}=-\infty}^{\infty} \sum_{n_{\sigma^-}=-\infty}^{\infty} \sum_{n_\xi=-\infty}^{\infty} \sum_{n_{\xi^-}=-\infty}^{\infty} \sum_{n_\omega=-\infty}^{\infty} \right. \\
& I_{S-n_\lambda+n_\kappa-n_{\sigma^+}-n_{\sigma^-}-2n_\xi-2n_{\xi^-}-3n_\omega} (2Z^{K^0}) \\
& I_{B+n_\lambda+n_\gamma+n_{\sigma^+}+n_{\sigma^-}+n_\xi+n_{\xi^-}+n_\omega} (2Z^n) \\
& \left. I_{Q+n_\kappa+n_\gamma+n_{\sigma^+}-n_{\sigma^-}-n_{\xi^-}-n_\omega} (2Z^{\pi^\pm}) I_{-n_\lambda} (2Z^{\Lambda^0}) I_{-n_\kappa} (2Z^{K^\pm}) \right\}
\end{aligned}$$

$$\begin{aligned}
& I_{-n_\gamma} (2Z^p) I_{-n_{\sigma^+}} (2Z^{\Sigma^+}) I_{-n_{\sigma^-}} (2Z^{\Sigma^-}) I_{-n_\xi} (2Z^{\Xi^0}) \\
& I_{-n_{\xi^-}} (2Z^{\Xi^-}) I_{-n_\omega} (2Z^{\Omega^-}) \} \cdot \exp(Z^{\pi^0}) \quad (4.18)
\end{aligned}$$

4.2.5 Case 4: Baryon number = 0, ±1, Strangeness = 0, ±1, ±2, ±3, Charge = 0, ±1, ±2

This is perhaps the most complete case since at this stage all the particles of the hadronic spectrum may be included. The Δ^{++} and $\overline{\Delta}^{++}$ particles which have strangeness 0 and charge ± 2 , are thus included and, the Δ^- is re-included.

The partition function may therefore be written from first principles as

$$\begin{aligned}
Z_{B,S,Q}^3(T, V) &= \frac{1}{(2\pi)^3} \int_0^{2\pi} d\phi \exp(-iS\phi) \int_0^{2\pi} d\psi \exp(-iB\psi) \int_0^{2\pi} d\alpha \exp(-iQ\alpha) \\
&\cdot \exp[2Z^{K^0} \cos \phi + 2Z^n \cos \psi + 2Z^{\pi^\pm} \cos \alpha + 2Z^{\Lambda^0} \cos \lambda \\
&+ 2Z^{K^\pm} \cos \kappa + 2Z^p \cos \gamma + 2Z^{\Delta^-} \cos \delta^- + 2Z^{\Sigma^+} \cos \sigma^+ \\
&+ 2Z^{\Sigma^-} \cos \sigma^- + 2Z^{\Xi^0} \cos \xi + 2Z^{\Xi^-} \cos \xi^- + 2Z^{\Omega^-} \cos \omega \\
&+ 2Z^{\Delta^{++}} \cos(\psi + 2\alpha)] \exp(Z^{\pi^0}) \quad (4.19)
\end{aligned}$$

Setting $\delta^{++} = \psi + 2\alpha$, we have that

$$\int \delta(\delta^{++} - \psi - 2\alpha) d\delta^{++} = \frac{1}{2\pi} \sum_{n_{\delta^{++}}=-\infty}^{\infty} \int_0^{2\pi} \exp(in_{\delta^{++}}(\delta^{++} - \psi - 2\alpha)) d\delta^{++}$$

Therefore, after using all the delta functions with variables λ to δ^{++} , the partition function in closed form for case 4 reads as

$$\begin{aligned}
Z_{B,S,Q}^3(T, V) &= \left\{ \sum_{n_\lambda=-\infty}^{\infty} \sum_{n_\kappa=-\infty}^{\infty} \sum_{n_\gamma=-\infty}^{\infty} \sum_{n_{\delta^-}=-\infty}^{\infty} \sum_{n_{\sigma^+}=-\infty}^{\infty} \sum_{n_{\sigma^-}=-\infty}^{\infty} \sum_{n_\xi=-\infty}^{\infty} \sum_{n_{\xi^-}=-\infty}^{\infty} \sum_{n_\omega=-\infty}^{\infty} \sum_{n_{\delta^{++}}=-\infty}^{\infty} \right. \\
& I_{S-n_\lambda+n_\kappa-n_{\sigma^+}-n_{\sigma^-}-2n_\xi-2n_{\xi^-}-3n_\omega} (2Z^{K^0}) \\
& I_{B+n_\lambda+n_\gamma+n_{\delta^-}+n_{\sigma^+}+n_{\sigma^-}+n_\xi+n_{\xi^-}+n_\omega+n_{\delta^{++}}} (2Z^n) \\
& I_{Q+n_\kappa+n_\gamma-n_{\delta^-}+n_{\sigma^+}-n_{\sigma^-}-n_{\xi^-}-n_\omega+2n_{\delta^{++}}} (2Z^{\pi^\pm}) I_{-n_\lambda} (2Z^{\Lambda^0}) I_{-n_\kappa} (2Z^{K^\pm}) \\
& I_{-n_\gamma} (2Z^p) I_{-n_{\delta^-}} (2Z^{\Delta^-}) I_{-n_{\sigma^+}} (2Z^{\Sigma^+}) I_{-n_{\sigma^-}} (2Z^{\Sigma^-}) I_{-n_\xi} (2Z^{\Xi^0}) \\
& \left. I_{-n_{\xi^-}} (2Z^{\Xi^-}) I_{-n_\omega} (2Z^{\Omega^-}) I_{-n_{\delta^{++}}} (2Z^{\Delta^{++}}) \right\} \cdot \exp(Z^{\pi^0}) \quad (4.20)
\end{aligned}$$

The canonical partition functions for a gas with three conserved quantum numbers have thus been derived and will be used in the following section to derive expressions for particle numbers.

$$\begin{aligned}
& +Z^{\overline{\Omega}^-} \exp(-i(-3\phi + \psi - \alpha)) \exp(\mu_{\overline{\Omega}^-}/T) \\
& +Z^{\Delta^{++}} \exp i(\psi + 2\alpha) \exp(\mu_{\Delta^{++}}/T) \\
& +Z^{\overline{\Delta}^{++}} \exp(-i(\psi + 2\alpha)) \exp(\mu_{\overline{\Delta}^{++}}/T) \} \cdot \exp(Z^{\pi^0}) \\
= & Z_{Total} \tag{4.21}
\end{aligned}$$

$\langle N_i \rangle$ can thus be obtained by differentiating Z_{Total} and setting $\mu_i = 0$. The results of this calculation follows.

4.3.1 Case 1: Baryon number = 0, ±1, Strangeness = 0, ±1, Charge = 0, ±1

$$\begin{aligned}
\left\langle N_{\frac{K^0}{K^0}} \right\rangle &= \frac{Z^{K^0}}{Z} \left\{ \sum_{n_\lambda=-\infty}^{\infty} \sum_{n_\kappa=-\infty}^{\infty} \sum_{n_\gamma=-\infty}^{\infty} \sum_{n_{\sigma^+}=-\infty}^{\infty} \sum_{n_{\sigma^-}=-\infty}^{\infty} I_{S-n_\lambda+n_\kappa-n_{\sigma^+}-n_{\sigma^-}-\mp 1} (2Z^{K^0}) \right. \\
& \cdot I_{B+n_\lambda+n_\gamma+n_{\sigma^+}+n_{\sigma^-}} (2Z^n) I_{Q+n_\kappa+n_\gamma+n_{\sigma^+}-n_{\sigma^-}} (2Z^{\pi^\pm}) I_{-n_\lambda} (2Z^{\Lambda^0}) \\
& \cdot I_{-n_\kappa} (2Z^{K^\pm}) I_{-n_\gamma} (2Z^p) I_{-n_{\sigma^+}} (2Z^{\Sigma^+}) I_{-n_{\sigma^-}} (2Z^{\Sigma^-}) \} \exp(Z^{\pi^0})
\end{aligned}$$

$$\begin{aligned}
\left\langle N_{\frac{n}{\pi}} \right\rangle &= \frac{Z^n}{Z} \left\{ \sum_{n_\lambda=-\infty}^{\infty} \sum_{n_\kappa=-\infty}^{\infty} \sum_{n_\gamma=-\infty}^{\infty} \sum_{n_{\sigma^+}=-\infty}^{\infty} \sum_{n_{\sigma^-}=-\infty}^{\infty} I_{S-n_\lambda+n_\kappa-n_{\sigma^+}-n_{\sigma^-}} (2Z^{K^0}) \right. \\
& \cdot I_{B+n_\lambda+n_\gamma+n_{\sigma^+}+n_{\sigma^-}-\mp 1} (2Z^n) I_{Q+n_\kappa+n_\gamma+n_{\sigma^+}-n_{\sigma^-}} (2Z^{\pi^\pm}) I_{-n_\lambda} (2Z^{\Lambda^0}) \\
& \cdot I_{-n_\kappa} (2Z^{K^\pm}) I_{-n_\gamma} (2Z^p) I_{-n_{\sigma^+}} (2Z^{\Sigma^+}) I_{-n_{\sigma^-}} (2Z^{\Sigma^-}) \} \exp(Z^{\pi^0})
\end{aligned}$$

$$\begin{aligned}
\left\langle N_{\frac{\pi^\pm}{\pi^\pm}} \right\rangle &= \frac{Z^{\pi^\pm}}{Z} \left\{ \sum_{n_\lambda=-\infty}^{\infty} \sum_{n_\kappa=-\infty}^{\infty} \sum_{n_\gamma=-\infty}^{\infty} \sum_{n_{\sigma^+}=-\infty}^{\infty} \sum_{n_{\sigma^-}=-\infty}^{\infty} I_{S-n_\lambda+n_\kappa-n_{\sigma^+}-n_{\sigma^-}} (2Z^{K^0}) \right. \\
& \cdot I_{B+n_\lambda+n_\gamma+n_{\sigma^+}+n_{\sigma^-}} (2Z^n) I_{Q+n_\kappa+n_\gamma+n_{\sigma^+}-n_{\sigma^-}-\mp 1} (2Z^{\pi^\pm}) I_{-n_\lambda} (2Z^{\Lambda^0}) \\
& \cdot I_{-n_\kappa} (2Z^{K^\pm}) I_{-n_\gamma} (2Z^p) I_{-n_{\sigma^+}} (2Z^{\Sigma^+}) I_{-n_{\sigma^-}} (2Z^{\Sigma^-}) \} \exp(Z^{\pi^0})
\end{aligned}$$

$$\begin{aligned}
\left\langle N_{\frac{\Lambda^0}{\Lambda^0}} \right\rangle &= \frac{Z^{\Lambda^0}}{Z} \left\{ \sum_{n_\lambda=-\infty}^{\infty} \sum_{n_\kappa=-\infty}^{\infty} \sum_{n_\gamma=-\infty}^{\infty} \sum_{n_{\sigma^+}=-\infty}^{\infty} \sum_{n_{\sigma^-}=-\infty}^{\infty} I_{S-n_\lambda+n_\kappa-n_{\sigma^+}-n_{\sigma^-}\pm 1} (2Z^{K^0}) \right. \\
& \cdot I_{B+n_\lambda+n_\gamma+n_{\sigma^+}+n_{\sigma^-}-\mp 1} (2Z^n) I_{Q+n_\kappa+n_\gamma+n_{\sigma^+}-n_{\sigma^-}} (2Z^{\pi^\pm}) I_{-n_\lambda} (2Z^{\Lambda^0}) \\
& \cdot I_{-n_\kappa} (2Z^{K^\pm}) I_{-n_\gamma} (2Z^p) I_{-n_{\sigma^+}} (2Z^{\Sigma^+}) I_{-n_{\sigma^-}} (2Z^{\Sigma^-}) \} \exp(Z^{\pi^0})
\end{aligned}$$

$$\begin{aligned}
\left\langle N_{\frac{K^+}{K^-}} \right\rangle &= \frac{Z^{K^\pm}}{Z} \left\{ \sum_{n_\lambda=-\infty}^{\infty} \sum_{n_\kappa=-\infty}^{\infty} \sum_{n_\gamma=-\infty}^{\infty} \sum_{n_{\sigma^+}=-\infty}^{\infty} \sum_{n_{\sigma^-}=-\infty}^{\infty} I_{S-n_\lambda+n_\kappa-n_{\sigma^+}-n_{\sigma^-}\mp 1} (2Z^{K^0}) \right. \\
&\quad \cdot I_{B+n_\lambda+n_\gamma+n_{\sigma^+}+n_{\sigma^-}} (2Z^n) I_{Q+n_\kappa+n_\gamma+n_{\sigma^+}-n_{\sigma^-}\mp 1} (2Z^{\pi^\pm}) I_{-n_\lambda} (2Z^{\Lambda^0}) \\
&\quad \left. \cdot I_{-n_\kappa} (2Z^{K^\pm}) I_{-n_\gamma} (2Z^p) I_{-n_{\sigma^+}} (2Z^{\Sigma^+}) I_{-n_{\sigma^-}} (2Z^{\Sigma^-}) \right\} \exp(Z^{\pi^0}) \\
\left\langle N_{\frac{p}{\bar{p}}} \right\rangle &= \frac{Z^p}{Z} \left\{ \sum_{n_\lambda=-\infty}^{\infty} \sum_{n_\kappa=-\infty}^{\infty} \sum_{n_\gamma=-\infty}^{\infty} \sum_{n_{\sigma^+}=-\infty}^{\infty} \sum_{n_{\sigma^-}=-\infty}^{\infty} I_{S-n_\lambda+n_\kappa-n_{\sigma^+}-n_{\sigma^-}} (2Z^{K^0}) \right. \\
&\quad \cdot I_{B+n_\lambda+n_\gamma+n_{\sigma^+}+n_{\sigma^-}\mp 1} (2Z^n) I_{Q+n_\kappa+n_\gamma+n_{\sigma^+}-n_{\sigma^-}\mp 1} (2Z^{\pi^\pm}) I_{-n_\lambda} (2Z^{\Lambda^0}) \\
&\quad \left. \cdot I_{-n_\kappa} (2Z^{K^\pm}) I_{-n_\gamma} (2Z^p) I_{-n_{\sigma^+}} (2Z^{\Sigma^+}) I_{-n_{\sigma^-}} (2Z^{\Sigma^-}) \right\} \exp(Z^{\pi^0}) \\
\left\langle N_{\frac{\Sigma^+}{\Sigma^-}} \right\rangle &= \frac{Z^{\Sigma^\pm}}{Z} \left\{ \sum_{n_\lambda=-\infty}^{\infty} \sum_{n_\kappa=-\infty}^{\infty} \sum_{n_\gamma=-\infty}^{\infty} \sum_{n_{\sigma^+}=-\infty}^{\infty} \sum_{n_{\sigma^-}=-\infty}^{\infty} I_{S-n_\lambda+n_\kappa-n_{\sigma^+}-n_{\sigma^-}\pm 1} (2Z^{K^0}) \right. \\
&\quad \cdot I_{B+n_\lambda+n_\gamma+n_{\sigma^+}+n_{\sigma^-}\mp 1} (2Z^n) I_{Q+n_\kappa+n_\gamma+n_{\sigma^+}-n_{\sigma^-}\mp 1} (2Z^{\pi^\pm}) I_{-n_\lambda} (2Z^{\Lambda^0}) \\
&\quad \left. \cdot I_{-n_\kappa} (2Z^{K^\pm}) I_{-n_\gamma} (2Z^p) I_{-n_{\sigma^+}} (2Z^{\Sigma^+}) I_{-n_{\sigma^-}} (2Z^{\Sigma^-}) \right\} \exp(Z^{\pi^0}) \\
\left\langle N_{\frac{\Sigma^-}{\Sigma^+}} \right\rangle &= \frac{Z^{\Sigma^\mp}}{Z} \left\{ \sum_{n_\lambda=-\infty}^{\infty} \sum_{n_\kappa=-\infty}^{\infty} \sum_{n_\gamma=-\infty}^{\infty} \sum_{n_{\sigma^+}=-\infty}^{\infty} \sum_{n_{\sigma^-}=-\infty}^{\infty} I_{S-n_\lambda+n_\kappa-n_{\sigma^+}-n_{\sigma^-}\pm 1} (2Z^{K^0}) \right. \\
&\quad \cdot I_{B+n_\lambda+n_\gamma+n_{\sigma^+}+n_{\sigma^-}\mp 1} (2Z^n) I_{Q+n_\kappa+n_\gamma+n_{\sigma^+}-n_{\sigma^-}\pm 1} (2Z^{\pi^\pm}) I_{-n_\lambda} (2Z^{\Lambda^0}) \\
&\quad \cdot I_{-n_\kappa} (2Z^{K^\pm}) I_{-n_\gamma} (2Z^p) I_{-n_{\sigma^+}} (2Z^{\Sigma^+}) I_{-n_{\sigma^-}} (2Z^{\Sigma^-}) \left. \right\} \\
&\quad \cdot \exp(Z^{\pi^0}) \tag{4.22}
\end{aligned}$$

The expressions of $\langle N \rangle$ for cases 2, 3 and 4 have been similarly derived and may be found in Appendix C.

This section thus concludes the derivation of expressions for particle numbers in the exact baryon number, strangeness and charge conservation formalism and, the results will be used in the next chapter to predict particle ratios which originate from the thermalized hadronic gas produced in the collision of nuclei.

Chapter 5

Results obtained using the B, S, Q Calculations

We now look at B, S, Q model calculations in terms of what it reveals beyond previous models and compare it to experimental results for Au-Au central collisions at Brookhaven.

5.1 Seeing beyond B, S Conservation with B, S, Q

What does a model conserving baryon number, strangeness and charge reveal that could not be seen in earlier models conserving only baryon number and strangeness? The motivation for the new model derives from the fact that the heavier nuclides tend to have many more neutrons than protons (Fig. 5.1). For example, ^{197}Au has 118 neutrons and only 79 protons, a neutron surplus of 39. In collisions involving heavier ions the effect arising from the neutron surplus substantially affects the particle abundance ratios leading to an increase in e.g. the π^-/π^+ ratio. This can be seen in Figure 5.2 which shows the theoretical plots (at different temperatures) for the π^-/π^+ ratio as a function of $B/2Q$ obtained by using the model equations. The baryon density is fixed at 0.05 for all plots. The deviation from unity for the n/p ratio is shown in the same figure. Note that the deviation from one for π^-/π^+ becomes more pronounced with decreasing temperature.

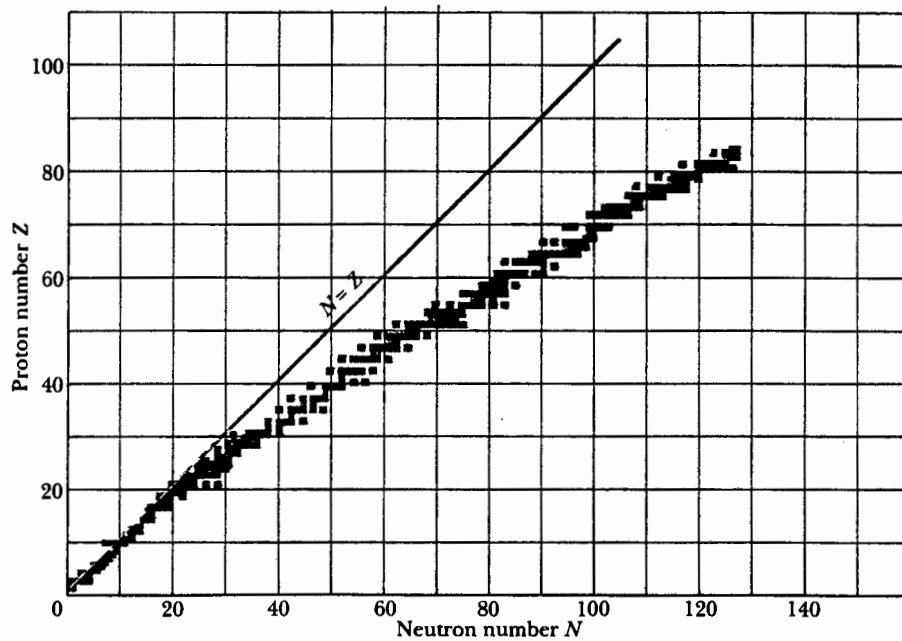


Figure 5.1: A plot of the known (stable) nuclides to show the deviation of neutron number, N , from Z as N increases [47].

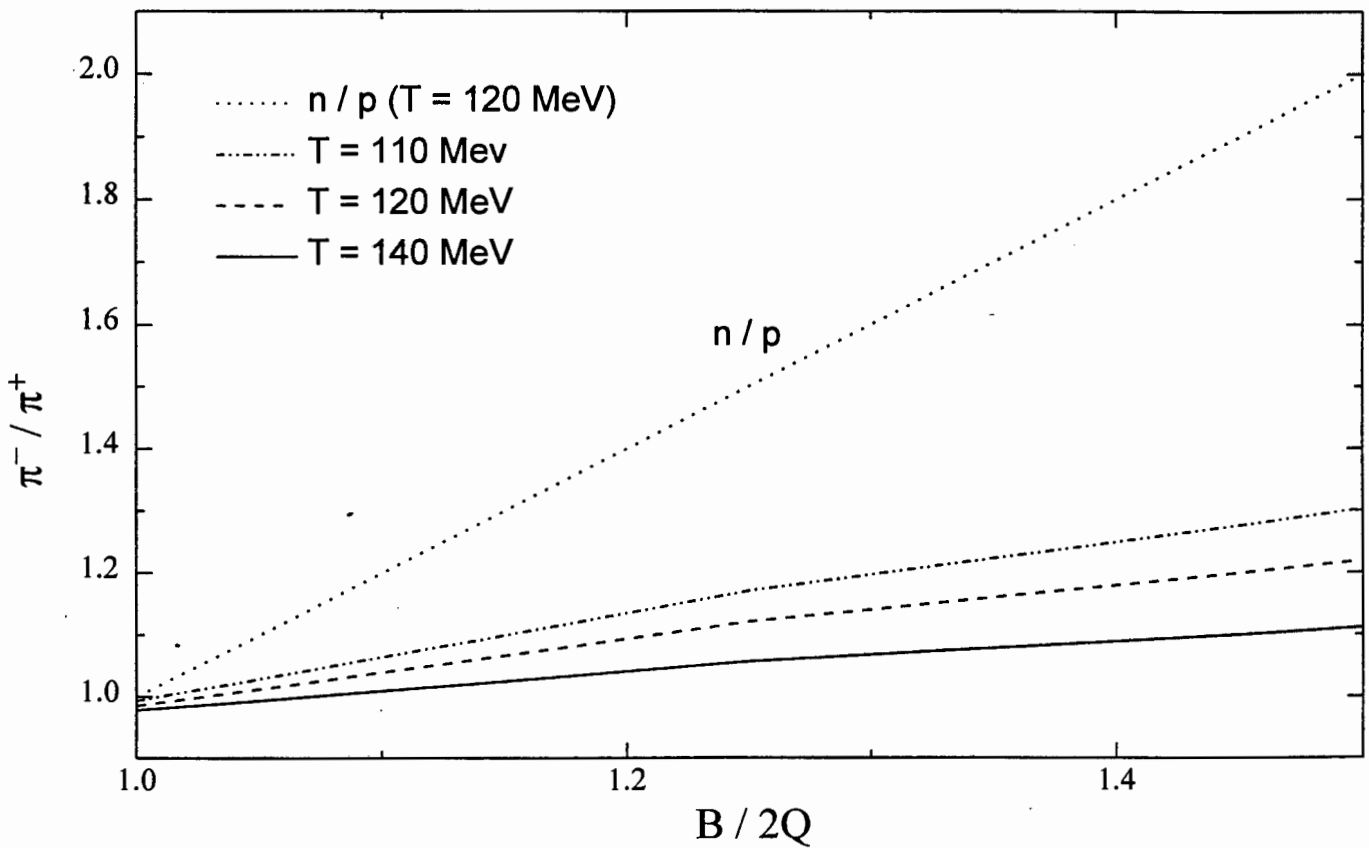


Figure 5.2: Plot showing the deviation from one for the π^-/π^+ ratio as the neutron surplus increases. The n/p ratio is also shown as a dotted line.

The effect of a neutron surplus on particle abundances can further be seen in plots of the ratios as a function of B where $B/2Q$ is kept fixed. The dashed line in each figure which we will examine is used for the case $B/2Q = 1.5$ and the solid line for $B/2Q = 1$. An increase in the particle ratios are obtained in all cases with the higher $B/2Q$ value i.e. with a neutron surplus of two times the proton number.

5.2 Comparisons with the BNL E866 data

Detailed measurements have been made by the E866 collaboration at the Brookhaven National Laboratory for relativistic $Au - Au$ collisions at a beam energy of $11 A GeV/c$. The experiment studies particle production in high baryon density matter created in central collisions[48]. The results give insight into the behaviour of the produced hadronic system as a function of the baryon number and of the size of the interaction volume.

Figure 5.3 shows the ratios of experimental particle yields obtained at mid-rapidity plotted against N_{pp} (number of projectile participants). We see that the π^+/π^- and p/π^+ ratios are almost unchanged, while the K^+/π^+ and K^-/π^- ratios increase with centrality. The systematic deviation from one for the π^+/π^- ratio can be largely attributed to the neutron surplus in Au ($B/2Q = 1.25$). The theoretical plots of the π^+/π^- ratio for $B/2Q = 1$ and $B/2Q = 1.5$ are shown in Figure 5.4.

The increase of the kaon ratios suggests that multiple interactions and rescattering play a large role in kaon/strangeness production in nucleus-nucleus collisions [48]. The following kaon ratios reached in the experiment

$$K^+/\pi^+ \sim 0.18 \pm 0.02$$

$$K^+/K^- \sim 5.0$$

compare well to those obtained in $Si + Au$ collisions. The kaon yield increases faster with centrality than the pion yield.

Figures 5.5 to 5.7 show the theoretical plots for the kaon ratios. A constant gradual rise with B is observed up till $B \approx 4$ for both the K^+/π^+ and K^-/π^- ratios before the slopes slowly begin to flatten out. The K^+/π^- ratio however, rises more gradually (if one considers the scale of

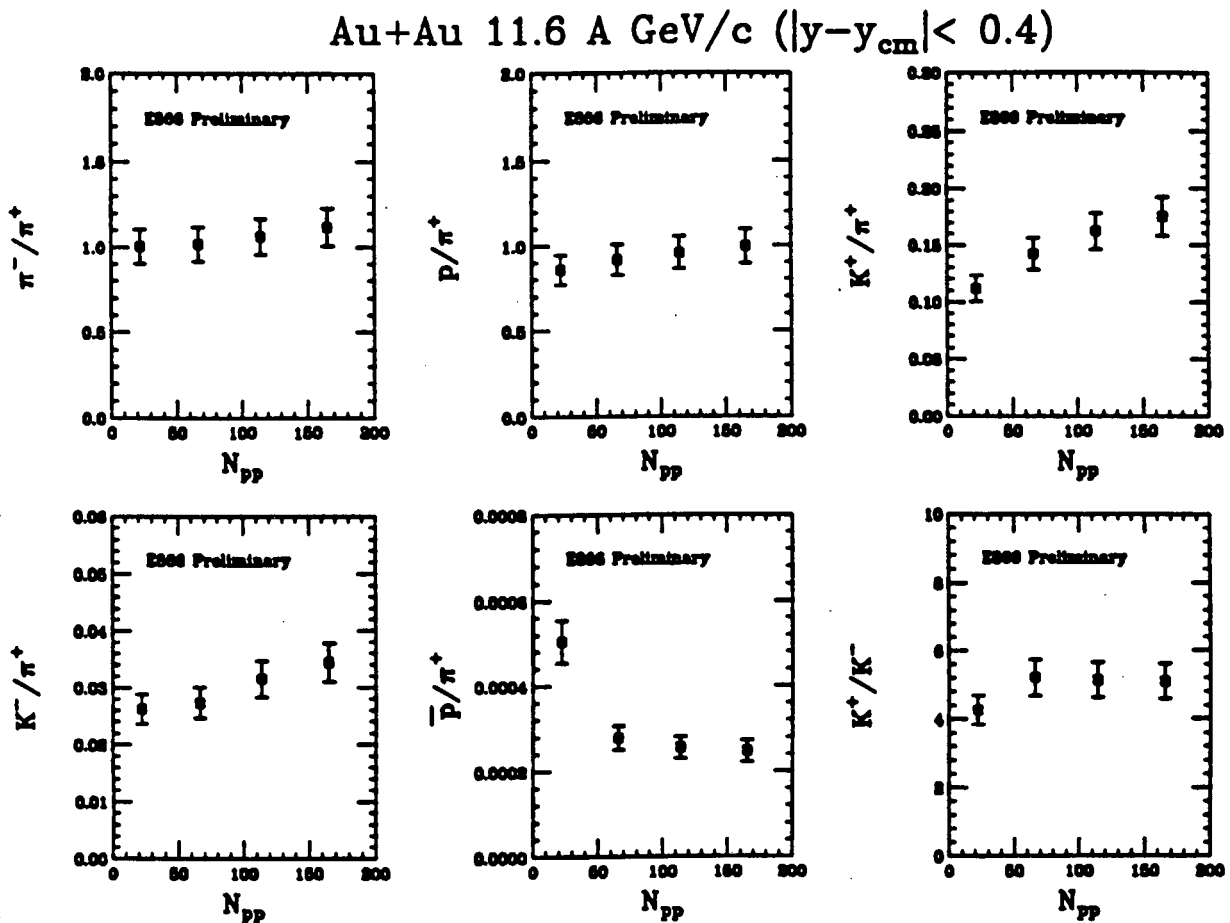


Figure 5.3: *Experimental particle ratios at mid-rapidity as a function of centrality [48].*

the plots) and this is reflected in the slight decreasing trend of the K^+/K^- ratio. The plot is systematically lower for $B/2Q = 1.5$ in the latter case. In the figures which follow, the model plots are drawn on a scale comparable with the experimental plots. It can be seen, even in the limited range of B , that the rise using model calculations is much faster than that seen in the experimental data for both the K^+/π^+ and K^-/π^- ratios. The K^+/K^- ratio is shown in Figure 5.7.

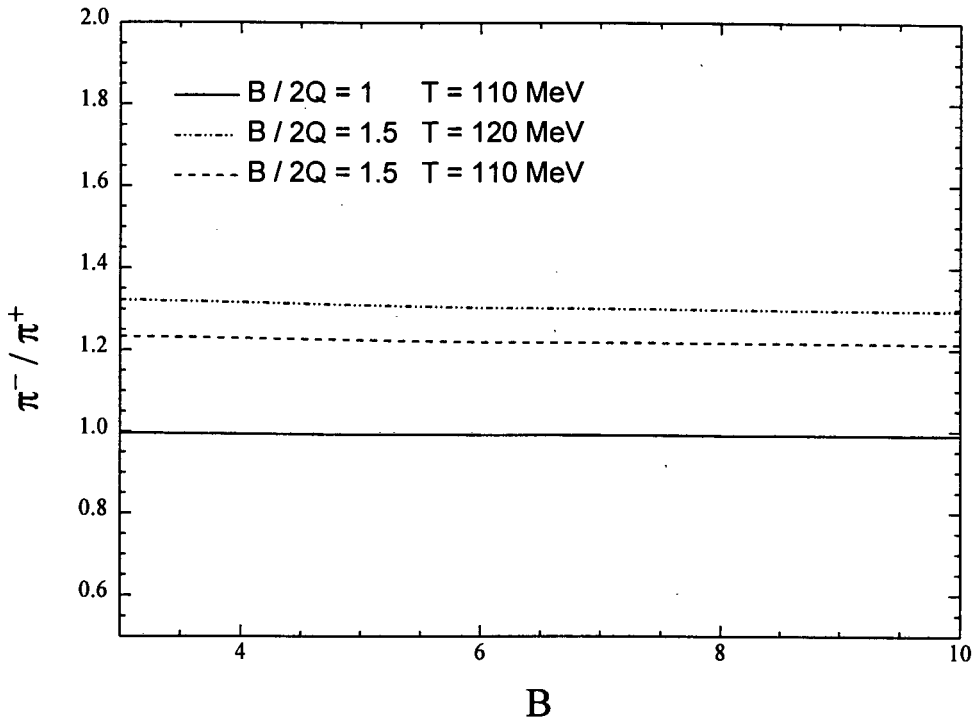


Figure 5.4: The π^-/π^+ ratio plotted as a function of B for different values of the temperature with $B/2Q$ remaining fixed at 1 and 1.5.

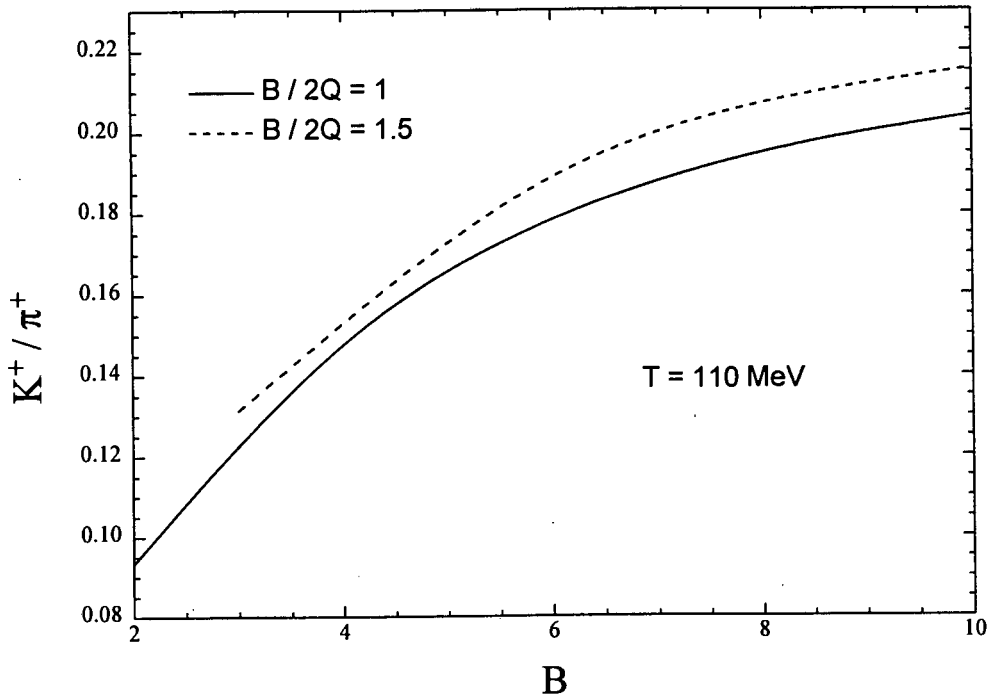


Figure 5.5: The K^+/π^+ ratio plotted as a function of B .

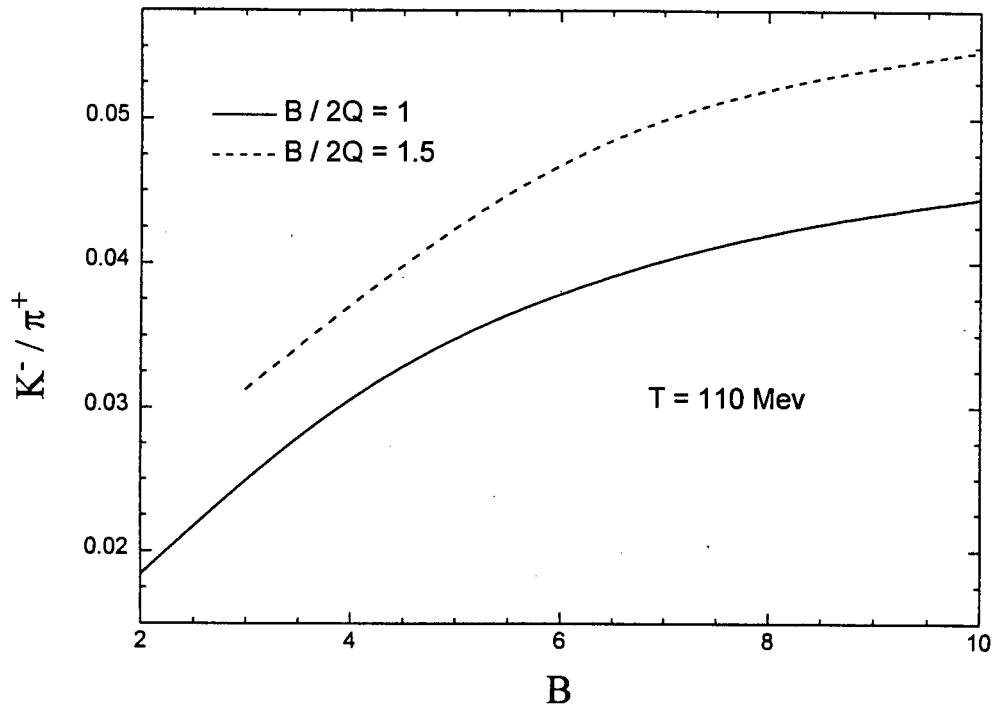


Figure 5.6: The K^-/π^+ ratio plotted as a function of B .

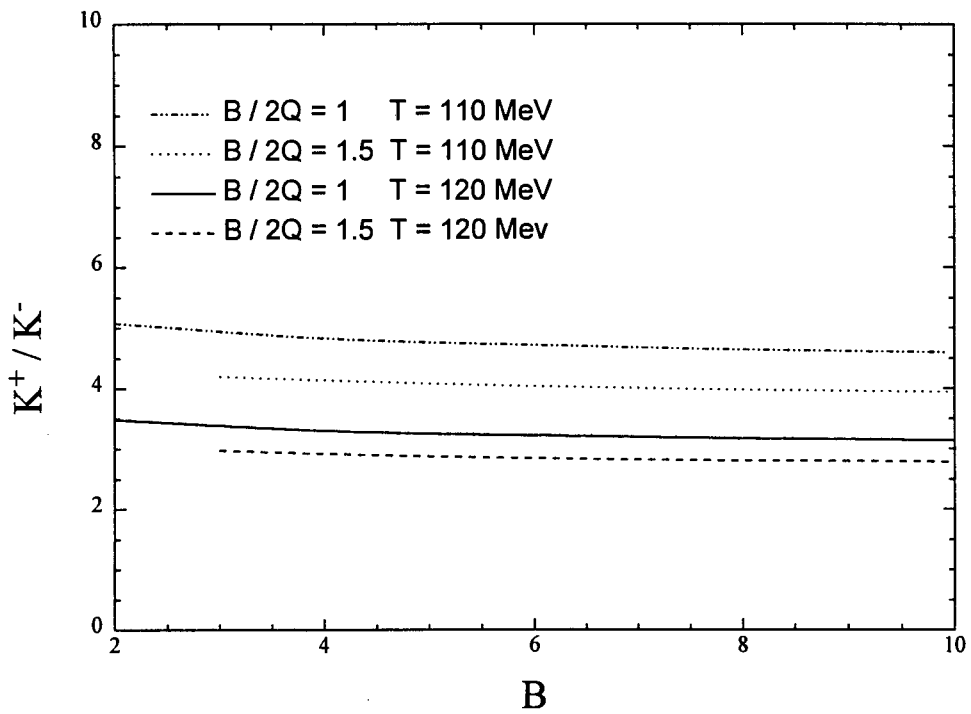


Figure 5.7: The K^+/K^- ratio plotted as a function of B .

Finally, we turn our attention to the \bar{p}/π^+ and p/π^+ ratios.

The observed \bar{p} production is the outcome of the competing processes of initial production and annihilation in nuclear matter. Antiproton production is interesting for a number of reasons. An example is the possibility of using antiprotons as a probe for baryon densities reached in collisions because of their large absorption cross-sections. Experimentally, a large drop is observed in the \bar{p}/π^+ ratio from peripheral to central collisions. The drop of the \bar{p} yield relative to other particles may be an indication of strong annihilation of \bar{p} in dense matter created in the collision. In Figure 5.8 we observe a slow increase in the \bar{p}/π^+ ratio opposite to the general tendency seen in the data. This can be explained by dynamical effects such as that which may be caused by the much smaller interaction volume and baryon density used for the theoretical fits compared to the experimental results. In the theoretical model the antiprotons will conceivably leave the fireball without sufficient rescattering to thermalize. For a small system such as that used in the model, initial \bar{p} production will almost certainly dominate annihilation and thermalization.

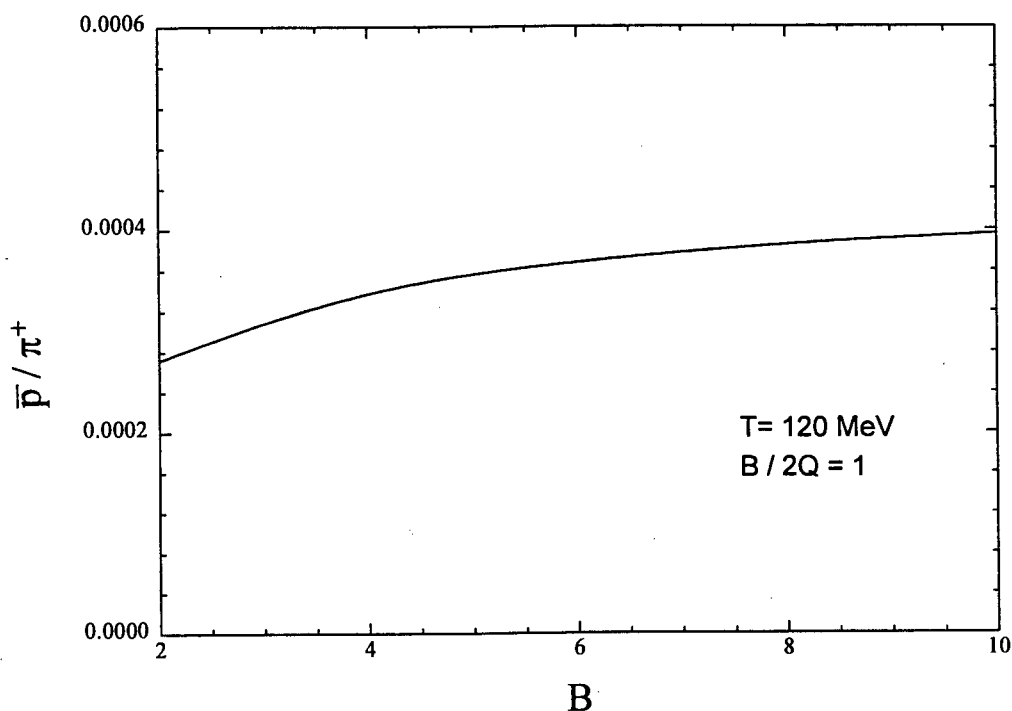


Figure 5.8: The \bar{p}/π ratio plotted as a function of B .

Lastly, Figure 5.9 shows the p/π^+ ratio. It can immediately be seen that the general tendency

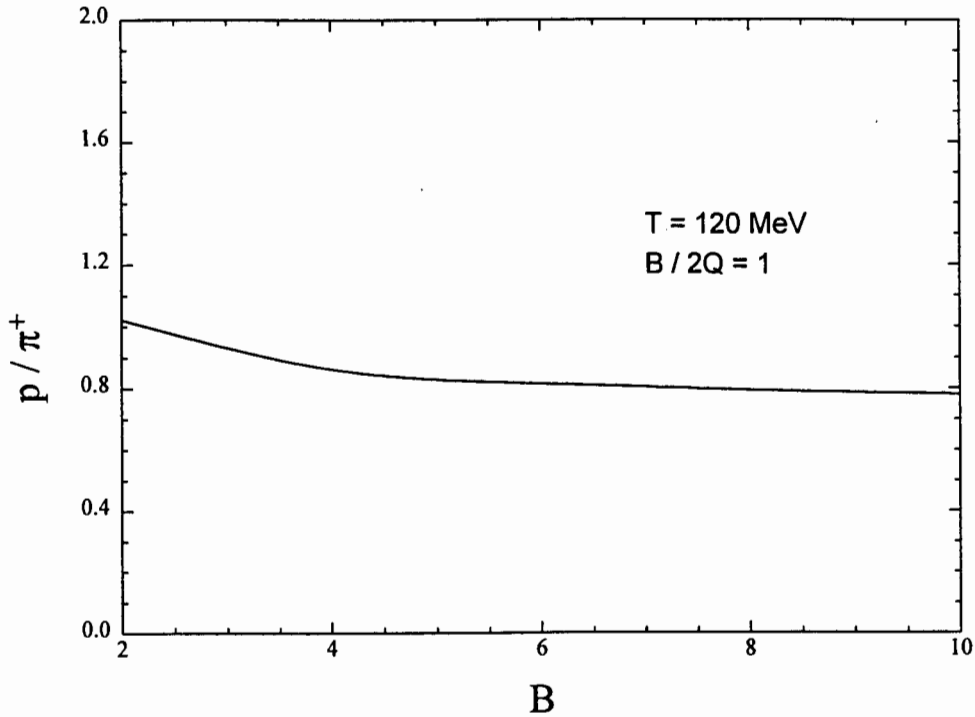


Figure 5.9: *The p/π^+ ratio plotted as a function of B .*

displayed by the model plot is different to that seen in the experimental data. The data show a slow increase with baryon number while the model gives just the opposite behaviour. Once again, dynamical effects outside the scope of the thermal model considered here need to be taken into account.

5.3 Summary and Conclusions

The particle abundance ratios have been computed in the canonical formalism using the formulation for the exact conservation of baryon number, strangeness and charge in the statistical thermodynamics of particle production. The volume and density of the system in the model calculations have been kept relatively small when compared to the experimental situation. The goal has been to stress the effect that the exact conservation of charge has on particle production in high energy collisions. This becomes particularly significant when the neutron number exceeds the charge in the colliding nuclei. Figure 5.2 shows the deviation from one for the π^-/π^+ ratio as $B/2Q$ increases i.e. as the overall neutron number exceeds the the overall charge in the collision. It is shown in the same figure that this effect becomes more pronounced with decreasing temperature. This can also be seen in the other particle ratio plots as a function of

baryon number, B .

In particular, in Figures 5.5 and 5.6, the K/π^+ ratios as a function of the baryon number are presented. The general tendencies displayed by these plots are consistent with the E866 experimental data. However, a steeper rise at lower volumes is attained by model calculations. It is also seen that the ratios are systematically increased as $B/2Q$ is increased.

Finally, we comment on the general tendency of the \bar{p}/π^+ and p/π^+ plots and, as with previous thermal model calculations, it is completely opposite to that seen in the experimental data. This clearly indicates dynamical effects outside the scope of these models and indeed, the limitation of current thermal models.

Appendix A

π^+ , π^- Production in a π, p, n Gas

The particle number expressions for the case of a gas containing pions, protons and neutrons is examined in closer detail. More specifically, we wish to show by analytical means that $\langle N_{\pi^+} \rangle = \langle N_{\pi^-} \rangle$ for such a gas if $Q = 0$.

The partition function may be determined using the same methods as before to yield

$$Z_{B,S,Q} = \sum_{n_{\text{proton}}=\infty}^{\infty} I_{B+n_{\text{proton}}} (2Z^n) I_{Q+n_{\text{proton}}} (2Z^\pi) I_{n_{\text{proton}}} (2Z^p) \quad (\text{A.1})$$

This leads to the following expressions for the particle numbers after differentiating $Z_{B,S,Q}$ in the usual way

$$\begin{aligned} \langle N_{\pi^+} \rangle &= \sum_{n_{\text{proton}}=\infty}^{\infty} I_{B+n_{\text{proton}}} (2Z^n) I_{Q+n_{\text{proton}}-1} (2Z^\pi) I_{n_{\text{proton}}} (2Z^p) \\ \langle N_{\pi^-} \rangle &= \sum_{n_{\text{proton}}=\infty}^{\infty} I_{B+n_{\text{proton}}} (2Z^n) I_{Q+n_{\text{proton}}+1} (2Z^\pi) I_{n_{\text{proton}}} (2Z^p) \end{aligned} \quad (\text{A.2})$$

We start our proof with the expression for $\langle N_{\pi^+} \rangle$ and manipulate the indices of the Bessel functions according to the following:

a) *change n_{proton} to $n_{\text{proton}} - B$*

$$\Rightarrow \langle N_{\pi^+} \rangle = \sum_{n_{\text{proton}}=\infty}^{\infty} I_{B-B+n_{\text{proton}}} (2Z^n) I_{Q-B+n_{\text{proton}}-1} (2Z^\pi) I_{n_{\text{proton}}-B} (2Z^p)$$

b) *change the sign of n_{proton}*

$$\Rightarrow \langle N_{\pi^+} \rangle = \sum_{n_{\text{proton}}=\infty}^{\infty} I_{-n_{\text{proton}}} (2Z^n) I_{Q-B-n_{\text{proton}}-1} (2Z^\pi) I_{-n_{\text{proton}}-B} (2Z^p)$$

c) *for $Q = 0$, $B = 2Q$*

$$\begin{aligned} \Rightarrow \langle N_{\pi^+} \rangle &= \sum_{n_{\text{proton}}=\infty}^{\infty} I_{-n_{\text{proton}}} (2Z^n) I_{Q-2Q-n_{\text{proton}}-1} (2Z^\pi) I_{-n_{\text{proton}}-B} (2Z^p) \\ &= \sum_{n_{\text{proton}}=\infty}^{\infty} I_{-n_{\text{proton}}} (2Z^n) I_{-Q-n_{\text{proton}}-1} (2Z^\pi) I_{-n_{\text{proton}}-B} (2Z^p) \end{aligned}$$

d) *change signs of all indices throughout*

$$\Rightarrow \langle N_{\pi^+} \rangle = \sum_{n_{\text{proton}}=\infty}^{\infty} I_{n_{\text{proton}}} (2Z^n) I_{Q+n_{\text{proton}}+1} (2Z^\pi) I_{n_{\text{proton}}+B} (2Z^p)$$

comparing this with $\langle N_{\pi^-} \rangle$, we find that $\langle N_{\pi^+} \rangle = \langle N_{\pi^-} \rangle$ provided $m_{\text{proton}} = m_{\text{neutron}}$.

The underlying principle in the above is the exchange of isospin symmetric partners in the baryon decuplet (while neglecting small mass differences such as that between protons and neutrons).

Appendix B

Analysis of a Q to I_3 Transformation

In this appendix the transformation from Q to I_3 is investigated mathematically to determine the usefulness of this for computation of numerical results.

The independent variables ϕ, ψ are changed to ϕ' and ψ' respectively to accommodate the inclusion of isospin since there will be no particles containing only baryon number or strangeness without containing isospin as well. The angle α is now used for isospin so that

$$\begin{aligned}\phi' &= \phi - \frac{1}{2}\alpha \\ \psi' &= \psi - \frac{1}{2}\alpha\end{aligned}$$

This change of variables will affect the limits of integration in the integral representation in the following way:

$$0 \leq \phi, \psi, \alpha \leq 2\pi \quad \rightarrow \quad 0 \leq \phi', \psi' \leq \pi, \quad 0 \leq \alpha \leq 2\pi$$

Since $Q = I_3 + \frac{B+S}{2}$, the exponentials can be changed accordingly to

$$\begin{aligned}e^{-iS\phi} &\rightarrow e^{-iS(\phi' + \frac{\alpha}{2})} \rightarrow e^{-iS\phi'} \\ e^{-iB\psi} &\rightarrow e^{-iB(\psi' + \frac{\alpha}{2})} \rightarrow e^{-iB\psi'} \\ e^{-iQ\alpha} &\rightarrow e^{-i(I_3 + \frac{B+S}{2})\alpha} \rightarrow e^{-i(I_3 + B + S)\alpha}\end{aligned}$$

The partition function in equation 4.10 can thus be rewritten as

$$Z_{B,S,Q}^1(T, V) = \frac{1}{(2\pi)^3} \int_0^\pi d\phi \exp(-iS\phi') \int_0^\pi d\psi \exp(-iB\psi') \int_0^{2\pi} d\alpha \exp -i(I_3 + B + S)\alpha$$

$$\begin{aligned}
& \cdot \exp[2Z^{K^0} \cos \phi' + 2Z^n \cos \psi' + 2Z^{\pi^\pm} \cos \alpha + 2Z^{\Lambda^0} \cos(\psi' - \phi') \\
& + 2Z^{K^\pm} \cos(\phi' + \alpha) + 2Z^p \cos(\psi' + \alpha) + 2Z^{\Sigma^+} \cos(\psi' - \phi' + \alpha) \\
& + 2Z^{\Sigma^-} \cos(\psi' - \phi' - \alpha)] \cdot \exp(Z^{\pi^0})
\end{aligned} \tag{B.1}$$

In the closed form of this equation $I_3 + B + S$ replaces Q as a bessel function index. Since $I_3 + B + S > Q$, the above procedure will not help in calculating numerical results more than before transforming from Q to I_3 .

Appendix C

Particle Number Expressions

In Appendix C expressions of $\langle N \rangle$ for cases 2, 3 and 4 discussed in chapter 3 are derived.

C.0.1 Case 2: Baryon number = $0, \pm 1$, Strangeness = $0, \pm 1, \pm 2$, Charge = $0, \pm 1$

$$\begin{aligned} \left\langle N_{\frac{K^0}{K^0}} \right\rangle &= \frac{Z^{K^0}}{Z} \left\{ \sum_{n_\lambda=-\infty}^{\infty} \sum_{n_\kappa=-\infty}^{\infty} \sum_{n_\gamma=-\infty}^{\infty} \sum_{n_{\sigma^+}=-\infty}^{\infty} \sum_{n_{\sigma^-}=-\infty}^{\infty} \sum_{n_\xi=-\infty}^{\infty} \sum_{n_{\xi^-}=-\infty}^{\infty} \right. \\ & I_{S-n_\lambda+n_\kappa-n_{\sigma^+}-n_{\sigma^-}-2n_\xi-2n_{\xi^-}-\mp 1} (2Z^{K^0}) I_{B+n_\lambda+n_\gamma+n_{\sigma^+}+n_{\sigma^-}+n_\xi+n_{\xi^-}} (2Z^n) \\ & I_{Q+n_\kappa+n_\gamma+n_{\sigma^+}-n_{\sigma^-}-n_{\xi^-}} (2Z^{\pi^\pm}) I_{-n_\lambda} (2Z^{\Lambda^0}) I_{-n_\kappa} (2Z^{K^\pm}) I_{-n_\gamma} (2Z^p) \\ & I_{-n_{\sigma^+}} (2Z^{\Sigma^+}) I_{-n_{\sigma^-}} (2Z^{\Sigma^-}) I_{-n_\xi} (2Z^{\Xi^0}) I_{-n_{\xi^-}} (2Z^{\Xi^-}) \left. \right\} \\ & \cdot \exp(Z^{\pi^0}) \end{aligned}$$

$$\begin{aligned} \left\langle N_{\frac{n}{n}} \right\rangle &= \frac{Z^n}{Z} \left\{ \sum_{n_\lambda=-\infty}^{\infty} \sum_{n_\kappa=-\infty}^{\infty} \sum_{n_\gamma=-\infty}^{\infty} \sum_{n_{\sigma^+}=-\infty}^{\infty} \sum_{n_{\sigma^-}=-\infty}^{\infty} \sum_{n_\xi=-\infty}^{\infty} \sum_{n_{\xi^-}=-\infty}^{\infty} \right. \\ & I_{S-n_\lambda+n_\kappa-n_{\sigma^+}-n_{\sigma^-}-2n_\xi-2n_{\xi^-}} (2Z^{K^0}) I_{B+n_\lambda+n_\gamma+n_{\sigma^+}+n_{\sigma^-}+n_\xi+n_{\xi^-}-\mp 1} (2Z^n) \\ & I_{Q+n_\kappa+n_\gamma+n_{\sigma^+}-n_{\sigma^-}-n_{\xi^-}} (2Z^{\pi^\pm}) I_{-n_\lambda} (2Z^{\Lambda^0}) I_{-n_\kappa} (2Z^{K^\pm}) I_{-n_\gamma} (2Z^p) \\ & I_{-n_{\sigma^+}} (2Z^{\Sigma^+}) I_{-n_{\sigma^-}} (2Z^{\Sigma^-}) I_\xi (2Z^{\Xi^0}) I_{-n_{\xi^-}} (2Z^{\Xi^-}) \left. \right\} \\ & \cdot \exp(Z^{\pi^0}) \end{aligned}$$

$$\left\langle N_{\frac{\pi^+}{\pi^+}} \right\rangle = \frac{Z^{\pi^\pm}}{Z} \left\{ \sum_{n_\lambda=-\infty}^{\infty} \sum_{n_\kappa=-\infty}^{\infty} \sum_{n_\gamma=-\infty}^{\infty} \sum_{n_{\sigma^+}=-\infty}^{\infty} \sum_{n_{\sigma^-}=-\infty}^{\infty} \sum_{n_\xi=-\infty}^{\infty} \sum_{n_{\xi^-}=-\infty}^{\infty} \right.$$

$$\begin{aligned}
& I_{S-n_\lambda+n_\kappa-n_{\sigma^+}-n_{\sigma^-}-2n_\xi-2n_{\xi^-}} (2Z^{K^0}) I_{B+n_\lambda+n_\gamma+n_{\sigma^+}+n_{\sigma^-}+n_\xi+n_{\xi^-}} (2Z^n) \\
& I_{Q+n_\kappa+n_\gamma+n_{\sigma^+}-n_{\sigma^-}-n_{\xi^-}-1} (2Z^{\pi^\pm}) I_{-n_\lambda} (2Z^{\Lambda^0}) I_{-n_\kappa} (2Z^{K^\pm}) I_{-n_\gamma} (2Z^p) \\
& I_{-n_{\sigma^+}} (2Z^{\Sigma^+}) I_{-n_{\sigma^-}} (2Z^{\Sigma^-}) I_\xi (2Z^{\Xi^0}) I_{-n_{\xi^-}} (2Z^{\Xi^-}) \} \\
& \cdot \exp(Z^{\pi^0})
\end{aligned}$$

$$\begin{aligned}
\left\langle N_{\frac{\Lambda^0}{\Lambda^0}} \right\rangle &= \frac{Z^{\Lambda^0}}{Z} \left\{ \sum_{n_\lambda=-\infty}^{\infty} \sum_{n_\kappa=-\infty}^{\infty} \sum_{n_\gamma=-\infty}^{\infty} \sum_{n_{\sigma^+}=-\infty}^{\infty} \sum_{n_{\sigma^-}=-\infty}^{\infty} \sum_{n_\xi=-\infty}^{\infty} \sum_{n_{\xi^-}=-\infty}^{\infty} \right. \\
& I_{S-n_\lambda+n_\kappa-n_{\sigma^+}-n_{\sigma^-}-2n_\xi-2n_{\xi^-}\pm 1} (2Z^{K^0}) I_{B+n_\lambda+n_\gamma+n_{\sigma^+}+n_{\sigma^-}+n_\xi+n_{\xi^-}\mp 1} (2Z^n) \\
& I_{Q+n_\kappa+n_\gamma+n_{\sigma^+}-n_{\sigma^-}-n_{\xi^-}} (2Z^{\pi^\pm}) I_{-n_\lambda} (2Z^{\Lambda^0}) I_{-n_\kappa} (2Z^{K^\pm}) I_{-n_\gamma} (2Z^p) \\
& I_{-n_{\sigma^+}} (2Z^{\Sigma^+}) I_{-n_{\sigma^-}} (2Z^{\Sigma^-}) I_\xi (2Z^{\Xi^0}) I_{-n_{\xi^-}} (2Z^{\Xi^-}) \} \\
& \cdot \exp(Z^{\pi^0})
\end{aligned}$$

$$\begin{aligned}
\left\langle N_{\frac{K^\pm}{K^-}} \right\rangle &= \frac{Z^{K^\pm}}{Z} \left\{ \sum_{n_\lambda=-\infty}^{\infty} \sum_{n_\kappa=-\infty}^{\infty} \sum_{n_\gamma=-\infty}^{\infty} \sum_{n_{\sigma^+}=-\infty}^{\infty} \sum_{n_{\sigma^-}=-\infty}^{\infty} \sum_{n_\xi=-\infty}^{\infty} \sum_{n_{\xi^-}=-\infty}^{\infty} \right. \\
& I_{S-n_\lambda+n_\kappa-n_{\sigma^+}-n_{\sigma^-}-2n_\xi-2n_{\xi^-}\mp 1} (2Z^{K^0}) I_{B+n_\lambda+n_\gamma+n_{\sigma^+}+n_{\sigma^-}+n_\xi+n_{\xi^-}} (2Z^n) \\
& I_{Q+n_\kappa+n_\gamma+n_{\sigma^+}-n_{\sigma^-}-n_{\xi^-}\mp 1} (2Z^{\pi^\pm}) I_{-n_\lambda} (2Z^{\Lambda^0}) I_{-n_\kappa} (2Z^{K^\pm}) I_{-n_\gamma} (2Z^p) \\
& I_{-n_{\sigma^+}} (2Z^{\Sigma^+}) I_{-n_{\sigma^-}} (2Z^{\Sigma^-}) I_\xi (2Z^{\Xi^0}) I_{-n_{\xi^-}} (2Z^{\Xi^-}) \} \\
& \cdot \exp(Z^{\pi^0})
\end{aligned}$$

$$\begin{aligned}
\left\langle N_{\frac{p}{p}} \right\rangle &= \frac{Z^p}{Z} \left\{ \sum_{n_\lambda=-\infty}^{\infty} \sum_{n_\kappa=-\infty}^{\infty} \sum_{n_\gamma=-\infty}^{\infty} \sum_{n_{\sigma^+}=-\infty}^{\infty} \sum_{n_{\sigma^-}=-\infty}^{\infty} \sum_{n_\xi=-\infty}^{\infty} \sum_{n_{\xi^-}=-\infty}^{\infty} \right. \\
& I_{S-n_\lambda+n_\kappa-n_{\sigma^+}-n_{\sigma^-}-2n_\xi-2n_{\xi^-}} (2Z^{K^0}) I_{B+n_\lambda+n_\gamma+n_{\sigma^+}+n_{\sigma^-}+n_\xi+n_{\xi^-}\mp 1} (2Z^n) \\
& I_{Q+n_\kappa+n_\gamma+n_{\sigma^+}-n_{\sigma^-}-n_{\xi^-}\mp 1} (2Z^{\pi^\pm}) I_{-n_\lambda} (2Z^{\Lambda^0}) I_{-n_\kappa} (2Z^{K^\pm}) I_{-n_\gamma} (2Z^p) \\
& I_{-n_{\sigma^+}} (2Z^{\Sigma^+}) I_{-n_{\sigma^-}} (2Z^{\Sigma^-}) I_\xi (2Z^{\Xi^0}) I_{-n_{\xi^-}} (2Z^{\Xi^-}) \} \\
& \cdot \exp(Z^{\pi^0})
\end{aligned}$$

$$\left\langle N_{\frac{\Delta^-}{\Delta^-}} \right\rangle = \frac{Z^{\Delta^-}}{Z} \left\{ \sum_{n_\lambda=-\infty}^{\infty} \sum_{n_\kappa=-\infty}^{\infty} \sum_{n_\gamma=-\infty}^{\infty} \sum_{n_{\sigma^+}=-\infty}^{\infty} \sum_{n_{\sigma^-}=-\infty}^{\infty} \sum_{n_\xi=-\infty}^{\infty} \sum_{n_{\xi^-}=-\infty}^{\infty} \right.$$

$$\begin{aligned}
& I_{S-n_\lambda+n_\kappa-n_{\sigma^+}-n_{\sigma^-}-2n_\xi-2n_{\xi^-}} (2Z^{K^0}) I_{B+n_\lambda+n_\gamma+n_{\sigma^+}+n_{\sigma^-}+n_\xi+n_{\xi^-}-1} (2Z^n) \\
& I_{Q+n_\kappa+n_\gamma+n_{\sigma^+}-n_{\sigma^-}-n_{\xi^-}-1} (2Z^{\pi^\pm}) I_{-n_\lambda} (2Z^{\Lambda^0}) I_{-n_\kappa} (2Z^{K^\pm}) I_{-n_\gamma} (2Z^P) \\
& I_{-n_{\sigma^+}} (2Z^{\Sigma^+}) I_{-n_{\sigma^-}} (2Z^{\Sigma^-}) I_\xi (2Z^{\Xi^0}) I_{-n_{\xi^-}} (2Z^{\Xi^-}) \} \\
& \cdot \exp(Z^{\pi^0})
\end{aligned}$$

$$\begin{aligned}
\left\langle N_{\frac{\Sigma^+}{\Sigma^+}} \right\rangle &= \frac{Z^{\Sigma^+}}{Z} \left\{ \sum_{n_\lambda=-\infty}^{\infty} \sum_{n_\kappa=-\infty}^{\infty} \sum_{n_\gamma=-\infty}^{\infty} \sum_{n_{\sigma^+}=-\infty}^{\infty} \sum_{n_{\sigma^-}=-\infty}^{\infty} \sum_{n_\xi=-\infty}^{\infty} \sum_{n_{\xi^-}=-\infty}^{\infty} \right. \\
& I_{S-n_\lambda+n_\kappa-n_{\sigma^+}-n_{\sigma^-}-2n_\xi-2n_{\xi^-}-1} (2Z^{K^0}) I_{B+n_\lambda+n_\gamma+n_{\sigma^+}+n_{\sigma^-}+n_\xi+n_{\xi^-}-1} (2Z^n) \\
& I_{Q+n_\kappa+n_\gamma+n_{\sigma^+}-n_{\sigma^-}-n_{\xi^-}-1} (2Z^{\pi^\pm}) I_{-n_\lambda} (2Z^{\Lambda^0}) I_{-n_\kappa} (2Z^{K^\pm}) I_{-n_\gamma} (2Z^P) \\
& I_{-n_{\sigma^+}} (2Z^{\Sigma^+}) I_{-n_{\sigma^-}} (2Z^{\Sigma^-}) I_\xi (2Z^{\Xi^0}) I_{-n_{\xi^-}} (2Z^{\Xi^-}) \} \\
& \cdot \exp(Z^{\pi^0})
\end{aligned}$$

$$\begin{aligned}
\left\langle N_{\frac{\Sigma^-}{\Sigma^-}} \right\rangle &= \frac{Z^{\Sigma^-}}{Z} \left\{ \sum_{n_\lambda=-\infty}^{\infty} \sum_{n_\kappa=-\infty}^{\infty} \sum_{n_\gamma=-\infty}^{\infty} \sum_{n_{\sigma^+}=-\infty}^{\infty} \sum_{n_{\sigma^-}=-\infty}^{\infty} \sum_{n_\xi=-\infty}^{\infty} \sum_{n_{\xi^-}=-\infty}^{\infty} \right. \\
& I_{S-n_\lambda+n_\kappa-n_{\sigma^+}-n_{\sigma^-}-2n_\xi-2n_{\xi^-}-1} (2Z^{K^0}) I_{B+n_\lambda+n_\gamma+n_{\sigma^+}+n_{\sigma^-}+n_\xi+n_{\xi^-}-1} (2Z^n) \\
& I_{Q+n_\kappa+n_\gamma+n_{\sigma^+}-n_{\sigma^-}-n_{\xi^-}-1} (2Z^{\pi^\pm}) I_{-n_\lambda} (2Z^{\Lambda^0}) I_{-n_\kappa} (2Z^{K^\pm}) I_{-n_\gamma} (2Z^P) \\
& I_{-n_{\sigma^+}} (2Z^{\Sigma^+}) I_{-n_{\sigma^-}} (2Z^{\Sigma^-}) I_\xi (2Z^{\Xi^0}) I_{-n_{\xi^-}} (2Z^{\Xi^-}) \} \\
& \cdot \exp(Z^{\pi^0})
\end{aligned}$$

$$\begin{aligned}
\left\langle N_{\frac{\Xi^0}{\Xi^0}} \right\rangle &= \frac{Z^{\Xi^0}}{Z} \left\{ \sum_{n_\lambda=-\infty}^{\infty} \sum_{n_\kappa=-\infty}^{\infty} \sum_{n_\gamma=-\infty}^{\infty} \sum_{n_{\sigma^+}=-\infty}^{\infty} \sum_{n_{\sigma^-}=-\infty}^{\infty} \sum_{n_\xi=-\infty}^{\infty} \sum_{n_{\xi^-}=-\infty}^{\infty} \right. \\
& I_{S-n_\lambda+n_\kappa-n_{\sigma^+}-n_{\sigma^-}-2n_\xi-2n_{\xi^-}-2} (2Z^{K^0}) I_{B+n_\lambda+n_\gamma+n_{\sigma^+}+n_{\sigma^-}+n_\xi+n_{\xi^-}-1} (2Z^n) \\
& I_{Q+n_\kappa+n_\gamma+n_{\sigma^+}-n_{\sigma^-}-n_{\xi^-}} (2Z^{\pi^\pm}) I_{-n_\lambda} (2Z^{\Lambda^0}) I_{-n_\kappa} (2Z^{K^\pm}) I_{-n_\gamma} (2Z^P) \\
& I_{-n_{\sigma^+}} (2Z^{\Sigma^+}) I_{-n_{\sigma^-}} (2Z^{\Sigma^-}) I_\xi (2Z^{\Xi^0}) I_{-n_{\xi^-}} (2Z^{\Xi^-}) \} \\
& \cdot \exp(Z^{\pi^0})
\end{aligned}$$

$$\left\langle N_{\frac{\Xi^-}{\Xi^-}} \right\rangle = \frac{Z^{\Xi^-}}{Z} \left\{ \sum_{n_\lambda=-\infty}^{\infty} \sum_{n_\kappa=-\infty}^{\infty} \sum_{n_\gamma=-\infty}^{\infty} \sum_{n_{\sigma^+}=-\infty}^{\infty} \sum_{n_{\sigma^-}=-\infty}^{\infty} \sum_{n_\xi=-\infty}^{\infty} \sum_{n_{\xi^-}=-\infty}^{\infty} \right.$$

$$\begin{aligned}
& I_{S-n_\lambda+n_\kappa-n_{\sigma^+}-n_{\sigma^-}-2n_\xi-2n_{\xi^-}\pm 2} (2Z^{K^0}) I_{B+n_\lambda+n_\gamma+n_{\sigma^+}+n_{\sigma^-}+n_\xi+n_{\xi^-}\mp 1} (2Z^n) \\
& I_{Q+n_\kappa+n_\gamma+n_{\sigma^+}-n_{\sigma^-}-n_{\xi^-}\pm 1} (2Z^{\pi^\pm}) I_{-n_\lambda} (2Z^{\Lambda^0}) I_{-n_\kappa} (2Z^{K^\pm}) I_{-n_\gamma} (2Z^p) \\
& I_{-n_{\sigma^+}} (2Z^{\Sigma^+}) I_{-n_{\sigma^-}} (2Z^{\Sigma^-}) I_\xi (2Z^{\Xi^0}) I_{-n_{\xi^-}} (2Z^{\Xi^-}) \} \\
& \cdot \exp(Z^{\pi^0})
\end{aligned} \tag{C.1}$$

C.0.2 Case 3: Baryon number = 0, ±1, Strangeness = 0, ±1, ±2, ±3, Charge = 0, ±1

$$\begin{aligned}
\left\langle N_{\frac{K^0}{K^0}} \right\rangle &= \frac{Z^{K^0}}{Z} \left\{ \sum_{n_\lambda=-\infty}^{\infty} \sum_{n_\kappa=-\infty}^{\infty} \sum_{n_\gamma=-\infty}^{\infty} \sum_{n_{\sigma^+}=-\infty}^{\infty} \sum_{n_{\sigma^-}=-\infty}^{\infty} \sum_{n_\xi=-\infty}^{\infty} \sum_{n_{\xi^-}=-\infty}^{\infty} \sum_{n_\omega=-\infty}^{\infty} \right. \\
& I_{S-n_\lambda+n_\kappa-n_{\sigma^+}-n_{\sigma^-}-2n_\xi-2n_{\xi^-}-3n_\omega\mp 1} (2Z^{K^0}) I_{B+n_\lambda+n_\gamma+n_{\sigma^+}+n_{\sigma^-}+n_\xi+n_{\xi^-}+n_\omega} (2Z^n) \\
& I_{Q+n_\kappa+n_\gamma+n_{\sigma^+}-n_{\sigma^-}-n_{\xi^-}-n_\omega} (2Z^{\pi^\pm}) I_{-n_\lambda} (2Z^{\Lambda^0}) I_{-n_\kappa} (2Z^{K^\pm}) I_{-n_\gamma} (2Z^p) \\
& I_{-n_{\sigma^+}} (2Z^{\Sigma^+}) I_{-n_{\sigma^-}} (2Z^{\Sigma^-}) I_{-n_\xi} (2Z^{\Xi^0}) I_{-n_{\xi^-}} (2Z^{\Xi^-}) I_{-n_\omega} (2Z^{\Omega^-}) \} \\
& \cdot \exp(Z^{\pi^0})
\end{aligned}$$

$$\begin{aligned}
\left\langle N_{\frac{n}{n}} \right\rangle &= \frac{Z^n}{Z} \left\{ \sum_{n_\lambda=-\infty}^{\infty} \sum_{n_\kappa=-\infty}^{\infty} \sum_{n_\gamma=-\infty}^{\infty} \sum_{n_{\sigma^+}=-\infty}^{\infty} \sum_{n_{\sigma^-}=-\infty}^{\infty} \sum_{n_\xi=-\infty}^{\infty} \sum_{n_{\xi^-}=-\infty}^{\infty} \sum_{n_\omega=-\infty}^{\infty} \right. \\
& I_{S-n_\lambda+n_\kappa-n_{\sigma^+}-n_{\sigma^-}-2n_\xi-2n_{\xi^-}-3n_\omega} (2Z^{K^0}) I_{B+n_\lambda+n_\gamma+n_{\sigma^+}+n_{\sigma^-}+n_\xi+n_{\xi^-}+n_\omega\mp 1} (2Z^n) \\
& I_{Q+n_\kappa+n_\gamma+n_{\sigma^+}-n_{\sigma^-}-n_{\xi^-}-n_\omega} (2Z^{\pi^\pm}) I_{-n_\lambda} (2Z^{\Lambda^0}) I_{-n_\kappa} (2Z^{K^\pm}) I_{-n_\gamma} (2Z^p) \\
& I_{-n_{\sigma^+}} (2Z^{\Sigma^+}) I_{-n_{\sigma^-}} (2Z^{\Sigma^-}) I_{-n_\xi} (2Z^{\Xi^0}) I_{-n_{\xi^-}} (2Z^{\Xi^-}) I_{-n_\omega} (2Z^{\Omega^-}) \} \\
& \cdot \exp(Z^{\pi^0})
\end{aligned}$$

$$\begin{aligned}
\left\langle N_{\frac{\pi^\pm}{\pi^\pm}} \right\rangle &= \frac{Z^{\pi^\pm}}{Z} \left\{ \sum_{n_\lambda=-\infty}^{\infty} \sum_{n_\kappa=-\infty}^{\infty} \sum_{n_\gamma=-\infty}^{\infty} \sum_{n_{\sigma^+}=-\infty}^{\infty} \sum_{n_{\sigma^-}=-\infty}^{\infty} \sum_{n_\xi=-\infty}^{\infty} \sum_{n_{\xi^-}=-\infty}^{\infty} \sum_{n_\omega=-\infty}^{\infty} \right. \\
& I_{S-n_\lambda+n_\kappa-n_{\sigma^+}-n_{\sigma^-}-2n_\xi-2n_{\xi^-}-3n_\omega} (2Z^{K^0}) I_{B+n_\lambda+n_\gamma+n_{\sigma^+}+n_{\sigma^-}+n_\xi+n_{\xi^-}+n_\omega} (2Z^n) \\
& I_{Q+n_\kappa+n_\gamma+n_{\sigma^+}-n_{\sigma^-}-n_{\xi^-}-n_\omega\mp 1} (2Z^{\pi^\pm}) I_{-n_\lambda} (2Z^{\Lambda^0}) I_{-n_\kappa} (2Z^{K^\pm}) I_{-n_\gamma} (2Z^p) \\
& I_{-n_{\sigma^+}} (2Z^{\Sigma^+}) I_{-n_{\sigma^-}} (2Z^{\Sigma^-}) I_{-n_\xi} (2Z^{\Xi^0}) I_{-n_{\xi^-}} (2Z^{\Xi^-}) I_{-n_\omega} (2Z^{\Omega^-}) \} \\
& \cdot \exp(Z^{\pi^0})
\end{aligned}$$

$$\begin{aligned}
\left\langle N_{\frac{\Lambda^0}{\Lambda^0}} \right\rangle &= \frac{Z^{\Lambda^0}}{Z} \left\{ \sum_{n_\lambda=-\infty}^{\infty} \sum_{n_\kappa=-\infty}^{\infty} \sum_{n_\gamma=-\infty}^{\infty} \sum_{n_{\sigma^+}=-\infty}^{\infty} \sum_{n_{\sigma^-}=-\infty}^{\infty} \sum_{n_\xi=-\infty}^{\infty} \sum_{n_{\xi^-}=-\infty}^{\infty} \sum_{n_\omega=-\infty}^{\infty} \right. \\
& I_{S-n_\lambda+n_\kappa-n_{\sigma^+}-n_{\sigma^-}-2n_\xi-2n_{\xi^-}-3n_\omega \pm 1} (2Z^{K^0}) I_{B+n_\lambda+n_\gamma+n_{\sigma^+}+n_{\sigma^-}+n_\xi+n_{\xi^-}+n_\omega \mp 1} (2Z^n) \\
& I_{Q+n_\kappa+n_\gamma+n_{\sigma^+}-n_{\sigma^-}-n_{\xi^-}-n_\omega} (2Z^{\pi^\pm}) I_{-n_\lambda} (2Z^{\Lambda^0}) I_{-n_\kappa} (2Z^{K^\pm}) I_{-n_\gamma} (2Z^P) \\
& I_{-n_{\sigma^+}} (2Z^{\Sigma^+}) I_{-n_{\sigma^-}} (2Z^{\Sigma^-}) I_{-n_\xi} (2Z^{\Xi^0}) I_{-n_{\xi^-}} (2Z^{\Xi^-}) I_{-n_\omega} (2Z^{\Omega^-}) \left. \right\} \\
& \cdot \exp(Z^{\pi^0})
\end{aligned}$$

$$\begin{aligned}
\left\langle N_{\frac{K^+}{K^-}} \right\rangle &= \frac{Z^{K^\pm}}{Z} \left\{ \sum_{n_\lambda=-\infty}^{\infty} \sum_{n_\kappa=-\infty}^{\infty} \sum_{n_\gamma=-\infty}^{\infty} \sum_{n_{\sigma^+}=-\infty}^{\infty} \sum_{n_{\sigma^-}=-\infty}^{\infty} \sum_{n_\xi=-\infty}^{\infty} \sum_{n_{\xi^-}=-\infty}^{\infty} \sum_{n_\omega=-\infty}^{\infty} \right. \\
& I_{S-n_\lambda+n_\kappa-n_{\sigma^+}-n_{\sigma^-}-2n_\xi-2n_{\xi^-}-3n_\omega \mp 1} (2Z^{K^0}) I_{B+n_\lambda+n_\gamma+n_{\sigma^+}+n_{\sigma^-}+n_\xi+n_{\xi^-}+n_\omega} (2Z^n) \\
& I_{Q+n_\kappa+n_\gamma+n_{\sigma^+}-n_{\sigma^-}-n_{\xi^-}-n_\omega \mp 1} (2Z^{\pi^\pm}) I_{-n_\lambda} (2Z^{\Lambda^0}) I_{-n_\kappa} (2Z^{K^\pm}) I_{-n_\gamma} (2Z^P) \\
& I_{-n_{\sigma^+}} (2Z^{\Sigma^+}) I_{-n_{\sigma^-}} (2Z^{\Sigma^-}) I_{-n_\xi} (2Z^{\Xi^0}) I_{-n_{\xi^-}} (2Z^{\Xi^-}) I_{-n_\omega} (2Z^{\Omega^-}) \left. \right\} \\
& \cdot \exp(Z^{\pi^0})
\end{aligned}$$

$$\begin{aligned}
\left\langle N_{\frac{P}{P}} \right\rangle &= \frac{Z^P}{Z} \left\{ \sum_{n_\lambda=-\infty}^{\infty} \sum_{n_\kappa=-\infty}^{\infty} \sum_{n_\gamma=-\infty}^{\infty} \sum_{n_{\sigma^+}=-\infty}^{\infty} \sum_{n_{\sigma^-}=-\infty}^{\infty} \sum_{n_\xi=-\infty}^{\infty} \sum_{n_{\xi^-}=-\infty}^{\infty} \sum_{n_\omega=-\infty}^{\infty} \right. \\
& I_{S-n_\lambda+n_\kappa-n_{\sigma^+}-n_{\sigma^-}-2n_\xi-2n_{\xi^-}-3n_\omega} (2Z^{K^0}) I_{B+n_\lambda+n_\gamma+n_{\sigma^+}+n_{\sigma^-}+n_\xi+n_{\xi^-}+n_\omega \mp 1} (2Z^n) \\
& I_{Q+n_\kappa+n_\gamma+n_{\sigma^+}-n_{\sigma^-}-n_{\xi^-}-n_\omega \mp 1} (2Z^{\pi^\pm}) I_{-n_\lambda} (2Z^{\Lambda^0}) I_{-n_\kappa} (2Z^{K^\pm}) I_{-n_\gamma} (2Z^P) \\
& I_{-n_{\sigma^+}} (2Z^{\Sigma^+}) I_{-n_{\sigma^-}} (2Z^{\Sigma^-}) I_{-n_\xi} (2Z^{\Xi^0}) I_{-n_{\xi^-}} (2Z^{\Xi^-}) I_{-n_\omega} (2Z^{\Omega^-}) \left. \right\} \\
& \cdot \exp(Z^{\pi^0})
\end{aligned}$$

$$\begin{aligned}
\left\langle N_{\frac{\Delta^-}{\Delta^-}} \right\rangle &= \frac{Z^{\Delta^-}}{Z} \left\{ \sum_{n_\lambda=-\infty}^{\infty} \sum_{n_\kappa=-\infty}^{\infty} \sum_{n_\gamma=-\infty}^{\infty} \sum_{n_{\sigma^+}=-\infty}^{\infty} \sum_{n_{\sigma^-}=-\infty}^{\infty} \sum_{n_\xi=-\infty}^{\infty} \sum_{n_{\xi^-}=-\infty}^{\infty} \sum_{n_\omega=-\infty}^{\infty} \right. \\
& I_{S-n_\lambda+n_\kappa-n_{\sigma^+}-n_{\sigma^-}-2n_\xi-2n_{\xi^-}-3n_\omega} (2Z^{K^0}) I_{B+n_\lambda+n_\gamma+n_{\sigma^+}+n_{\sigma^-}+n_\xi+n_{\xi^-}+n_\omega \mp 1} (2Z^n) \\
& I_{Q+n_\kappa+n_\gamma+n_{\sigma^+}-n_{\sigma^-}-n_{\xi^-}-n_\omega \pm 1} (2Z^{\pi^\pm}) I_{-n_\lambda} (2Z^{\Lambda^0}) I_{-n_\kappa} (2Z^{K^\pm}) I_{-n_\gamma} (2Z^P) \\
& I_{-n_{\sigma^+}} (2Z^{\Sigma^+}) I_{-n_{\sigma^-}} (2Z^{\Sigma^-}) I_{-n_\xi} (2Z^{\Xi^0}) I_{-n_{\xi^-}} (2Z^{\Xi^-}) I_{-n_\omega} (2Z^{\Omega^-}) \left. \right\} \\
& \cdot \exp(Z^{\pi^0})
\end{aligned}$$

$$\begin{aligned}
\left\langle N_{\frac{\Sigma^+}{\Sigma^+}} \right\rangle &= \frac{Z^{\Sigma^+}}{Z} \left\{ \sum_{n_\lambda=-\infty}^{\infty} \sum_{n_\kappa=-\infty}^{\infty} \sum_{n_\gamma=-\infty}^{\infty} \sum_{n_{\sigma^+}=-\infty}^{\infty} \sum_{n_{\sigma^-}=-\infty}^{\infty} \sum_{n_\xi=-\infty}^{\infty} \sum_{n_{\xi^-}=-\infty}^{\infty} \sum_{n_\omega=-\infty}^{\infty} \right. \\
&I_{S-n_\lambda+n_\kappa-n_{\sigma^+}-n_{\sigma^-}-2n_\xi-2n_{\xi^-}-3n_\omega \pm 1} (2Z^{K^0}) I_{B+n_\lambda+n_\gamma+n_{\sigma^+}+n_{\sigma^-}+n_\xi+n_{\xi^-}+n_\omega \mp 1} (2Z^n) \\
&I_{Q+n_\kappa+n_\gamma+n_{\sigma^+}-n_{\sigma^-}-n_{\xi^-}-n_\omega \mp 1} (2Z^{\pi^\pm}) I_{-n_\lambda} (2Z^{\Lambda^0}) I_{-n_\kappa} (2Z^{K^\pm}) I_{-n_\gamma} (2Z^P) \\
&I_{-n_{\sigma^+}} (2Z^{\Sigma^+}) I_{-n_{\sigma^-}} (2Z^{\Sigma^-}) I_{-n_\xi} (2Z^{\Xi^0}) I_{-n_{\xi^-}} (2Z^{\Xi^-}) I_{-n_\omega} (2Z^{\Omega^-}) \left. \right\} \\
&\cdot \exp(Z^{\pi^0})
\end{aligned}$$

$$\begin{aligned}
\left\langle N_{\frac{\Sigma^-}{\Sigma^-}} \right\rangle &= \frac{Z^{\Sigma^-}}{Z} \left\{ \sum_{n_\lambda=-\infty}^{\infty} \sum_{n_\kappa=-\infty}^{\infty} \sum_{n_\gamma=-\infty}^{\infty} \sum_{n_{\sigma^+}=-\infty}^{\infty} \sum_{n_{\sigma^-}=-\infty}^{\infty} \sum_{n_\xi=-\infty}^{\infty} \sum_{n_{\xi^-}=-\infty}^{\infty} \sum_{n_\omega=-\infty}^{\infty} \right. \\
&I_{S-n_\lambda+n_\kappa-n_{\sigma^+}-n_{\sigma^-}-2n_\xi-2n_{\xi^-}-3n_\omega \pm 1} (2Z^{K^0}) I_{B+n_\lambda+n_\gamma+n_{\sigma^+}+n_{\sigma^-}+n_\xi+n_{\xi^-}+n_\omega \mp 1} (2Z^n) \\
&I_{Q+n_\kappa+n_\gamma+n_{\sigma^+}-n_{\sigma^-}-n_{\xi^-}-n_\omega \pm 1} (2Z^{\pi^\pm}) I_{-n_\lambda} (2Z^{\Lambda^0}) I_{-n_\kappa} (2Z^{K^\pm}) I_{-n_\gamma} (2Z^P) \\
&I_{-n_{\sigma^+}} (2Z^{\Sigma^+}) I_{-n_{\sigma^-}} (2Z^{\Sigma^-}) I_{-n_\xi} (2Z^{\Xi^0}) I_{-n_{\xi^-}} (2Z^{\Xi^-}) I_{-n_\omega} (2Z^{\Omega^-}) \left. \right\} \\
&\cdot \exp(Z^{\pi^0})
\end{aligned}$$

$$\begin{aligned}
\left\langle N_{\frac{\Xi^0}{\Xi^0}} \right\rangle &= \frac{Z^{\Xi^0}}{Z} \left\{ \sum_{n_\lambda=-\infty}^{\infty} \sum_{n_\kappa=-\infty}^{\infty} \sum_{n_\gamma=-\infty}^{\infty} \sum_{n_{\sigma^+}=-\infty}^{\infty} \sum_{n_{\sigma^-}=-\infty}^{\infty} \sum_{n_\xi=-\infty}^{\infty} \sum_{n_{\xi^-}=-\infty}^{\infty} \sum_{n_\omega=-\infty}^{\infty} \right. \\
&I_{S-n_\lambda+n_\kappa-n_{\sigma^+}-n_{\sigma^-}-2n_\xi-2n_{\xi^-}-3n_\omega \pm 2} (2Z^{K^0}) I_{B+n_\lambda+n_\gamma+n_{\sigma^+}+n_{\sigma^-}+n_\xi+n_{\xi^-}+n_\omega \mp 1} (2Z^n) \\
&I_{Q+n_\kappa+n_\gamma+n_{\sigma^+}-n_{\sigma^-}-n_{\xi^-}-n_\omega} (2Z^{\pi^\pm}) I_{-n_\lambda} (2Z^{\Lambda^0}) I_{-n_\kappa} (2Z^{K^\pm}) I_{-n_\gamma} (2Z^P) \\
&I_{-n_{\sigma^+}} (2Z^{\Sigma^+}) I_{-n_{\sigma^-}} (2Z^{\Sigma^-}) I_{-n_\xi} (2Z^{\Xi^0}) I_{-n_{\xi^-}} (2Z^{\Xi^-}) I_{-n_\omega} (2Z^{\Omega^-}) \left. \right\} \\
&\cdot \exp(Z^{\pi^0})
\end{aligned}$$

$$\begin{aligned}
\left\langle N_{\frac{\Xi^-}{\Xi^-}} \right\rangle &= \frac{Z^{\Xi^-}}{Z} \left\{ \sum_{n_\lambda=-\infty}^{\infty} \sum_{n_\kappa=-\infty}^{\infty} \sum_{n_\gamma=-\infty}^{\infty} \sum_{n_{\sigma^+}=-\infty}^{\infty} \sum_{n_{\sigma^-}=-\infty}^{\infty} \sum_{n_\xi=-\infty}^{\infty} \sum_{n_{\xi^-}=-\infty}^{\infty} \sum_{n_\omega=-\infty}^{\infty} \right. \\
&I_{S-n_\lambda+n_\kappa-n_{\sigma^+}-n_{\sigma^-}-2n_\xi-2n_{\xi^-}-3n_\omega \pm 2} (2Z^{K^0}) I_{B+n_\lambda+n_\gamma+n_{\sigma^+}+n_{\sigma^-}+n_\xi+n_{\xi^-}+n_\omega \mp 1} (2Z^n) \\
&I_{Q+n_\kappa+n_\gamma+n_{\sigma^+}-n_{\sigma^-}-n_{\xi^-}-n_\omega \pm 1} (2Z^{\pi^\pm}) I_{-n_\lambda} (2Z^{\Lambda^0}) I_{-n_\kappa} (2Z^{K^\pm}) I_{-n_\gamma} (2Z^P) \\
&I_{-n_{\sigma^+}} (2Z^{\Sigma^+}) I_{-n_{\sigma^-}} (2Z^{\Sigma^-}) I_{-n_\xi} (2Z^{\Xi^0}) I_{-n_{\xi^-}} (2Z^{\Xi^-}) I_{-n_\omega} (2Z^{\Omega^-}) \left. \right\} \\
&\cdot \exp(Z^{\pi^0})
\end{aligned}$$

$$\begin{aligned}
\left\langle N_{\frac{\Omega^-}{\Omega^-}} \right\rangle &= \frac{Z^{\Omega^-}}{Z} \left\{ \sum_{n_\lambda=-\infty}^{\infty} \sum_{n_\kappa=-\infty}^{\infty} \sum_{n_\gamma=-\infty}^{\infty} \sum_{n_{\sigma^+}=-\infty}^{\infty} \sum_{n_{\sigma^-}=-\infty}^{\infty} \sum_{n_\xi=-\infty}^{\infty} \sum_{n_{\xi^-}=-\infty}^{\infty} \sum_{n_\omega=-\infty}^{\infty} \right. \\
& I_{S-n_\lambda+n_\kappa-n_{\sigma^+}-n_{\sigma^-}-2n_\xi-2n_{\xi^-}-3n_\omega \pm 3} (2Z^{K^0}) I_{B+n_\lambda+n_\gamma+n_{\sigma^+}+n_{\sigma^-}+n_\xi+n_{\xi^-}+n_\omega \mp 1} (2Z^n) \\
& I_{Q+n_\kappa+n_\gamma+n_{\sigma^+}-n_{\sigma^-}-n_{\xi^-}-n_\omega \pm 1} (2Z^{\pi^\pm}) I_{-n_\lambda} (2Z^{\Lambda^0}) I_{-n_\kappa} (2Z^{K^\pm}) I_{-n_\gamma} (2Z^P) \\
& I_{-n_{\sigma^+}} (2Z^{\Sigma^+}) I_{-n_{\sigma^-}} (2Z^{\Sigma^-}) I_{-n_\xi} (2Z^{\Xi^0}) I_{-n_{\xi^-}} (2Z^{\Xi^-}) I_{-n_\omega} (2Z^{\Omega^-}) \left. \right\} \\
& \cdot \exp(Z^{\pi^0}) \tag{C.2}
\end{aligned}$$

C.0.3 Case 4: Baryon number = 0,±1, Strangeness = 0,±1,±2, ±3, Charge = 0,±1,±2

$$\begin{aligned}
\left\langle N_{\frac{K^0}{K^0}} \right\rangle &= \frac{Z^{K^0}}{Z} \left\{ \sum_{n_\lambda=-\infty}^{\infty} \sum_{n_\kappa=-\infty}^{\infty} \sum_{n_\gamma=-\infty}^{\infty} \sum_{n_{\delta^-}=-\infty}^{\infty} \sum_{n_{\sigma^+}=-\infty}^{\infty} \sum_{n_{\sigma^-}=-\infty}^{\infty} \sum_{n_\xi=-\infty}^{\infty} \sum_{n_{\xi^-}=-\infty}^{\infty} \sum_{n_\omega=-\infty}^{\infty} \sum_{n_{\delta^{++}}=-\infty}^{\infty} \right. \\
& I_{S-n_\lambda+n_\kappa-n_{\sigma^+}-n_{\sigma^-}-2n_\xi-2n_{\xi^-}-3n_\omega \mp 1} (2Z^{K^0}) \\
& I_{B+n_\lambda+n_\gamma+n_{\delta^-}+n_{\sigma^+}+n_{\sigma^-}+n_\xi+n_{\xi^-}+n_\omega+n_{\delta^{++}} (2Z^n) \\
& I_{Q+n_\kappa+n_\gamma-n_{\delta^-}+n_{\sigma^+}-n_{\sigma^-}-n_{\xi^-}-n_\omega+2n_{\delta^{++}} (2Z^{\pi^\pm}) \\
& I_{-n_\lambda} (2Z^{\Lambda^0}) I_{-n_\kappa} (2Z^{K^\pm}) I_{-n_\gamma} (2Z^P) I_{-n_{\delta^-}} (2Z^{\Delta^-}) I_{-n_{\sigma^+}} (2Z^{\Sigma^+}) I_{-n_{\sigma^-}} (2Z^{\Sigma^-}) \\
& I_{-n_\xi} (2Z^{\Xi^0}) I_{-n_{\xi^-}} (2Z^{\Xi^-}) I_{-n_\omega} (2Z^{\Omega^-}) I_{-n_{\delta^{++}}} (2Z^{\Delta^{++}}) \left. \right\} \cdot \exp(Z^{\pi^0})
\end{aligned}$$

$$\begin{aligned}
\left\langle N_{\frac{\pi^0}{\pi^0}} \right\rangle &= \frac{Z^n}{Z} \left\{ \sum_{n_\lambda=-\infty}^{\infty} \sum_{n_\kappa=-\infty}^{\infty} \sum_{n_\gamma=-\infty}^{\infty} \sum_{n_{\delta^-}=-\infty}^{\infty} \sum_{n_{\sigma^+}=-\infty}^{\infty} \sum_{n_{\sigma^-}=-\infty}^{\infty} \sum_{n_\xi=-\infty}^{\infty} \sum_{n_{\xi^-}=-\infty}^{\infty} \sum_{n_\omega=-\infty}^{\infty} \sum_{n_{\delta^{++}}=-\infty}^{\infty} \right. \\
& I_{S-n_\lambda+n_\kappa-n_{\sigma^+}-n_{\sigma^-}-2n_\xi-2n_{\xi^-}-3n_\omega} (2Z^{K^0}) \\
& I_{B+n_\lambda+n_\gamma+n_{\delta^-}+n_{\sigma^+}+n_{\sigma^-}+n_\xi+n_{\xi^-}+n_\omega+n_{\delta^{++}} \mp 1} (2Z^n) \\
& I_{Q+n_\kappa+n_\gamma-n_{\delta^-}+n_{\sigma^+}-n_{\sigma^-}-n_{\xi^-}-n_\omega+2n_{\delta^{++}} (2Z^{\pi^\pm}) \\
& I_{-n_\lambda} (2Z^{\Lambda^0}) I_{-n_\kappa} (2Z^{K^\pm}) I_{-n_\gamma} (2Z^P) I_{-n_{\delta^-}} (2Z^{\Delta^-}) I_{-n_{\sigma^+}} (2Z^{\Sigma^+}) I_{-n_{\sigma^-}} (2Z^{\Sigma^-}) \\
& I_{-n_\xi} (2Z^{\Xi^0}) I_{-n_{\xi^-}} (2Z^{\Xi^-}) I_{-n_\omega} (2Z^{\Omega^-}) I_{-n_{\delta^{++}}} (2Z^{\Delta^{++}}) \left. \right\} \cdot \exp(Z^{\pi^0})
\end{aligned}$$

$$\left\langle N_{\frac{\pi^\pm}{\pi^\pm}} \right\rangle = \frac{Z^{\pi^\pm}}{Z} \left\{ \sum_{n_\lambda=-\infty}^{\infty} \sum_{n_\kappa=-\infty}^{\infty} \sum_{n_\gamma=-\infty}^{\infty} \sum_{n_{\delta^-}=-\infty}^{\infty} \sum_{n_{\sigma^+}=-\infty}^{\infty} \sum_{n_{\sigma^-}=-\infty}^{\infty} \sum_{n_\xi=-\infty}^{\infty} \sum_{n_{\xi^-}=-\infty}^{\infty} \sum_{n_\omega=-\infty}^{\infty} \sum_{n_{\delta^{++}}=-\infty}^{\infty} \right.$$

$$\begin{aligned}
& I_{S-n_\lambda+n_\kappa-n_{\sigma^+}-n_{\sigma^-}-2n_\xi-2n_{\xi^-}-3n_\omega} (2Z^{K^0}) \\
& I_{B+n_\lambda+n_\gamma+n_{\delta^-}+n_{\sigma^+}+n_{\sigma^-}+n_\xi+n_{\xi^-}+n_\omega+n_{\delta^{++}}} (2Z^n) \\
& I_{Q+n_\kappa+n_\gamma-n_{\delta^-}+n_{\sigma^+}-n_{\sigma^-}-n_{\xi^-}-n_\omega+2n_{\delta^{++}} \mp 1} (2Z^{\pi^\pm}) \\
& I_{-n_\lambda} (2Z^{\Lambda^0}) I_{-n_\kappa} (2Z^{K^\pm}) I_{-n_\gamma} (2Z^p) I_{-n_{\delta^-}} (2Z^{\Delta^-}) I_{-n_{\sigma^+}} (2Z^{\Sigma^+}) I_{-n_{\sigma^-}} (2Z^{\Sigma^-}) \\
& I_{-n_\xi} (2Z^{\Xi^0}) I_{-n_{\xi^-}} (2Z^{\Xi^-}) I_{-n_\omega} (2Z^{\Omega^-}) I_{-n_{\delta^{++}}} (2Z^{\Delta^{++}}) \} \cdot \exp(Z^{\pi^0})
\end{aligned}$$

$$\begin{aligned}
\left\langle N_{\frac{\Lambda^0}{\Lambda^0}} \right\rangle &= \frac{Z^{\Lambda^0}}{Z} \left\{ \sum_{n_\lambda=-\infty}^{\infty} \sum_{n_\kappa=-\infty}^{\infty} \sum_{n_\gamma=-\infty}^{\infty} \sum_{n_{\delta^-}=-\infty}^{\infty} \sum_{n_{\sigma^+}=-\infty}^{\infty} \sum_{n_{\sigma^-}=-\infty}^{\infty} \sum_{n_\xi=-\infty}^{\infty} \sum_{n_{\xi^-}=-\infty}^{\infty} \sum_{n_\omega=-\infty}^{\infty} \sum_{n_{\delta^{++}}=-\infty}^{\infty} \right. \\
& I_{S-n_\lambda+n_\kappa-n_{\sigma^+}-n_{\sigma^-}-2n_\xi-2n_{\xi^-}-3n_\omega \pm 1} (2Z^{K^0}) \\
& I_{B+n_\lambda+n_\gamma+n_{\delta^-}+n_{\sigma^+}+n_{\sigma^-}+n_\xi+n_{\xi^-}+n_\omega+n_{\delta^{++}} \mp 1} (2Z^n) \\
& I_{Q+n_\kappa+n_\gamma-n_{\delta^-}+n_{\sigma^+}-n_{\sigma^-}-n_{\xi^-}-n_\omega+2n_{\delta^{++}}} (2Z^{\pi^\pm}) \\
& I_{-n_\lambda} (2Z^{\Lambda^0}) I_{-n_\kappa} (2Z^{K^\pm}) I_{-n_\gamma} (2Z^p) I_{-n_{\delta^-}} (2Z^{\Delta^-}) I_{-n_{\sigma^+}} (2Z^{\Sigma^+}) I_{-n_{\sigma^-}} (2Z^{\Sigma^-}) \\
& \left. I_{-n_\xi} (2Z^{\Xi^0}) I_{-n_{\xi^-}} (2Z^{\Xi^-}) I_{-n_\omega} (2Z^{\Omega^-}) I_{-n_{\delta^{++}}} (2Z^{\Delta^{++}}) \right\} \cdot \exp(Z^{\pi^0})
\end{aligned}$$

$$\begin{aligned}
\left\langle N_{\frac{K^+}{K^-}} \right\rangle &= \frac{Z^{K^\pm}}{Z} \left\{ \sum_{n_\lambda=-\infty}^{\infty} \sum_{n_\kappa=-\infty}^{\infty} \sum_{n_\gamma=-\infty}^{\infty} \sum_{n_{\delta^-}=-\infty}^{\infty} \sum_{n_{\sigma^+}=-\infty}^{\infty} \sum_{n_{\sigma^-}=-\infty}^{\infty} \sum_{n_\xi=-\infty}^{\infty} \sum_{n_{\xi^-}=-\infty}^{\infty} \sum_{n_\omega=-\infty}^{\infty} \sum_{n_{\delta^{++}}=-\infty}^{\infty} \right. \\
& I_{S-n_\lambda+n_\kappa-n_{\sigma^+}-n_{\sigma^-}-2n_\xi-2n_{\xi^-}-3n_\omega \mp 1} (2Z^{K^0}) \\
& I_{B+n_\lambda+n_\gamma+n_{\delta^-}+n_{\sigma^+}+n_{\sigma^-}+n_\xi+n_{\xi^-}+n_\omega+n_{\delta^{++}}} (2Z^n) \\
& I_{Q+n_\kappa+n_\gamma-n_{\delta^-}+n_{\sigma^+}-n_{\sigma^-}-n_{\xi^-}-n_\omega+2n_{\delta^{++}} \mp 1} (2Z^{\pi^\pm}) \\
& I_{-n_\lambda} (2Z^{\Lambda^0}) I_{-n_\kappa} (2Z^{K^\pm}) I_{-n_\gamma} (2Z^p) I_{-n_{\delta^-}} (2Z^{\Delta^-}) I_{-n_{\sigma^+}} (2Z^{\Sigma^+}) I_{-n_{\sigma^-}} (2Z^{\Sigma^-}) \\
& \left. I_{-n_\xi} (2Z^{\Xi^0}) I_{-n_{\xi^-}} (2Z^{\Xi^-}) I_{-n_\omega} (2Z^{\Omega^-}) I_{-n_{\delta^{++}}} (2Z^{\Delta^{++}}) \right\} \cdot \exp(Z^{\pi^0})
\end{aligned}$$

$$\begin{aligned}
\left\langle N_{\frac{p}{p}} \right\rangle &= \frac{Z^p}{Z} \left\{ \sum_{n_\lambda=-\infty}^{\infty} \sum_{n_\kappa=-\infty}^{\infty} \sum_{n_\gamma=-\infty}^{\infty} \sum_{n_{\delta^-}=-\infty}^{\infty} \sum_{n_{\sigma^+}=-\infty}^{\infty} \sum_{n_{\sigma^-}=-\infty}^{\infty} \sum_{n_\xi=-\infty}^{\infty} \sum_{n_{\xi^-}=-\infty}^{\infty} \sum_{n_\omega=-\infty}^{\infty} \sum_{n_{\delta^{++}}=-\infty}^{\infty} \right. \\
& I_{S-n_\lambda+n_\kappa-n_{\sigma^+}-n_{\sigma^-}-2n_\xi-2n_{\xi^-}-3n_\omega} (2Z^{K^0}) \\
& I_{B+n_\lambda+n_\gamma+n_{\delta^-}+n_{\sigma^+}+n_{\sigma^-}+n_\xi+n_{\xi^-}+n_\omega+n_{\delta^{++}} \mp 1} (2Z^n) \\
& I_{Q+n_\kappa+n_\gamma-n_{\delta^-}+n_{\sigma^+}-n_{\sigma^-}-n_{\xi^-}-n_\omega+2n_{\delta^{++}} \mp 1} (2Z^{\pi^\pm})
\end{aligned}$$

$$I_{-n_\lambda} (2Z^{\Lambda^0}) I_{-n_\kappa} (2Z^{K^\pm}) I_{-n_\gamma} (2Z^p) I_{-n_{\delta^-}} (2Z^{\Delta^-}) I_{-n_{\sigma^+}} (2Z^{\Sigma^+}) I_{-n_{\sigma^-}} (2Z^{\Sigma^-}) \\ I_{-n_\xi} (2Z^{\Xi^0}) I_{-n_{\xi^-}} (2Z^{\Xi^-}) I_{-n_\omega} (2Z^{\Omega^-}) I_{-n_{\delta^{++}}} (2Z^{\Delta^{++}}) \} \cdot \exp (Z^{\pi^0})$$

$$\left\langle N_{\frac{\Delta^-}{\Delta^-}} \right\rangle = \frac{Z^{\Delta^-}}{Z} \left\{ \sum_{n_\lambda=-\infty}^{\infty} \sum_{n_\kappa=-\infty}^{\infty} \sum_{n_\gamma=-\infty}^{\infty} \sum_{n_{\delta^-}=-\infty}^{\infty} \sum_{n_{\sigma^+}=-\infty}^{\infty} \sum_{n_{\sigma^-}=-\infty}^{\infty} \sum_{n_\xi=-\infty}^{\infty} \sum_{n_{\xi^-}=-\infty}^{\infty} \sum_{n_\omega=-\infty}^{\infty} \sum_{n_{\delta^{++}}=-\infty}^{\infty} \right. \\ I_{S-n_\lambda+n_\kappa-n_{\sigma^+}-n_{\sigma^-}-2n_\xi-2n_{\xi^-}-3n_\omega} (2Z^{K^0}) \\ I_{B+n_\lambda+n_\gamma+n_{\delta^-}+n_{\sigma^+}+n_{\sigma^-}+n_\xi+n_{\xi^-}+n_\omega+n_{\delta^{++}} \mp 1} (2Z^n) \\ I_{Q+n_\kappa+n_\gamma-n_{\delta^-}+n_{\sigma^+}-n_{\sigma^-}-n_{\xi^-}-n_\omega+2n_{\delta^{++}} \pm 1} (2Z^{\pi^\pm}) \\ I_{-n_\lambda} (2Z^{\Lambda^0}) I_{-n_\kappa} (2Z^{K^\pm}) I_{-n_\gamma} (2Z^p) I_{-n_{\delta^-}} (2Z^{\Delta^-}) I_{-n_{\sigma^+}} (2Z^{\Sigma^+}) I_{-n_{\sigma^-}} (2Z^{\Sigma^-}) \\ I_{-n_\xi} (2Z^{\Xi^0}) I_{-n_{\xi^-}} (2Z^{\Xi^-}) I_{-n_\omega} (2Z^{\Omega^-}) I_{-n_{\delta^{++}}} (2Z^{\Delta^{++}}) \} \cdot \exp (Z^{\pi^0})$$

$$\left\langle N_{\frac{\Sigma^+}{\Sigma^+}} \right\rangle = \frac{Z^{\Sigma^+}}{Z} \left\{ \sum_{n_\lambda=-\infty}^{\infty} \sum_{n_\kappa=-\infty}^{\infty} \sum_{n_\gamma=-\infty}^{\infty} \sum_{n_{\delta^-}=-\infty}^{\infty} \sum_{n_{\sigma^+}=-\infty}^{\infty} \sum_{n_{\sigma^-}=-\infty}^{\infty} \sum_{n_\xi=-\infty}^{\infty} \sum_{n_{\xi^-}=-\infty}^{\infty} \sum_{n_\omega=-\infty}^{\infty} \sum_{n_{\delta^{++}}=-\infty}^{\infty} \right. \\ I_{S-n_\lambda+n_\kappa-n_{\sigma^+}-n_{\sigma^-}-2n_\xi-2n_{\xi^-}-3n_\omega \pm 1} (2Z^{K^0}) \\ I_{B+n_\lambda+n_\gamma+n_{\delta^-}+n_{\sigma^+}+n_{\sigma^-}+n_\xi+n_{\xi^-}+n_\omega+n_{\delta^{++}} \mp 1} (2Z^n) \\ I_{Q+n_\kappa+n_\gamma-n_{\delta^-}+n_{\sigma^+}-n_{\sigma^-}-n_{\xi^-}-n_\omega+2n_{\delta^{++}} \mp 1} (2Z^{\pi^\pm}) \\ I_{-n_\lambda} (2Z^{\Lambda^0}) I_{-n_\kappa} (2Z^{K^\pm}) I_{-n_\gamma} (2Z^p) I_{-n_{\delta^-}} (2Z^{\Delta^-}) I_{-n_{\sigma^+}} (2Z^{\Sigma^+}) I_{-n_{\sigma^-}} (2Z^{\Sigma^-}) \\ I_{-n_\xi} (2Z^{\Xi^0}) I_{-n_{\xi^-}} (2Z^{\Xi^-}) I_{-n_\omega} (2Z^{\Omega^-}) I_{-n_{\delta^{++}}} (2Z^{\Delta^{++}}) \} \cdot \exp (Z^{\pi^0})$$

$$\left\langle N_{\frac{\Sigma^-}{\Sigma^-}} \right\rangle = \frac{Z^{\Sigma^-}}{Z} \left\{ \sum_{n_\lambda=-\infty}^{\infty} \sum_{n_\kappa=-\infty}^{\infty} \sum_{n_\gamma=-\infty}^{\infty} \sum_{n_{\delta^-}=-\infty}^{\infty} \sum_{n_{\sigma^+}=-\infty}^{\infty} \sum_{n_{\sigma^-}=-\infty}^{\infty} \sum_{n_\xi=-\infty}^{\infty} \sum_{n_{\xi^-}=-\infty}^{\infty} \sum_{n_\omega=-\infty}^{\infty} \sum_{n_{\delta^{++}}=-\infty}^{\infty} \right. \\ I_{S-n_\lambda+n_\kappa-n_{\sigma^+}-n_{\sigma^-}-2n_\xi-2n_{\xi^-}-3n_\omega \pm 1} (2Z^{K^0}) \\ I_{B+n_\lambda+n_\gamma+n_{\delta^-}+n_{\sigma^+}+n_{\sigma^-}+n_\xi+n_{\xi^-}+n_\omega+n_{\delta^{++}} \mp 1} (2Z^n) \\ I_{Q+n_\kappa+n_\gamma-n_{\delta^-}+n_{\sigma^+}-n_{\sigma^-}-n_{\xi^-}-n_\omega+2n_{\delta^{++}} \pm 1} (2Z^{\pi^\pm}) \\ I_{-n_\lambda} (2Z^{\Lambda^0}) I_{-n_\kappa} (2Z^{K^\pm}) I_{-n_\gamma} (2Z^p) I_{-n_{\delta^-}} (2Z^{\Delta^-}) I_{-n_{\sigma^+}} (2Z^{\Sigma^+}) I_{-n_{\sigma^-}} (2Z^{\Sigma^-}) \\ I_{-n_\xi} (2Z^{\Xi^0}) I_{-n_{\xi^-}} (2Z^{\Xi^-}) I_{-n_\omega} (2Z^{\Omega^-}) I_{-n_{\delta^{++}}} (2Z^{\Delta^{++}}) \} \cdot \exp (Z^{\pi^0})$$

$$\begin{aligned}
\left\langle N_{\frac{\Xi^0}{\Xi^0}} \right\rangle &= \frac{Z^{\Xi^0}}{Z} \left\{ \sum_{n_\lambda=-\infty}^{\infty} \sum_{n_\kappa=-\infty}^{\infty} \sum_{n_\gamma=-\infty}^{\infty} \sum_{n_\delta=-\infty}^{\infty} \sum_{n_{\sigma^+}=-\infty}^{\infty} \sum_{n_{\sigma^-}=-\infty}^{\infty} \sum_{n_\xi=-\infty}^{\infty} \sum_{n_{\xi^-}=-\infty}^{\infty} \sum_{n_\omega=-\infty}^{\infty} \sum_{n_{\delta^{++}}=-\infty}^{\infty} \right. \\
&I_{S-n_\lambda+n_\kappa-n_{\sigma^+}-n_{\sigma^-}-2n_\xi-2n_{\xi^-}-3n_\omega \pm 2} (2Z^{K^0}) \\
&I_{B+n_\lambda+n_\gamma+n_{\delta^-}+n_{\sigma^+}+n_{\sigma^-}+n_\xi+n_{\xi^-}+n_\omega+n_{\delta^{++}} \mp 1} (2Z^n) \\
&I_{Q+n_\kappa+n_\gamma-n_{\delta^-}+n_{\sigma^+}-n_{\sigma^-}-n_{\xi^-}-n_\omega+2n_{\delta^{++}}} (2Z^{\pi^\pm}) \\
&I_{-n_\lambda} (2Z^{\Lambda^0}) I_{-n_\kappa} (2Z^{K^\pm}) I_{-n_\gamma} (2Z^p) I_{-n_{\delta^-}} (2Z^{\Delta^-}) I_{-n_{\sigma^+}} (2Z^{\Sigma^+}) I_{-n_{\sigma^-}} (2Z^{\Sigma^-}) \\
&I_{-n_\xi} (2Z^{\Xi^0}) I_{-n_{\xi^-}} (2Z^{\Xi^-}) I_{-n_\omega} (2Z^{\Omega^-}) I_{-n_{\delta^{++}}} (2Z^{\Delta^{++}}) \left. \right\} \cdot \exp(Z^{\pi^0})
\end{aligned}$$

$$\begin{aligned}
\left\langle N_{\frac{\Xi^-}{\Xi^-}} \right\rangle &= \frac{Z^{\Xi^-}}{Z} \left\{ \sum_{n_\lambda=-\infty}^{\infty} \sum_{n_\kappa=-\infty}^{\infty} \sum_{n_\gamma=-\infty}^{\infty} \sum_{n_\delta=-\infty}^{\infty} \sum_{n_{\sigma^+}=-\infty}^{\infty} \sum_{n_{\sigma^-}=-\infty}^{\infty} \sum_{n_\xi=-\infty}^{\infty} \sum_{n_{\xi^-}=-\infty}^{\infty} \sum_{n_\omega=-\infty}^{\infty} \sum_{n_{\delta^{++}}=-\infty}^{\infty} \right. \\
&I_{S-n_\lambda+n_\kappa-n_{\sigma^+}-n_{\sigma^-}-2n_\xi-2n_{\xi^-}-3n_\omega \pm 2} (2Z^{K^0}) \\
&I_{B+n_\lambda+n_\gamma+n_{\delta^-}+n_{\sigma^+}+n_{\sigma^-}+n_\xi+n_{\xi^-}+n_\omega+n_{\delta^{++}} \mp 1} (2Z^n) \\
&I_{Q+n_\kappa+n_\gamma-n_{\delta^-}+n_{\sigma^+}-n_{\sigma^-}-n_{\xi^-}-n_\omega+2n_{\delta^{++}} \pm 1} (2Z^{\pi^\pm}) \\
&I_{-n_\lambda} (2Z^{\Lambda^0}) I_{-n_\kappa} (2Z^{K^\pm}) I_{-n_\gamma} (2Z^p) I_{-n_{\delta^-}} (2Z^{\Delta^-}) I_{-n_{\sigma^+}} (2Z^{\Sigma^+}) I_{-n_{\sigma^-}} (2Z^{\Sigma^-}) \\
&I_{-n_\xi} (2Z^{\Xi^0}) I_{-n_{\xi^-}} (2Z^{\Xi^-}) I_{-n_\omega} (2Z^{\Omega^-}) I_{-n_{\delta^{++}}} (2Z^{\Delta^{++}}) \left. \right\} \cdot \exp(Z^{\pi^0})
\end{aligned}$$

$$\begin{aligned}
\left\langle N_{\frac{\Omega^-}{\Omega^-}} \right\rangle &= \frac{Z^{\Omega^-}}{Z} \left\{ \sum_{n_\lambda=-\infty}^{\infty} \sum_{n_\kappa=-\infty}^{\infty} \sum_{n_\gamma=-\infty}^{\infty} \sum_{n_\delta=-\infty}^{\infty} \sum_{n_{\sigma^+}=-\infty}^{\infty} \sum_{n_{\sigma^-}=-\infty}^{\infty} \sum_{n_\xi=-\infty}^{\infty} \sum_{n_{\xi^-}=-\infty}^{\infty} \sum_{n_\omega=-\infty}^{\infty} \sum_{n_{\delta^{++}}=-\infty}^{\infty} \right. \\
&I_{S-n_\lambda+n_\kappa-n_{\sigma^+}-n_{\sigma^-}-2n_\xi-2n_{\xi^-}-3n_\omega \pm 3} (2Z^{K^0}) \\
&I_{B+n_\lambda+n_\gamma+n_{\delta^-}+n_{\sigma^+}+n_{\sigma^-}+n_\xi+n_{\xi^-}+n_\omega+n_{\delta^{++}} \mp 1} (2Z^n) \\
&I_{Q+n_\kappa+n_\gamma-n_{\delta^-}+n_{\sigma^+}-n_{\sigma^-}-n_{\xi^-}-n_\omega+2n_{\delta^{++}} \pm 1} (2Z^{\pi^\pm}) \\
&I_{-n_\lambda} (2Z^{\Lambda^0}) I_{-n_\kappa} (2Z^{K^\pm}) I_{-n_\gamma} (2Z^p) I_{-n_{\delta^-}} (2Z^{\Delta^-}) I_{-n_{\sigma^+}} (2Z^{\Sigma^+}) I_{-n_{\sigma^-}} (2Z^{\Sigma^-}) \\
&I_{-n_\xi} (2Z^{\Xi^0}) I_{-n_{\xi^-}} (2Z^{\Xi^-}) I_{-n_\omega} (2Z^{\Omega^-}) I_{-n_{\delta^{++}}} (2Z^{\Delta^{++}}) \left. \right\} \cdot \exp(Z^{\pi^0})
\end{aligned}$$

$$\left\langle N_{\frac{\Delta^{++}}{\Delta^{++}}} \right\rangle = \frac{Z^{\Delta^{++}}}{Z} \left\{ \sum_{n_\lambda=-\infty}^{\infty} \sum_{n_\kappa=-\infty}^{\infty} \sum_{n_\gamma=-\infty}^{\infty} \sum_{n_\delta=-\infty}^{\infty} \sum_{n_{\sigma^+}=-\infty}^{\infty} \sum_{n_{\sigma^-}=-\infty}^{\infty} \sum_{n_\xi=-\infty}^{\infty} \sum_{n_{\xi^-}=-\infty}^{\infty} \sum_{n_\omega=-\infty}^{\infty} \sum_{n_{\delta^{++}}=-\infty}^{\infty} \right.$$

$$\begin{aligned}
& I_{S-n_\lambda+n_\kappa-n_{\sigma^+}-n_{\sigma^-}-2n_\xi-2n_{\xi^-}-3n_\omega} (2Z^{K^0}) \\
& I_{B+n_\lambda+n_\gamma+n_{\delta^-}+n_{\sigma^+}+n_{\sigma^-}+n_\xi+n_{\xi^-}+n_\omega+n_{\delta^{++}} \mp 1} (2Z^n) \\
& I_{Q+n_\kappa+n_\gamma-n_{\delta^-}+n_{\sigma^+}-n_{\sigma^-}-n_{\xi^-}-n_\omega+2n_{\delta^{++}} \mp 2} (2Z^{\pi^\pm}) \\
& I_{-n_\lambda} (2Z^{\Lambda^0}) I_{-n_\kappa} (2Z^{K^\pm}) I_{-n_\gamma} (2Z^p) I_{-n_{\delta^-}} (2Z^{\Delta^-}) I_{-n_{\sigma^+}} (2Z^{\Sigma^+}) I_{-n_{\sigma^-}} (2Z^{\Sigma^-}) \\
& I_{-n_\xi} (2Z^{\Xi^0}) I_{-n_{\xi^-}} (2Z^{\Xi^-}) I_{-n_\omega} (2Z^{\Omega^-}) I_{-n_{\delta^{++}}} (2Z^{\Delta^{++}}) \} \cdot \exp(Z^{\pi^0}) \quad (C.3)
\end{aligned}$$

Bibliography

- [1] L. Willets, Quark Models of Hadronic Interactions, in *Hadrons and Heavy Ions*, edited by W.D. Heiss; Springer-Verlag, (1985).
- [2] J. Rafelski, M. Danos, Nuclear Matter Under Extreme Conditions, in *Hadrons and Heavy Ions*, edited by W.D. Heiss; Springer-Verlag, (1985).
- [3] J. Rafelski, M. Danos, Perspectives in High Energy Nuclear Collisions, NBSIR 83-2725, Washington, D.C., (1983).
- [4] Workshop on Future Relativistic Heavy Ion Experiments, Proceedings edited by R. Stock and R. Bock, GSI 81-6, Orange Report, (1981).
- [5] Workshop on Quark Matter Formation and Heavy Ion Collisions, Proceedings edited by M. Jacob and H. Satz, World Scientific Publ. Co., Singapore, (1982).
- [6] H. Satz, Critical Behaviour in Statistical QCD, in *The Quark Structure of Matter*, edited by M. Jacob and K. Winter; World Scientific Publ. Co., Singapore, (1986).
- [7] L. McLerran, Quark-Gluon Plasma and Space-Time Picture of Ultra-relativistic Nuclear Collisions, in *Hadrons and Hadronic Matter*, edited by D. Vautherin, F. Lenz and J.W. Negele; Plenum Press, New York, (1990).
- [8] R. Hagedorn, Suppl. Nuovo Cimento 6, 311, (1968).
- [9] R. Hagedorn, The Long Way to the Statistical Bootstrap Model, in *Hadrons and Hadronic Matter*, edited by J. Letessier, H. Gutbrod and J. Rafelski; Plenum Press, New York, (1995).
- [10] W. Heisenberg, Z. Phys. 101, 533, (1936).

- [11] F. Becattini, University of Florence preprint DFF 263-12, (1996), (to be published in the proceedings of the XXXIII Eloisatron Workshop, Erice (Italy), October 19-25, 1996).
- [12] V.F. Weisskopf, *Phys. Rev.* 52, 295, (1937).
- [13] H. Koppe, *Phys. Rev.* 76, 688, (1949).
- [14] H. Koppe, *Zs .f. Naturfoschung* 3a, 251, (1948).
- [15] E. Fermi, *Progr. Theor. Phys.* 5, 570, (1950).
- [16] W. Blümel, P. Koch and U. Heinz, *Z. f. Physik, C* 63, 637 (1994).
- [17] W.H. Barkas et al., *Phys. Rev.* 5, 570, (1950).
- [18] V.M Maksimonto, *Soviet Phys. JETP* 6, 180, (1958).
- [19] N. Yajima and K. Kobayakawa, *Progr. Theor. Phys.* 19, 192, (1958).
- [20] F. Cerulus, *Nuovo Cimento* 14, 827, (1959).
- [21] M. Kretzschmar, *Ann. Rev. Nucl. Sci.* 11, 1-40, (1960).
- [22] K. Redlich and L. Turko, *Z. Phys. C5*, 201, (1980).
- [23] H. Elze, W. Greiner and J. Rafelski, *Phys. Lett.*, B124, 515, (1983).
- [24] L. Turko, *Phys. Lett.* 104B, 153, (1981).
- [25] H.Th. Elze and W. Greiner, *Phys. Rev.* A33, 1879, (1986); K. Redlich and D.E. Miller, *Phys. Rev.* D37, 3716, (1988); *Phys. Rev.* D35, 2524, (1987); D.S. Skagerstam, *Z. Phys.* C24, 97, (1984); *J. Phys.* A18, 1, (1985); *Phys. Lett.* 133B, 419, (1985).
- [26] R. Hagedorn, K. Redlich, *Statistical Thermodynamics in Relativistic Particle and Ion Physics : Canonical or Grand Canonical?*, *Z. Phys. C-Particles and Fields* 27, 541-551, (1985).
- [27] J. Rafelski and M. Danos, *Phys. Lett.* 97B, 279, (1980).

- [28] J. Cleymans, M. Marais, A. Muronga, Talk presented by M. Marais at the 40th Annual Conference of the South African Institute of Physics, University of the Western Cape, July 1995.
- [29] T. Matsui and H. Satz, *Phys. Lett.* 178B, 416, (1986).
- [30] U. Heinz, *Nucl. Phys.* A566, 205c, (1994).
- [31] J. Letessier, A Tounsi, U. Heinz, J. Sollfrank and J. Rafelski, Strangeness Conservation in Hot Fireballs, preprint TPR-92-28, revised Aug. 1993, submitted to *Phys. Rev. D.*; J. Letessier, A Tounsi, U. Heinz, J. Sollfrank and J. Rafelski, *Phys. Rev. Lett.* 70, 3530, (1993).
- [32] E. Schnedermann, J. Sollfrank and U. Heinz, *Phys. Rev.* C48, 2462, (1993); U. Heinz, Particle Spectra, in *Hadrons and Hadronic Matter*, edited by J. Letessier, H. Gutbrod and J. Rafelski; Plenum Press, New York, (1995).
- [33] R. Hagedorn, *Thermodynamics of Strong Interactions*, CERN 71-12, Geneva, (1971).
- [34] J. Bjorken, *Phys. Rev.* D27, 140, (1983).
- [35] Y.M. Sinyukov, V.Averchenkov and B. Lärstadt, *Z Phys.* C49, 417, (1991); M.Kataja, *Z Phys.* C38, 419, (1988).S
- [36] A.J. Pointon, *Statistical Physics*, Longmans, Green and Co., (1967).
- [37] A.L Fetter, J.D. Walecka, *Quantum Theory of Many Particle Systems*, McGraw-Hill, (1971).
- [38] R.K. Pathria, *Statistical Mechanics*, Pergamon Press, (1984).
- [39] F.Solms, H.G. Miller and A. Plastino, *Phys. Lett.*, A157, 286, (1991) (and references therein).
- [40] B. Müller, *The Physics of the Quark-Gluon Plasma*, Springer-Verlag (1985).
- [41] J. Kapusta, *Finite Temperature Field Theory*, Cambridge University Press (1989).

- [42] J. Cleymans, K. Redlich and E. Suhonen, Canonical Description of Strangeness Conservation and Particle Production, *Z.Phys. C-Particles and Fields* 51, 137, (1991).
- [43] J. Cleymans, E. Suhonen, G.M. Weber, Conserved Quantum Numbers in Relativistic Ion Collisions, Seminar on Theoretical Physics, Bloemfontein, South Africa, (1991).
- [44] J. Cleymans, E. Suhonen, G.M. Weber, Exact Baryon and Strangeness Conservation in Hadronic Gas Models, *Z.Phys. C-Particles and Fields* 53, 485-491, (1992).
- [45] D. Perkins, *Introduction to High Energy Physics* (Second Edition), Addison -Wesley Publishing Company, (1983).
- [46] K. Nishijima, *Fundamental Particles*, W.A. Benjamin Inc., (1964).
- [47] D. Halliday, R. Resnick and J. Walker, *Fundamentals of Physics* (Fifth Edition), John Wiley and Sons, Inc., (1997).
- [48] E866 Collaboration, Y. Akiba, Talk presented at Quark Matter '96, Heidelberg, May 1996; Y. Akiba for the E802 collaboration, *Nuclear Physics, A610*, 139c-152c, (1996).

Acknowledgements

I would like to thank my supervisor, Prof. Jean Cleymans, for all his support and encouragement and, the stimulating discussions enjoyed with him. I would also like to thank Prof. Cleymans for being such a good teacher.

Many thanks to Prof. Esko Suhonen from Oulu, Finland for his collaboration with us and his quiet encouragement. Thank-you for making more computers available and for lunch on the mountain.

Also, to the ever patient Mrs. Joan Parsons, thank-you for all those times of impromptu Latex tutorials even when you had tons of other work.

To my wonderful parents, for everything including their endearing impatience to see the end-product and wondering whether I'd be done by the next day - thank-you for putting up with me.

Thanks to my brother, Adrian, for his aesthetic appreciation of my thesis and for helping me with some of the more artistic impressions of high energy collisions.



"PARTICLES, PARTICLES, PARTICLES!"

A cartoon by Sidney Harris

*From ghoulies and ghosties and long-leggety beasties
And things that go bump in the night,
Good Lord, deliver us!*

Anonymous